STRUCTURAL AND EPITOPE CHARACTERIZATION OF MAJOR ALLERGENS FROM DUST MITE, BLO T 21 AND DER F 7

TAN KANG WEI

NATIONAL UNIVERSITY OF SINGAPORE
2011

STRUCTURAL AND EPITOPE CHARACTERIZATION OF MAJOR ALLERGENS FROM DUST MITE, BLO T 21 AND DER F 7

TAN KANG WEI
(B. Sc., UKM)

A THESIS SUBMITTED
FOR THE DEGREE OF DOCTOR OF PHILOSOPHY
DEPARTMENT OF BIOLOGICAL SCIENCES
NATIONAL UNIVERSITY OF SINGAPORE
2011

Acknowledgements

I am heartily thankful to my supervisor, Assoc. Prof. Dr. Henry Mok, for his encouragement, patience, guidance and support throughout these years of my study. His critical thinking and advices really inspired me in doing my research.

I would also like to extend my gratitude to Assoc. Prof. Dr. Chew, for being a resourceful and understanding collaborator. Special thanks to Prof. Yang and Assoc. Prof. Dr. Sivaraman for their sharing of ideas that have been wonderfully insightful for my studies in NMR and X-ray crystallography.

Many thanks to Dr. Chan. Dr. Kartik, Dr. Shiva, Dr. Lin Zhi, Dr. Ong, Dr. Kumar, Dr. Chiradeep and Dr. Jobi for their generosity in sharing invaluable experience whenever I requested. You have been a great help throughout my candidature. Sang, Jack, Rishi, Jana, Wentao, and everyone in SBL as well as functional genomic lab 1 and 2, my heartfelf thanks for your delightful companionships and helpful advices for designing my experiments.

To my beloved Xin Yu, thank you for always being there for me. Your love is a great motivation for my research that I will forever cherish. Special thanks for helping me to proofread this thesis with admirable patience and critical comments.

My family and relatives who have been emotionally supportive from the day I stepped foot in Singapore, I am forever indebted to you for your understanding, patience and love. Without you, I won't be who I am today, thank you very much.

Table of Contents

Summary

Allergic diseases have drawn worldwide attention since its discovery for more than a century ago. Currently, the prevalence of allergic diseases is rising steadily to an alarming state in both developed and developing countries, taking a toll on millions of lives. These diseases include asthma, atopic dermatitis (AD), rhinitis, anaphylaxis as well as food, drug and insect allergy. House dust mite (HDM) stands out as one of the major causative agents of allergic diseases owing to its ubiquitous presence in both temperate and tropical regions. To date, more than twenty groups of allergens have been isolated from dust mites and were shown to be highly antigenic. However, the underlying reasons of their allergenicity remain largely unknown. Therefore, extensive immune characterization aided by sophisticated structural studies is imperative in order to decipher the inherent features of these allergens and to develop a hypoallergen for specific immune therapy.

This thesis aims to describe the 3D structures and the IgE epitopes of two major allergens from dust mites, namely, Blo t 21 and Der f 7. The first part of this thesis focuses on Blo t 21, a major allergen from *Blomia tropicalis*. Blo t 21 showed limited cross-reactivity with its paralogue, Blo t 5, thus inferring that Blo t 21 should use unique epitopes to interact with IgE antibodies. The 3D structures of Blo t 21 and Blo t 5 (PDB: 2JMH) determined by NMR approaches shared high structural homology. However, some disparities of the local structure could be detected. The allergenicity test on the Blo t 21 mutants using ELISA demonstrated that residues Glu-74, Asp-79, Glu-89 and Asp-96 were the major IgE epitopes, with residues Glu-89 and Asp-96 forming a conformational epitope. The subsequent peptide ELISA experiments suggested the presence of a linear IgE epitope in Blo t 21, which exhibited distinct allergenicity compared to that described in Blo t 5 previously. These data could help to explain the limited cross reactivity between Blo t 21 and Blo t 5. The allergenicity and cross inhibition tests conducted on the homologous proteins, Der f 21 and Der p 5, indicated different antigenic properties as compared to Blo t 21 and Blo t 5. Further

analysis implied that the primary sequence, stability and 3D structure could contribute to the differences in these proteins. Therefore, the fundamental biophysical and structural characterizations on these allergens should be included while mapping their IgE epitopes.

The second part of this thesis describes the crystal structure and the IgE epitope mapping of Der f 7, a major group 7 allergen from *Dermatophagoides farinae*. Studies have shown that this allergen elicits strong immune response in mite-sensitized individuals. The crystal structure of Der f 7 is very similar to that of Der p 7, which was also solved by X-ray crystallography method (PDB: 3H4Z). However, it was reported that these two allergens showed dissimilar IgE binding activity, with a majority of the test subjects indicating higher sensitivity to Der p 7. Recently, attempts to map the IgE epitopes have been reported in two separate accounts. However, our results suggested that the proposed IgE binding residues, Leu-48, Phe-50 and Asp-159, might not be the major IgE epitopes of Der f 7. Based on the mapping of different residues between Der f 7 and Der p 7 on the crystal structures, we proposed that residues Lys-25, Asp-55 and Glu-124 could be responsible for the higher IgE binding activity of Der p 7. Nevertheless, the IgE epitopes of Der f 7 remained elusive thus far. In addition, the data pertaining to physical characterization and ligand binding studies of Der f 7 will be presented as well. These results may pave a way for understanding the allergenic properties of these proteins, and aid in the development of hypoallergens suitable for immunotherapy purposes.

LIST OF TABLE

.

LIST OF FIGURES

LIST OF ABBREVIATIONS

Amino Acids

One letter code	Three letter code	Amino acid
A	Ala	Alanine
C	Cys	Cystein
D	Asp	Aspartic acid
E	Glu	Glutamic acid
F	Phe	Phenylalanine
G	Gly	Glycine
H	His	Histidine
I	Ile	Isoleucine
K	Lys	Lysine
L	Leu	Leucine
M	Met	Methionine
N	Asn	Asparagine
P	Pro	Proline
Q	Gln	Glutamine
R	Arg	Arginine
S	Ser	Serine
T	Thr	Threonine
V	Val	Valine
W	Trp	Tyrptophan
Y	Tyr	Tyrosine

Chemicals and reagents

BSA	Bovine serum albumine
$CaCl_2$	Calcium chloride
dATP	2’ deoxyadenosine 5’ triphosphate
dCTP	2’ deoxycytidine 5’ triphosphate
dGTP	2’ deoxyguanosine 5’ triphosphate
dNTP	Deoxynucleotide triphosphate
dTTP	2’ deoxythymidine 5’ triphosphate
IPTG	Isopropyl-D-thiogalactoside
KCl	Potassium chloride
$MgCl_2$	Magnesium chloride
Ni	Nickel
Ni-NTA	Nickel-Nitrilotriacetic
PBS	Phospate buffer saline
PBS-T	Phospate buffer saline with 0.05% Tween
PEG MME	Polyethylene glycol monomethyl ether
PNPP	*p*-Nitrophenyl phosphate disodium
SDS	Sodium dodecyl-sulphate
TEMED	N,N,N,N’-Tetramethylethylenediamine
TMB	3,3,’5,5’-Tetramethylbenzidine
Tris	Tris (hydoxymethyl)-aminomenthane

Units and measurement

bp	Base pair
Da	Dalton
Hz	Hertz
K	Kelvin
kDa	Kilo Dalton
M	Molar
pH	Potential of hydrogen
ppm	Parts per million
rpm	Rotation per minute
SGD	Singapore Dollar
U	Unit (enzyme)
V	Volt

Others

1D/2D/3D/4D	One dimentional/Two dimensional/3D/ Four dimensional
α	alpha
β	beta
γ	gamma
δ	delta
ε	epsilon
APC	Antigen-presenting cell
CCP4	Collaborative Computational Project Number 4
CD	Circular dichroism

CD4/8	Cluster of differentiation 4/8
CD23	Fc epsilon RII
CD25	alpha chain of the IL-2 receptor
CSI	Chemical shift index
DNA	Deoxyribonucleic acid
ELISA	Enzyme-Linked ImmunoSorbent Assay
EST	Expressed Sequence Tag
FcεRI	IgE receptor type-I
FPLC	Fast Protein Liquid Chromatography
GST	Glutathione S-transferase
HRP	Horseradish peroxidase
HSQC	Heteronuclear Single-Quantum Correlation
IFN-γ	Interferon gamma
IgA	Immunoglobulin A
IgE	Immunoglobulin E
IgG	Immunoglobulin G
IL	Interleukin
ITAM	Immunoreceptor tyrosine-based activation motif
LB	Luria Bertani
MALDI-TOF	Matrix-assisted laser desorption/ionization
MHC	Major histocompatibility complex
NMR	Nuclear Magnetic Resonance
NOE	Nuclear Overhauser Effect
NOESY	Nuclear Overhauser Effect Spectroscopy
NPC2	Niemann Pick protein type C2
OD	Optical density
PCR	Polymerase chain reaction

RIA	Radio-immuno assay
R.M.S.D.	Root mean square deviation
SeMet	Selenium methionine
SDS-PAGE	Sodium Dodecyl-Sulphate Polyacrylamide Gel Electrophoresis
Th1	Type-1 Helper T-cells
Th2	Type-2 Helper T-cells
TNF-α	Tumor necrosis factor alpha
TOCSY	Total correlation spectroscopy

CHAPTER 1 INTRODUCTION

1. Allergy

1.1 An introduction to allergy

Clemens von Pirquet, an Austrian pediatrician, coined the word “Allergy” in 1906. Originated from the Greek word 'allos', which means “change in the native state”, the term 'allergy' is now used to describe the altered immune response in a human body in response to the supposedly innocuous foreign substances, commonly known as allergens. The immune system in a healthy human body will function with an intricate balance to react appropriately to the intruding foreign substances while preventing the over-reaction against self-antigens or harmless foreign antigens. An occurrence of the excessive or uncontrolled immune response will lead to an immune disease known as “Hypersensitivity”. Hypersensitivity disorders include autoimmune diseases, in which the body immune system mistakes own cells or tissues as antigens, and the diseases that result in the hyper-reactive responses against non-harmful environmental proteins or microbes. Gell and Coombs (1963) proposed that there are four types of hypersensitivity, distinguished by the immune-pathologenic mechanism and the type of mediators involved (Gell and Coombs 1963). The fifth type of hypersensitivity (Type V Hypersensitivity) was described as a rare, type 2-like hypersensitivity (Rajan 2003). Based on these classifications, allergy is synonymous with “Type I Hypersensitivity”, in which the immunoglobulin E (IgE) and IgG4 mediate the immune responses against foreign antigens. Commonly mentioned disorders observed in Type I Hypersensitivity include atopy, systemic anaphylaxis and asthma.

Atopy or atopic syndrome refers to the hereditary predisposition of an individual toward producing specific IgE antibodies against environmental antigens and subsequent development of immediate and acute allergic reactions (Abbas and Lichtman 2003). The cross-linking of the allergens to the IgE antibodies bound on the surface of mast cells or basophils triggers the release of the pro-inflammatory mediators (histamine, proteases,

chemokines, heparin), resulting in the clinical manifestation of diseases like atopic eczema, asthma and allergic rhinitis (Bousquet, Holt et al. 2008).

An antigen that can trigger immediate allergic responses upon exposure is defined as an allergen. Allergens are usually soluble proteins or chemicals that can induce the proliferation of the IgE antibodies circulating in the atopic patients. Some common allergens' sources include animal products, drugs, foods, insect stings, fungal and pollens. Animal products include fur, dander, wool and the dust mite (*Dermatophagoides pteronyssinus* and *Dermatophagoides farinae*; and storage mite *Blomia tropicalis*) excretion (Hurtado and Parini 1987; Fernandez, Martin-Esteban et al. 1993). Many atopic patients are known to be hypersensitive to certain drugs like penicillin, sulfonamides and local anesthetics, which sometimes cause complications in the medical practices. A more commonly known source of allergen is food. Some commonly known food allergens are celery, corn, eggs, certain fruits, seafood and nuts. Insect stings like bee venom and wasp venom are also widely known as a major source of allergens. Several genera of fungus are implicated as major allergen sources comprising *Aspergillus, Cladosporium, Alternaria, Penicillium* and *Fusarium* (Cromwell, 1997). Pollen allergens which are known to cause hay fever include some species of grass like ryegrass *Lolium perenne* and timothy grass *Phleum pratense*; weeds such as ragweed *Ambrosia* and nettle (*Urtica dioica*); as well as those from trees like birch *Betula verrucosa*, alder *Alnus serrulata* and willow *Salix fragilis* (Cromwell,1997).

In the past three decades, there has been a spectacular increase in the prevalence of asthma and allergic disease worldwide (Holgate 2004). The prevalence of asthma increased 75% from 1980 – 1994, with 160% increment in asthma rates among the children under the age of five (Centers for Disease Control, USA, 1998). World Health Organization (WHO) reported that in 2007, more than 300 million people suffered from asthma worldwide, with 250,000 fatalities attributed to the disease annually. Asthma and allergic diseases have caused millions of people to suffer physical impairments and decrease in quality of life. For example, approximately 10.1 million missed work days for adults annually in US (Akinbami 2006); asthma was also responsible for 3,384 deaths in US (ALA age group analysis of NHIS

through 2005). Besides that, asthma also adds to the healthcare financial burden bore by a nation. In Singapore, for every 10,000 students examined in 2001, 1026 male students (~10 %) and 757 (~7.5%) female students had asthma; and the incidence of asthma increased for both genders between 1991 and 2001 (Statistics Singapore Newsletter, 2003). In US, the annual economic cost of asthma is US$19.7 Million (ALA, USA, 2007) and according to the survey conducted in 2009 by National Heart, Lung and Blood Institute, USA, over USD$20 billion were spent due to asthma per annum. On the other hand, around SGD$54 million were spent yearly by asthmatic patients in Singapore (Chew, Goh et al. 1999).

Conventional clinical treatment for allergic diseases is designed to alleviate the symptoms and to suppress the allergic inflammation. For example, antihistamines drugs, anticholinergic agents or topical corticosteroids are commonly used to treat allergic rhinitis (Kay, 2001). Atopic dermatitis is normally treated with antihistamines and corticosteroids to control and suppress inflammation of the affected site (Roos, Geuer et al. 2004). Anti-asthmatic drugs salbutamol and salmeterol are predominantly used to relieve asthmatic symptoms and for maintenance therapy (Kon and Barnes 1997). However, relieving the symptoms is not the most effective choice for long-term therapy. The advent of allergen-specific immunotherapy provides a novel avenue to reverse the course of the disease and for prolonged protection against progression of allergic diseases (Valenta 2002; Niederberger and Valenta 2004).

1.2 Mechanisms of allergy

There are three major components involved in an allergic reaction, namely, the allergen, the IgE and at least one type of effector cells such as mast cells, basophils or eosinophils (Abbas and Lichtman 2003). Besides that, the immune system also requires other cellular members such as antigen-presenting cells (APC) and lymphocyte cells to initiate and regulate of allergic reaction and disease progression. An invading allergen is captured by APC such as dendritic cells or cutaneous Langerhans' cells and presented as T-cell peptide to

CD4+ T-cells in a major histocompatibility complex MHC class II-restricted manner (Abbas and Lichtman, 2003 and Kay, 2001). Consequently, the CD4+ cells are primed to differentiate into T helper 2 cells (Th2) followed by the release of Th2-type cytokines such as IL-4, IL-5, IL-9 and IL-13 (Kay, 2001).

The APC presents the antigen in the form of peptide fragments to the T-cells. The fragments bearing the T-cell epitopes are loaded onto the MHC and the formation of the MHC-peptides complexes will be recognized by the T-cells. Generally, there are two classes of MHC molecules; Class I MHC presents the peptides to the CD8+ cytolytic T-cells while the Class II MHC presents the peptides to the CD4+ helper T-cells. The Class II MHC-peptide complex is recognized by the T-cell receptor (TCR) located on the surface of the T-cells. Dendritic cells, macrophages and B lymphocyte cells are the common APCs that initiate the helper T-cells (Th). Dendritic cells and cutaneous Langerhans cells are known to present the allergens to Th2 cells in an MHC Class II manner in cases of asthma and eczema, respectively (Kay, 2001).

The Th2 cells will respond upon recognition of the MHC-peptide complexes by releasing an array of cytokines. Subsequently, the proliferation of specific IgE antibodies and the development of inflammation cells such as mast cells, basophils and eosinophils will be implemented. The cytokines that mediate the inflammatory and immune reactions are termed as “interleukin”. Interleukins-4 (IL-4) and IL-13 initiate the differentiation of B cells to undergo class switching of the constant region of immunoglobulin heavy chain (C_H) to Fcε to produce IgE class antibodies specifically (Valenta 2002). IL-4 and IL-9 promote the development of mast cells, the major effector cells in releasing inflammation mediators (Kay, 2001). IL-13 plays a key role in inducing airway hyper-responsiveness, goblet cell metaplasia and mucus hypersecretion (Wills-Karp, Luyimbazi et al. 1998), while the expansion and recruitment of eosinophils and basophils are induced collectively by IL-4, IL-5, IL-9 and IL-13 (Kay, 2001). The cytokines secreted by Th1 or Th2 cells act as an autocrine growth factor to promote the proliferation of these cells while inhibiting the growth of the opposite cell type (Fernandez-Botran, Sanders et al. 1988; Gajewski and Fitch 1988; Liew and McInnes 2002).

For instance, IL-4 induces the growth of Th2 cells while inhibiting the proliferation of Th1 cells. On the other hand, IFN-γ, a cytokine released by Th1 subset of cells promotes the expansion of Th1 cells but inhibits the proliferation of Th2 cells.

IgE antibodies bind to its receptor (Fc receptor) via the constant region, Fcε, on the heavy chain. Cross-linking of the FcεRI (high-affinity IgE receptor) present on the mast cells or basophils by allergen-bound IgE releases inflammatory mediators such as histamine, leukotrienes and lipid mediators (Kay 2008). This receptor is also present on the surface of APC where it assists in the IgE-mediated capturing of the allergen, enabling the allergen to be presented to the T-cells (Stingl and Maurer 1997). Based on the crystal structure of the FcεRIα and IgE-Fc complex, the α-chain of FcεRIα binds to the dimeric molecules of Cε3 domain of the IgE (Garman, Wurzburg et al. 2000). FcεRIα does not aggregate in the absence of antigen; the aggregation of the receptors occurs only when IgE antibodies are bound to the receptor and cross-linked by allergens. Numerous signaling pathways initiated by the aggregation of FcεRI receptors on the surface of mast cells result in the secretion of various inflammatory mediators and cytokines (Turner and Kinet 1999).

The FcεRIα receptor is expressed on the surface of mast cells and basophils as a multimeric αβγ2 complex (Nadler, Matthews et al. 2000). The β chain and two γ chains act as a phosphoreceptor for Tyr kinases that are involved in signaling cascades. Each β and γ chains contains one Immunoreceptor Tyr-based Activation Motif (ITAM) in their respective cytosolic portions. The aggregation of FcεRIα receptors triggers the signal transduction that activates two main Tyr kinases, Lyn and Syk. The first kinase, Lyn, phosphorylates ITAMs of β and γ chains followed by the recruitment and activation of the second kinase, Syk to the ITAMs of γ chains (Abbas and Lichtman, 2003). The recruitment and activation of the kinases lead to the elaborated signalling events that ultimately result in the phosphorylation of myosin light chains by an activated protein kinase C. Finally, degranulation occurs when the actin-myosin complexes are broken down (Nadler, Matthews et al. 2000; Abbas and Lichtman 2003).

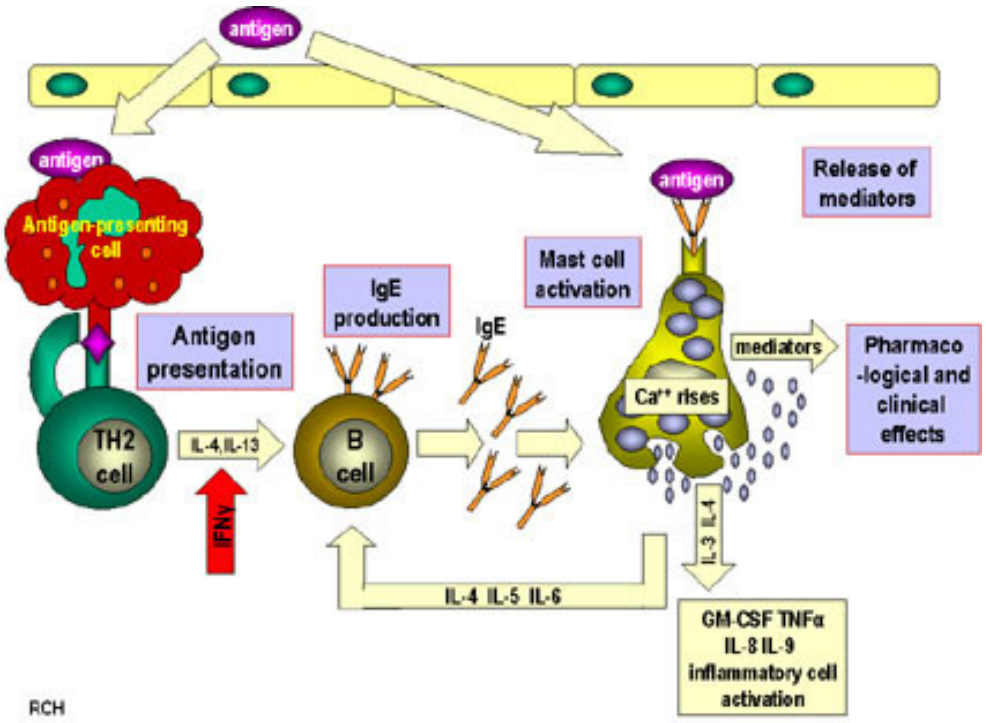

Figure 1.1 Mechanism of allergy diseases. During the first encounter, the allergen will be presented by the APCs to Th2 cells triggering release of cytokines like IL-4 and Il-13. These cytokines stimulate antibody class switching and production of IgE antibodies. Pro-inflammatory mediators will be released by mast cells once mast cells-bound IgE antibodies are cross-linked by the allergen, which ultimately results in acute allergic reactions such as wheezing, asthma and sneezing.

1.3 Dust mite

House dust mites are arachnids related to ticks, spiders and harvestmen (Colloff 2009). These microscopic organisms belong to the phylum Arthropoda, subphylum Chelicerata, class Arachnida, order Acari, and suborder Astigmata. Dust mites are ubiquitously found, especially in human habitats, where the dust is accumulated in bedding, carpets and furniture. House dust provides a sustaining habitat for dust mites, where the food source - shed human skin scales – is abundant. The predominant dust mites species found in household dust, and the major source of allergens belong to the family Pyroglyphidae. The top three pyroglyphid species of house dust mites in terms of the frequency and abundance worldwide are *D. farinae, D. pteronyssinus* and *Euroglyphus maynei* (Colloff 2009). These species are more common in temperate climate such as continental Europe and North

America. On the other hand, storage mite *B. tropicalis* (family Echymyopodidae) has emerged as a more important species in tropics and subtropical regions.

Dust mites reproduce sexually and the stages in its life cycle are the egg, a six-legged larva, two eight legged nymphal stages (protonymph and tritonymph) and adult. Similar to insects, adult mites have exoskeleton, jointed appendages and a blood-filled body cavity (hemocoel) (Fernandez-Caldas 2002). However, instead of having three pairs of legs like insects, mites have four. Dust mites are poikilothermic (unable to control body temperature), the length of their life cycle is thus dependent on the temperature of the habitat. The growth in population and egg-to-adult development of dust mites are controlled by both humidity and temperature (Hart 1998). In laboratory, dust mite requires a high relative humidity (RH) from 75% to 80% to complete their life cycle, with an optimum temperature of approximately 25 °C to 30 °C (Fernandez-Caldas 2002). The life span of the adults is approximately 4-6 weeks, during which time each female can produce 40-80 eggs.

The abundance of dust mites in household area is one of the main reasons why dust mite is the major cause of asthma attacks in the world. The body and the feces of dust mite are the major source of allergens. These "allergens" are the enzymes and other proteins from the mites that react potently as antigenic molecule. For example, Der p 1, a group 1 allergen isolated from *D. pteronysinnus* was shown to be strongly associated with the gut and faecal pellets, based on its amino acid sequence; the group 4 allergens are amylase, common functional enzymes found in most of the organisms (Colloff 2009). Based on the online resource Allergome (www.allergome.org), more than 20 groups of proteins from dust mites have been isolated and characterized, indicating the wide diversity of different proteins that are involved in causing allergic reactions (Table 1.1). These allergens are grouped according to their function, molecular weight and sequence identity, and numbered according to their chronological characterization. As it can be seen, group 1 and group 2 are the two predominant group of allergens from dust mites, with each of them accounting for more than 80% in IgE binding prevalence among patients sensitized to dust mites (Trombone, Tobias et al. 2002).

World Health Organization / International Union of Immunologic Societies Subcommittee (WHO/IUIS) recommended the nomenclature of allergens. This system comprises of the first three letters designating the genus, followed by one alphabet from the species and one numeral that describe the order of discovery of the allergen (King, Hoffman et al. 1994; Chapman, Pomes et al. 2007). For example, Der p 1 defines the first allergen proteins isolated from dust mite *Dermatophagoides pteronyssinus* while Der p 2 will be referring to the second isolated from the same mite. Similarly, Ara h 1 describes the first allergen isolated from peanut *Arachis hypogaea.*

Group 1 allergens are glycoproteins with sequence homology and protease function similar to cysteine proteases such as papain, actinidin and bromelin (Enrique, Malek et al. 2008). The molecular weight of these allergens are around 25kD and were cloned from *D. farinae, D. pteronyssinus, B. tropicalis* and *E. maynei*. The IgE binding prevalence for group 1 mite allergens is more than 90% of the tested population (Table 1.1). Group 2 allergens are another important group of allergen identified in dust mites. These proteins are highly heat resistant and have a molecular weight of about 14 kDa. They consist of predominantly beta-sheet structure with an immunoglobulin-like fold (ML-like) (Colloff 2009). Similarly, Group 2 allergens have very high IgE prevalence of more than 90% (Table 1.1).

Group	Biological Function	Mw (kDa)	% Prevalence
1	Cystein protease	25	>90
2	Niemann-Pick C2 homologue	14	>90
3	Tyrpsin/serine protease	25	16-97
4	Amylase	57	30-74
5	Unknown	15	50-70
6	Chymotrypsin/serine protease	27	40
7	Innate Immunity	24	50
8	Glutathaione-S-transferase	26	40
9	Collagenolytic serine protease	26	90
10	Tropomyosin	37	50-95
11	Paramyosine	102	80
12	Unknown	16	50
13	Fatty acid binding protein	15	10-23
14	Vitellogenien/apolipophorin-like	17.7	90
15	98K Chitinase	62.5	70
16	Gelsolin	55	35
17	Calcium-binding protein	30	35
18	Chitinase	60	60
19	Anti-microbial peptide	7	10
20	Arginine kinase	40	40
21	Unknown (Group 5 analogue)	12	>50
22	Group 2 analogue	14	50
23	Unknown	14	-

Table 1.1 Classification of dust mite allergens (adapted and modified from www.allergome.org and (Thomas, Smith et al. 2002). The allergens are grouped based on their function and sequence similarity, and are numbered in chronological order of first isolation.

1.4 From structure determination to IgE epitope mapping

1.4.1 Structural biology of allergens

The first available three-dimensional (3D) structure of an allergen was Bev t 1, a major birch pollen allergen identified in *Betula verrucosa* (Gajhede, Osmark et al. 1996). That was the first attempt to identify the structural attributes that would make a protein an allergen.

The structures of several other major allergens like Der f 2, a major dust mite allergen from *D. pteronyssinus* (Ichikawa, Hatanaka et al. 1998), and Phl p 2 (De Marino, Morelli et al. 1999), a timothy grass pollen allergen from *Phleum pratense* were also solved using both X-ray crystallography and NMR (Nuclear Magnetic Resonance). However, the structural analysis of the allergens was not fruitful as there were no conserved structural motifs or common structural themes that could indicate allergenicity due to the diversity of tertiary folds of different allergens (Valenta and Kraft 2002).

By classifying allergens into four structural families based on the experimental 3D structures and homology models, Aalberse (2000) has provided a systematic way to categorize allergens. In the same review, Aalberse proposed that all IgE epitopes are conformational as it involves residues from different parts of the linear protein sequence. However, this statement is questionable, as the recent study on Blo t 5, a major dust mite allergen isolated from *B. tropicalis,* has shown that this novel allergen harbors a linear epitope (Chan, Ong et al. 2008). Bet v 1, a major allergen which causes the birch pollen allergy, has been well characterized for its 3D structure and IgE epitope (Gajhede, Osmark et al. 1996; Mirza, Henriksen et al. 2000; Spangfort, Mirza et al. 2003). The 3D structure of Bet v 1 consists of 7 β-strands and 3 α-helices forming a globular protein with molecular weight of around 17.5 kilo Dalton (kD). Holm and coworkers (2004) conducted a very comprehensive study in an attempt to mutate several surface residues of Bet v 1 to modulate its IgE binding properties. In this study, two mutants with four and nine surface amino acids substitutions respectively were generated. These mutations which cover up to five different areas on the surface of the allergen, have significantly changed the IgE binding properties of Bet v 1 (Holm, Gajhede et al. 2004).

Der p 2 from dust mite *D. Pteronyssinus* is another major allergen that was extensively characterized. Both the NMR and X-ray crystallography structure of this 14-kDa protein have been solved. Der p 2 has a human immunoglobulin-like fold which consists of predominantly β-sheets, with a β barrel formed by two 3-stranded antiparallel β-sheets (Mueller, Benjamin et al. 1998; Derewenda, Li et al. 2002). The overall fold is being

maintained by 3 disulfide bridges; these disulfide bridges have been shown to be crucial for the structural integrity of the group 2 allergens. Derewenda et al (2002) identified a large hydrophobic cavity between the two β-sheets, which inferred that the group 2 allergens may bind to hydrophobic ligands and the binding could be important to its physiological function in dust mites (Derewenda, Li et al. 2002). However, there is no concrete evidence that describes any ligand as well as its binding to the protein.

The structure of another important allergen from dust mite, Der p 1 has been resolved using X-ray crystallography technique (Meno, Thorsted et al. 2005; de Halleux, Stura et al. 2006). Both forms of Der p 1, pro-Der p 1 and mature Der p 1, exhibited α-β structure, with a typical papain-like cysteine protease fold. The pro-peptide region comprised of 4 α -helices which extended and interacted with the active site, and was shown to cover several IgE epitopes on the mature protein domain (Meno, Thorsted et al. 2005). Similar to group 2 allergens, three disulfide bridges were used to stabilize the overall structure of the mature protein, which also contained a magnesium binding site and dimerizes with an extensive dimeric interface (Kon and Barnes 1997). The crystal structure of the homologous protein, Der f 1 from *D. farinae*, which shared 80% sequence identity Der p 1 was also solved later (Chruszcz, Chapman et al. 2009). In this controversial report, the authors claimed that despite a high sequence and structural homology between these two proteins, the closer analysis of both structures revealed four different patches of surface exposed residues that may affect antibody binding. However, there is no proper assay or conclusive experimental data such as mutagenesis studies that can support their hypothesis.

There is experimental evidence implying that some allergens are capable of "reversible plasticity", which describes that an allergen could assume different conformations and thus exposing varying degree of its IgE epitopes (Valenta and Kraft 2002). For example, the calcium-binding activity of birch pollen allergen, Bet v 3, was shown to influence the IgE binding capacity drastically. When a calcium ion was removed from Bet v 3 via EGTA treatment, the IgE binding was strongly reduced (Seiberler, Scheiner et al. 1994). Similar calcium-mediated modulation of the allergenicity was also observed in other calcium-binding

allergens from plants and fish (Wopfner, Dissertori et al. 2007). The calcium-binding induced structural changes had been reported in Bet v 4 and Phl p 7, in which the local movement within the EF-hand motif was involved (Valenta, Hayek et al. 1998; Wopfner, Dissertori et al. 2007). It was proposed that the calcium-bound (open) form would expose the IgE epitopes that were buried in the calcium-depleted (apo-closed) form (Hayek, Vangelista et al. 1998; Niederberger, Hayek et al. 1999). Plasticity of allergen was also observed in the enhanced IgE binding following the interaction with IgG antibodies to the major birch pollen allergen, Bet v 1 (Visco, Dolecek et al. 1996; Denepoux, Eibensteiner et al. 2000). However, there is no evidence that can prove the any alteration in the structure of Bet v 1 upon binding to IgG antibodies. Nevertheless, these data strongly suggest that allergens can exist in a highly dynamic form that could present their IgE epitope in varying degrees. In conclusion, the structural changes induced by biological functions or interaction with other molecules may affect the IgE binding activity of some allergens.

1.4.2 IgE epitope mapping of allergens

Determination of the IgE epitope will help to distinguish the part of the protein that is responsible for IgE binding and thus cross-linking of the Fcε receptor to release pro-inflammatory mediators. Strategic scanning mutations can be employed based on IgE epitope mapping, to modify the wild-type allergen into a hypoallergenic molecule (hypoallergen) that can be used as a potential vaccine for immunotherapy. In addition, information on the locations of the epitopes, their charges and distribution are crucial for understanding the basis of interaction between IgE antibodies and allergens.

Site-directed mutagenesis (SDM) is one of the most widely used and simplest methods to study the IgE epitope by identifying the individual residues that are involved in IgE binding. Subsequently, IgE detection assays like ELISA and immunoblot experiments are used to determine the viability of the potential hypoallergens. A single substitution of a putative IgE binding residue to Ala usually will not disrupt the secondary or tertiary structures

of the protein; hence, this is a powerful strategy that can be used to identify unique residues that are involved in IgE binding. In broad, potential candidates for mutagenesis study can be chosen either based on the sequence alignment with non-allergenic/allergic homologous proteins, or by analyzing the 3D structure of an allergen. Multiple sequence alignment with allergenic homologous proteins \enable\s the identification of conserved amino acid residues among other cross-reactive allergens; while the alignment with non-allergenic homologous proteins help to determine unique residues in allergens that share different properties from those in the non-allergenic ones. Structural based selection provides more information like surface exposed/solvent accessible residues and their location in the 3D structure, e.g. surface exposed residues are most likely to be involved in the surface-surface interaction with IgE antibodies. Site-directed mutagenesis approaches have been successfully employed to map the IgE epitopes of Hev b 6.02 (Karisola, Mikkola et al. 2004), Der p 2 (Mueller, Smith et al. 2001), Bet v 1 (Spangfort, Mirza et al. 2003), Der f 13 and Blo t 5 (Chan, Ong et al. 2006; Chan, Ong et al. 2008)

X-ray crystallography proves to be an important tool to study the structure of protein complexes. However, there is no available structure on the complex formed between IgE and allergen so far. To form the IgE-allergen complex, a large amount of homogenous IgE will need to be extracted. Unfortunately, the IgE antibodies are usually present in a very low titer in sera as compared to the other types of immunoglobulin. In addition, an allergen usually contains multiple IgE epitope that may bind to more than one IgE molecule, thus making the crystallization process more difficult (Fedorov, Ball et al. 1997). An indirect approach has been introduced using a monoclonal antibody (IgG) to form a complex with the allergen of interest. The monoclonal antibody used must be able to cross-inhibit sera IgE from binding to the allergen. Mirza and coworkers had successfully employed this approach to determine the structure of the complex formed between Fab fragment of a murine monoclonal antibody IgG, BV16 and the major pollen allergen Bet v 1. The limitation of this approach, however, is that the monoclonal IgG which inhibits the binding of IgE to Bet v 1 does not necessarily bind at the IgE epitope. The inhibition of IgE binding may be due to the steric hindrance caused by

the monoclonal IgG binding to adjacent IgE epitope (Mirza, Henriksen et al. 2000). To date, this is the only structure of an allergen-antibody complex; nevertheless, the structure of an allergen-IgE complex is yet to be determined.

Several other methods that are commonly employed to map the IgE epitopes include peptide mapping and specific point mutation involving proline or cysteine residues. In peptide mapping strategy, the whole allergen protein is fragmented into peptides with overlapping N-terminal/ C-terminal sequences, which are used to estimate the region that interacts with the IgE antibodies. This method was proven to be successful in identifying the IgE epitopes of a major food allergen from English walnut (*Juglans regia*), Jug r 1 (Robotham, Teuber et al. 2002), a major pollen allergen *Juniperus* ashei, Jun a 1 (Midoro-Horiuti, Mathura et al. 2003), and 13S globulin allergen from buckwheat *Fagopyrum esculentum* (Fag13S) (Sordet, Culerrier et al. 2009). However, peptide mapping strategy is only applicable in identifying the sequential/linear epitopes while most of the IgE epitopes are conformational (Aalberse *et al*., 2000). Point mutations targeting prolines and cysteines have been shown to reduce the IgE binding capability of Der p 2, a major allergen from dust mite *D. pteronysinnus* (Takai, Ichikawa et al. 2000) and Asp f 2, a major fungus allergen from *Aspergillus fumigatus* (Banerjee, Kurup et al. 2002) respectively. However, the substitution of either proline or cysteine residues resulted in the disruption of the tertiary structure of proteins as these amino acids are essential in maintaining the structural integrity. Therefore, this strategy may not be reliable in identifying the IgE epitopes since the resulting conformational change of a protein does not delineate the true nature of the residues that are interacting with the IgE antibodies. Though these strategies may not be useful in defining the IgE epitope of an allergen, it had been demonstrated that they can be used to generate hypoallergenic molecules.

It has been shown that the IgE epitope can also be determined by measuring the amide proton exchange rates of the backbone amides in an allergen while binding to an antibody. In this technique, ^{15}N-labeled allergen is allowed to bind to the antibody, which is immobilized on a column before the buffer containing 100 % D_2O was added. Free amide hydrogen will exchange with deuterium in the buffer, while the amide hydrogen of the

residues in contact with antibody will be protected from exchange. Hence, the IgE epitope can be identified by assigning the remaining peaks in the ^{1}H-^{15}N HSQC spectrum. This approach has been successfully applied to map the IgE epitopes on Der p 2 which were also confirmed by mutagenesis studies (Mueller, Smith et al. 2001). However, this technique still employed monoclonal IgG as a large amount of antibody is required.

1.5 Specific immunotherapy

Specific immunotherapy was practiced about a century ago even before humankind knew the IgE-mediated mechanism. With the rationale of "vaccination" against "airborne toxins", this method was first used to alleviate the symptoms of hay fever and proved to be successful by Noon (1911). To date, specific immunotherapy has been extensively employed in numerous cases of allergy diseases. Several variations of administrating this method have been devised and it remains the only curative approach against allergy. However, thus far, respiratory allergy and hymenoptera venom allergy are the only accepted indications for specific immunotherapy. Jutel and coworkers demonstrated the depletion of Th2 cytokines such as IL-4 and IL-5 but the augmentation of Th1 cytokines' secretion such as IFN-γ and IL-12 with the immunotherapy using bee venom (Jutel, Pichler et al. 1995). Interleukin-4 (IL-4), IL-5 and IL-13 are involved in the development of Th2 cells while IFN-γ and IL-12 are the Th1-type cytokines that negatively regulate the development of Th2 cells. The main idea is to divert the T-cell responses from Th2 to Th1, in which the production of IgE antibodies is reduced while the production of IgG antibodies is induced. The IgG antibodies are also known as "blocking IgG antibodies" due to its ability to inhibit the IgE antibodies interacting with an allergen, thus preventing the cross-linking of Fcε receptors and the subsequent release of pro-inflammatory mediators (van Neerven, Wikborg et al. 1999; Holm, Gajhede et al. 2004; Niederberger and Valenta 2004; Valenta, Niespodziana et al. 2011).

The major problem associated with the use of native allergen extracts as means of immunotherapy is the resultant local and systemic side effects such as anaphylactic shock

(Valenta, 2002). The British Committee for the Safety of Medicines reported 26 deaths due to immunotherapy administered via subcutaneous injection using natural allergens' extracts in 1986. More recently, immunotherapy attempts using birch pollen extracts have resulted in the production of IgE antibodies that bind to new allergenic components (Moverare, Elfman et al. 2002). These incidents had raised concerns on the usefulness and risk/benefit ratio of immunotherapy using natural allergens' extracts and therefore, prompted the development of the allergenic molecules with reduced allergenicity, known as hypoallergens. The main idea of hypoallergen is the modification of an allergenic molecule to reduce or abolish its allergenicity so it will not cause the IgE-mediated side effects (Valenta, 2002). Chemical modification has been shown to be able to reduce the allergenicity of Fel d 1, a major cat allergen (Versteeq *et al*., 2004). Nevertheless, recombinant DNA technology proves to be more a versatile tool in creating hypoallergen based on many promising results.

Recombinant DNA technology was widely used in the past few decades to modify allergens for allergen-specific immunotherapy. By modifying the specific regions in the DNA sequence, the corresponding IgE binding epitopes can be removed from an allergen, hence generating the hypoallergen. The hypoallergen should preserve the T-cell epitopes to retain its immunogenicity, enabling the induction of a non-Th2 type response (Akdis and Blaser 2001). At the same time, the proliferation of Th1 or regulatory T-cells leading to a secretion of cytokines associated to these T-cells is expected (Kay, 2001). This is followed by the production of "blocking" IgG4 or IgA antibodies that can inhibit the binding of IgE to allergens. In this section, several strategies that are commonly used to remove the IgE epitope of an allergen while retaining its T-cell epitope will be discussed.

The IgE epitopes mapping strategies have been discussed in the earlier sections. As mentioned, point mutation approach was used to identify and to remove the residues involved in the binding with IgE antibodies. (Chan et al 2006) used site-directed mutagenesis to create the hypoallergenic mutant of Der f 13 with four point mutations. The integrity of the overall structure of the quadruple mutant was verified using circular dichroism (CD). Various immuno-assays have shown that the mutant demonstrated reduced IgE binding, but are still

capable of inducing T-cells proliferation. Blocking IgG antibodies were also raised from mice immunized with the quadruple mutant, indicating that this mutant retained its T-cell epitopes although the IgE epitopes have been removed. Similar methodology has been used to create a hypoallergen for the major dust mite allergen, Blo t 5 by mutating its sequential IgE epitope (Chan, Ong et al. 2008).

Most of the B-cell epitopes of an allergen is conformational (Aalberse *et al.* 2000), thus, the 3D structure of an allergen plays an important role in eliciting IgE-mediated responses. The disruption of the structural integrity has been attempted to generate the hypoallergen for the group 2 allergens from dust mites (Olsson, van Hage-Hamsten et al. 1998; Takai, Ichikawa et al. 2000). The group 2 allergens from dust mites have 3 disulfide bonds formed by 6 conserved cysteine residues. It was demonstrated that by altering the cysteine residues of these allergens, the IgE binding capacities were drastically reduced; while the T-cell epitopes remained intact, thus making them a good candidate for hypoallergens. Similar approach was used to reduce the IgE binding capability of Asp f 2, a major fungus allergen (Banerjee *et* al., 2002). However, this approach seems to be useful for the allergens that maintain their structural integrity using disulfide bonds. In addition, these structurally compromised mutants may not be able to raise blocking IgG antibodies if the IgG antibodies are specific to both the structure and sequence of the wild-type allergen.

An interesting approach was proposed by Norman *et al* (1996) with the rationale of fragmenting the allergens in order to disrupt its IgE epitope while retaining the T-cell epitope. This method was first used on Fel d 1, a major cat allergen, in which a mixture of long peptides' fragments (27 amino acids), which represent the major T-cell epitopes were derived from the allergen. However, the use of long peptides seemed to cause various adverse effects, including severe asthma (Norman, Ohman et al. 1996; Simons, Imada et al. 1996). It was suggested that the long peptide fragments might have retained a residual IgE binding capability and therefore, shorter peptides were designed for the subsequent experiments. This modification achieved an overall positive clinical efficacy without relevant adverse effects. Similar strategy was employed on Bet v 1, a major pollen allergen as well. In that experiment,

two recombinant fragments of Bet v 1 comprising residues 1-74 and residues 75-160 showed reduced allergenicity, while retaining their lymphoproliferative activity (Vrtala, Akdis et al. 2000). Other studies on bee venom allergies such as Api m 1 using the peptide immunotherapy have shown an increased production of allergen-specific IgG4 in serum and IL-10 production in allergen-stimulated PBMC cultures (Mueller, Benjamin et al. 1998; Vrtala, Akdis et al. 2000).

Another approach to create a hypoallergens is to generate oligomers of allergens. In this method, several recombinant allergens are fused and expressed together as a single molecule. It was demonstrated that the generation of dimers and trimers of Bet v 1 could significantly reduce the skin prick reactivity while maintaining the ability to stimulate Bet v 1-specific T-cell (Vrtala, Hirtenlehner et al. 1999). The recombinant fusion protein combining two bee venom major allergens, Api m 1 and Api m 2 from *Apis mellifera*, was shown to induce the T-cell proliferation but reduce IgE reactivity and histamine release (Kussebi, Karamloo et al. 2005). Karamloo and coworkers adopted the similar idea to generate a chimeric protein fusing three bee venom major allergens, Api m 1/2/3 that preserved the T-cell epitopes from all three different allergens, but with the IgE epitopes disrupted (Karamloo, Schmid-Grendelmeier et al. 2005).

Recombinant DNA technology is a powerful method that has enabled the identification of IgE epitopes as well as the generation of immunogenic hypoallergens with reduced allergenicity. This engineered hypoallergen should have reduced IgE binding capacity, thus reducing incidences of adverse side effects; and deviated T-cells pathway that favors the production of Th1 or regulatory T-cells cytokines. There is no perfect strategy to engineer a hypoallergen, but the availability of various strategies should enable the engineering of a more effective hypoallergen.

1.7 Group 21 allergen from dust mite

Group 21 is a relatively new group of allergen isolated from dust mite. To date, only three of its counterparts have been reported, i.e. Blo t 21, Der p 21 and Der f 21 based on the Allergome database (www.allergome.org). The biophysical and immunological characterization of Blot 21 and Der p 21 were described in separate accounts (Gao, Wang de et al. 2007; Weghofer, Dall'Antonia et al. 2008), but no structural information and cross-reactivity data between these allergens is available thus far.

Gao and coworkers first described Blo t 21 as a paralogue to Blo t 5, a major group 5 allergen isolated from *B. tropicalis*. The authors showed that Blo t 21 was a product of a single-copy gene that shared 39% protein sequence identity with Blo t 5. This 113-amino acid novel allergen reacted with 57.9% of the individuals attending outpatient allergy clinics over 1.5 years; and more than 75% of the sensitized patients were shown to be co-sensitized to both Blo t 21 and Blo t 5. The major finding of that study was the low-to-moderate cross-reactivity between Blo t 21 and Blo t 5, based on thirteen patients' sera. In three patients' sera, it was demonstrated that Blo t 21 was able to partially inhibit the IgE binding to Blo t 5, but Blo t 5 was not able to inhibit the IgE binding to Blo t 21. This result implied that Blo t 21 could bear some unique IgE epitopes that was not found in Blo t 5. In order to prove the hypothesis, it would be necessary to solve the 3D structure to aid in the IgE epitopes mapping of Blo t 21.

Another well characterized group 21 allergen from dust mite is Der p 21, isolated from *D. pteronysinnus.* This allergen was shown to have high thermal stability and could be refolded easily based on the CD experiments. In terms of allergenicity, Der p 21 could bind to high levels of IgE antibodies and able to elicit high allergenic activity in the basophil activation experiments. One unique characteristic of Der p 21 as reported by Weghofer and coworkers (2008) was the dimerization of the protein based on the small-angle X-ray scattering experiments. It was later revealed that Blo t 21, despite being homologous to Der p 21, in fact exists as a monomer in solution, regardless of its final concentration. Another

notable finding was the specific reactivity of the rabbit anti-Der p 21 serum with the crude extracts from *D. pteronysinnus* and *D. farinae* at 14 kDa and 28 kDa, which represent the approximate molecular weight of Der p 21 monomer and dimer, respectively. This anti-Der p 21 serum was not able to exhibit visible reaction at the same position in other dust mites tested, including *B. tropicalis*. Additionally, it was also demonstrated that the rabbit anti-Der p 21 IgG antibodies could inhibit the IgE binding in the mite-allergic patients' sera. These results indicated that Der p 21 and Blo t 21 were using different epitope residues to interact with specific IgE antibodies. However, there is no direct evidence showing that Der p 21 and Blo t 21 are not cross-reacting to each other.

1.8 Group 7 allergen from dust mite

Recently, the crystal structure of Der p 7, a major group 7 allergen from dust mite *D. pteronysinnus* has been reported (Mueller, Edwards et al. 2010). In the skin tests study, about 53% of mite-allergic individuals were shown to react to Der p 7 (Shen, Lin et al. 1997). A more extensive study on the allergenic properties, however, was conducted on the homologous protein, Der f 7, which was isolated from *D. farinae*. Der f 7 shares 86% sequence identity with Der p 7 and these two allergens were shown to cross-react to each other. The homology modeling of Der f 7 using the crystal structure of Der p 7 as the template was used for the monoclonal antibody HD12 (mAbs HD12) and polyclonal IgE binding studies. Based on the immunodot blot experiments using overlapping peptides derived from Der f 7, Shen and coworkers (2011) identified Leu-48 and Phe-50 as the important residues interacting with the Der f 7-specific mAbs HD12. Interestingly, the substitution of Leu-48 to Ile-48 and Phe-50 to Leu-50 in Der p 7 resulted in the non-responsiveness towards the Der f 7-specific mAbs HD12, thus suggesting that residues Leu-48 and Phe-50 were unique epitopes in Der f 7 (Shen, Tam et al. 2011). Subsequently, Chou and coworkers identified residue Asp-159, which is located in the loop region based on the model of Der f 7, as an important residue that interacted with the specific IgE antibody. It was also demonstrated that

Asp-159 was responsible for the IgE-mediated cross-reactivity between Der f 7 and Der p 7. However, this phenomenon was shown in only 2 of 30 sera tested (Chou, Tam et al. 2011). The characterization of the IgE/IgG epitopes of Der f 7 based on the homology model might not be accurate; high-resolution 3D structure of Der f 7 would provide detailed information such as the orientation of these IgE/IgG binding residues and correct surface charge distribution that could explain the allergenicity of this protein. Previously, the protein crystal of Der p 7 was obtained by adding the modified maltose-binding protein (MBP) to the N-terminal of the protein. Even though the recombinant Der p 7 was readily crystallized at room temperature, they did not show good diffraction (Mueller, Edwards et al. 2010).

1.9 Objectives and significance of this study

The first part focused on the studies on Blo t 21. Blo t 21 was shown to bind specific IgE antibodies in more than 50% of atopic patients allergic to dust mite and thus is considered as a major dust mite allergen. Previous study concluded that the overall cross-reactivity between Blo t 21 and Blo t 5 was low-to-moderate despite their similarities (Gao, Wang de et al. 2007). In most cases, Blo t 5 was unable to inhibit the binding of IgE to Blo t 21, thus implying that the latter may harbor a different set of IgE epitopes as compared to Blo t 5. However, there is no report on the 3D structure and the IgE epitope responsible for the allergenicity of Blo t 21 thus far.

The general objectives of this part were to study the structural characteristics of Blo t 21, a novel group 21 allergen isolated from *B. tropicalis* using NMR experiments and to investigate its IgE binding epitopes. The foundation of this research was based on the results of the previous study (Gao, Wang de et al. 2007). The blood sera obtained from the volunteers for all immunological experiments in our study was different from those that were used in the previous studies. Therefore, there are bound to be some inevitable discrepancies between our results, since the IgE profile is different among individuals. *In vivo* experiment such as mouse immunization was not conducted since it is not relevant to this study.

The specific aims and the significance of the first part were:

1) To solve the NMR structure of Blo t 21 and to examine its structural differences with Blo t 5. This is important as the differences in terms of allergenicity between these allergens could be due to the structural properties.
2) To map the IgE epitopes of Blo t 21 by site-directed mutagenesis in order to identify specific residues involved in the binding to IgE antibodies. Information of the major IgE epitopes may help in understanding the antigenic properties of Blo t 21.
3) To generate stable mutants of Blo t 21 with reduced IgE binding and mast cell cross-linking ability. The mutant with significant reduction in IgE binding when compared to the wild-type protein can be used as a potential hypoallergen for immunotherapy purposes.
4) To explain the differences in the allergenicity and lack of cross-reactivity between Blo t 21 and Blo t 5, as well as other similar allergens (Der f 21 and Der p 5) using their structural and immunological information. This may provide insight into the allergenic properties of these proteins.

The second part of this thesis focused on Der f 7, a major group 7 allergen from dust mite. Der f 7 shared 86% sequence identity with Der p 7, however, there were evidence showing that these two proteins shared different allergencity (Shen, Chua et al. 1995). Additionally, the IgE epitope mapping of group 7 protein was inconclusive (Chou, Tam et al. 2011). Therefore, by comparing the 3D structure of Der f 7 and Der p 7, we hoped to be able to identify their IgE epitopes. Apart from allergenicity, the ligand binding studies on Der f 7 would be interesting as well. Previously, Mueller and coworkers (2010) showed that Der p 7 was able to interact with polymyxin B (PB) but not the other ligands tested. Based on the structure-based homology search, there could be other ligands that were not tested previously. This is important as it was shown in other allergens that ligand binding could affect their allergencity (Thomas, Hales et al. 2005).

The general objectives of this part included structural determination of Der f 7 and identification of its IgE epitopes. In addition, the comparison of the structure, biophysical properties and allergenicity between Der f 7 and Der p 7 would be studied as well. Notably, most of the immunological studies on these proteins were done using monoclonal antibodies (Shen, Chua et al. 1993; Shen, Chua et al. 1995; Shen, Chua et al. 1995; Shen, Tam et al. 2011), only polyclonal IgE antibodies were used in our study as the study on monoclonal antibodies' interaction with these proteins was beyond the scope of this thesis.

The specific aims and significance of the second part included:

1. Structure determination of Der f 7 using NMR/X-ray crystallography approaches. The structure could be useful for the IgE epitope mapping studies.
2. Comparing the physical properties between Der f 7 and Der p 7 using SDS-PAGE, circular dichroim, and NMR experiments. This may contribute to a better understanding of the differences of these allergens in terms of their allergenicity.
3. Identifying the IgE epitopes of Der f 7 using site-directed mutagenesis approaches with the aid of the 3D structures. Information of the IgE epitopes may be important in explaining the allergenicity of this protein.
4. Identifying the ligand(s) that bind to Der f 7 using NMR approaches. Ligand binding study may shed a light on the probable function of this protein. Additionally, investigating the allergenicity of its bound form would also be interesting.

CHAPTER 2 MATERIALS & METHODS

2.1 Generation and subcloning of Blo t 21 and its mutants into expression vector

2.1.1 Bacterial host strains

Strain	Genotye
DH5-α	F^- Φ80d*lac*ZΔM15 &(*lac*ZYA-*arg*F) U169 *rec*A1 *end*A1 *hsd*R17(r_k^-,m_k^+) *pho*A *sup*E44 λ^- *thi*-1 *gyr*A96 *rel*A1
BL21-DE3	F^- *omp*T *hsd*S_B($r_B^-m_B^-$) *gal dcm*

2.1.2 Generation of DNA insert and Polymerase Chain Reaction

DNA insert was generated by polymerase chain reaction (PCR), using upstream oligonucleotide primer containing BamH I restriction site and downstream oligonucleotide primer containing stop codon and EcoR I restriction site. PCR reaction mix was prepared in 50 µl mix containing 1 X Pfu buffer (20 mM Tris-HCl (pH 7.5 at 25°C), 8 mM $MgCl_2$, 0.5 mM DTT, 50 mg/ml BSA), 1 µl of wild-type Blo t 21 DNA template, 0.4 µM of each primers, 200 µM of each dATP, dCTP, dGTP and dCTP, and 1 µl of 1 U KOD Hot Start Pfu DNA Polymerase (Novagen).

PCR was carried out for 30 cycles using 94°C for denaturation (15 sec), ~50 °C for annealing (30 sec) and 72°C for elongation (10 sec). The annealing temperature was adjusted accordingly to the melting temperature, Tm, of the primers used. The PCR product was analyzed on 1% agarose gel and purified using Gel Extraction Kit (QIAGEN) according to standard manufacturer's protocol.

2.2 Generation of DNA mutant insert for site-directed mutagenesis

Mutants were generated by employing the modified QuikChange™ Site-Directed Mutagenesis Kit (Stratagene) designed oligonucleotide primers (1st Base) with mismatches.

Primers were designed with mismatches base pairing being flanked on both 5' and 3' ends with about 9 to 15 bases each using the software GeneRunner. The list of mismatched primers for Blo t 21 could be seen in Table 2.1. The PCR using the high fidelity KOD Hot Start Pfu DNA Polymerase (Novagen) generated the whole plasmid consisting of mismatched bases. The methylated wild-type plasmids were digested by adding 1 µl of 1 U Dpn 1 Fast Digest^{TM} restriction enzyme at 37°C for 30 minutes. The mixture was subsequently purified using the spin columns (QIAGEN) followed by direct transformation into BL21 (DE3) competent cells. The list of primers used is shown in Table 2.1. PCR amplification was carried out with similar procedure as described in section 2.1.2 except that the elongation time was adjusted to 3 min. A flow chart of this method could be seen in Figure 2.1.

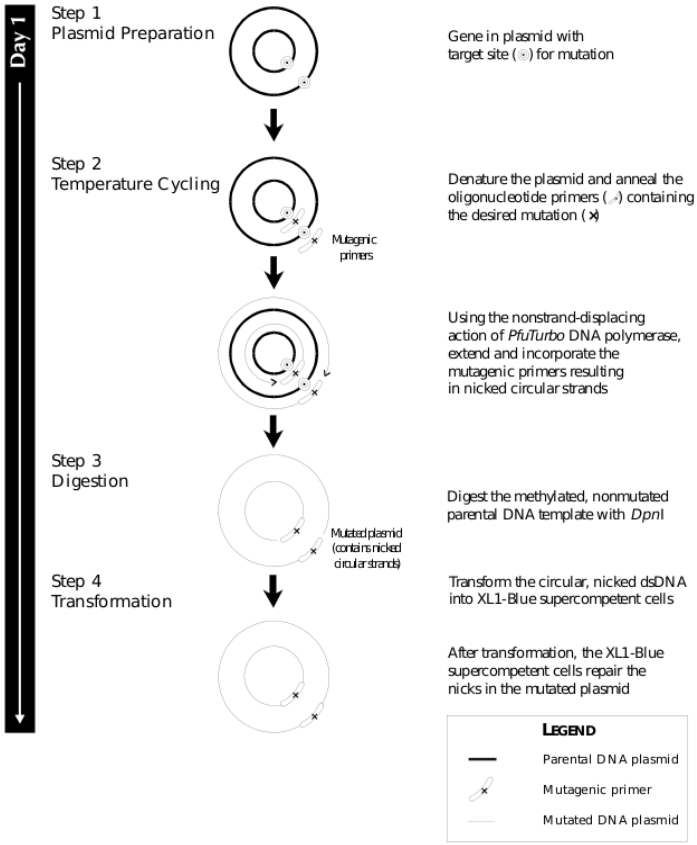

Figure 2.1 Generation of site-directed mutants. The high fidelity Hot Start KOD DNA Polymerase enabled the amplification of the DNA insert together with the vector. Dpn 1 restriction enzyme was used to digest the methylated unmutated parental DNA template. Finally, the nicked dsDNA was repaired in the BL21 (DE3) competent cells.

Blot21_E74A_up	5' TTC CAA CGG GCA CTC AAG CGA 3'
Blot21_E74A_down	5' TCG CTT GAG TGC CCG TTG GAA 3'
Blot21_K76A_down	5' CGG GAA CTC GCA CGA ACT GAT 3'
Blot21_K76A_down	5' ATC AGT TCG TGC GAG TTC CCG 3'
Blot21_D79A_up	5' AAG CGA ACT GCA TTG GAT TTG 3'
Blot21_D79A_down	5' CAA ATC CAA TGC AGT TCG CTT 3'
Blot21_E84A_up	5' GAT TTG CTC GCA AAA TTC AAC TTT G 3'
Blot21_E84A_down	5' C AAA GTT GAA TTT TGC GAG CAA ATC 3'
Blot21_R23A_up	5' GCT ACT CAA GCA TTC CAT GAG 3'
Blot21_R23A_down	5' CTC ATG GAA TGC TTG AGT AGC 3'
Blot21_E26A_up	5' CGA TTC CAT GCA ATT GAA AAA TTC TTG 3'
Blot21_E26A_down	5' CAA GAA TTT TTC AAT TGC ATG GAA TCG 5'
Blot21_E37A_up	5' G CAT ATT ACT CAT GCA GTT GAT GAT 3'
Blot21_E37A_down	5' ATC ATC AAC TGC ATG AGT AAT ATG C 3'
Blot21_E42A_up	5' GAT GAT TTG GCA AAA ACC GGC 3'
Blot21_E42A_down	5' GCC GGT TTT TGC CAA ATC ATC 3'
Blot21_K43A_up	5' GAT TTG GAA GCA ACC GGC AAC 3'
Blot21_K43A_down	5' GTT GCC GGT TGC TTC CAA ATC 3'
Blot21 _K47A_up	5' GGC AAC GCA GAT GAG AAG 3'
Blot21_K47A_down	5' CTT CTC ATC TGC GTT GCC GGT 3'
Blot21_D48A_up	5' GGC AAC AAA GCA GAG AAG GCA 3'
Blot21_D48A_down	5' TGC CTT CTC TGC TTT GTT GCC 3'
Blot21_E49A_up	5' GC AAC AAA GAT GCA AAG GCA CGA 3'
Blot21_E49A_down	5' TCG TGC CTT TGC ATC TTT GTT GC 3'
Blot21_K50A_up	5' C AAA GAT GAG GCA GCA CGA CTT 3'
Blot21_K50A_down	5' AAG TCG TGC TGC CTC ATC TTT G 3'
Blot21_E61A_up	5' ACC GTT TCT GCA GCT TTC ATC 3'
Blot21_E61A_down	5' GAT GAA AGC TGC AGA AAC GGT 3'
Blot21_R68A_up	5' GAA GGA TCA GCA GGA TAT TTC C 3'
Blot21_R68A_down	5' G GAA ATA TCC TGC TGA TCC TTC 3'
Blot21_D96A_up	5' GCA ACC GGT GCA TTG TTG TTG AAG3'
Blot21_D96A_down	5' CTT CAA CAA CAA TGC ACC GGT TGC 3'
Blot21_K107A_up	5' GCT CTC CAA GCA CGA GTC CAA 3'
Blot21_K107A_down	5' TTG GAC TCG TGC TTG GAG AGC 3'

Table 2.1 List of primers used for PCR and mutagenesis studies. Primers with mismatches on primers used to generate site-directed mutations to Ala residues were underlined.

2.3 Preparation of DH5-α competent cells

Frozen glycerol stock of DH5α was streaked onto plain LB agar plate and incubated overnight at 37 °C. A fresh single colony was inoculated into 8 ml of LB broth and incubated in a shaker overnight at 37 °C. 1 ml of overnight culture was transferred into 100 ml of LB broth and incubated in a shaker at 37 °C with shaking speed of 200 rpm. Cells were grown until $O.D_{600}$ reached 0.4 and then transferred into 50 ml tubes and spun at 3,500 rpm for 10 minutes at 4

°C. Supernatant was removed and cell pellets were resuspended gently with 40 ml of cold glycerol buffer (0.1 M $CaCl_2$, 15% glycerol) and then incubated on ice for 30 minutes. Cells were spun at 3,500 rpm for another 10 minutes at 4 °C and the supernatant was removed. The pellet was resuspended carefully in 4 ml of cold glycerol buffer and incubated on ice for 2 hours before aliquoted at 50 µl per tube and store at -80 °C.

2.4 Subcloning

For preparation of His-tagged proteins, DNA inserts were subcloned into pET-M, a modified pET-32a vector with S-tag and thioredoxin tag removed. For preparation of GST-tagged proteins, the inserts were subcloned into pGEX-4T-1 vector (Novagen). The DNA insert (about 50 ng/µl) was digested usingusing 10 U of BamH I Fast Digest ™ and EcoR 1 Fast Digest ™ (Fermentes) in total reaction volume of 20 µl. Two microliter of expression vector (about 50 ng/µl) was digested in a separate tube with another 10 U of the similar restriction enzyme in total reaction volume of 10 µl. Concentrated 10 X Fast Digest ™ buffer was added accordingly. Both tubes were incubated in 37°C water bath for 30 minutes.

The plasmid and DNA insert digestion mixtures were purified using the spin column (QIAGEN) after the incubation and the ligation of DNA insert and plasmid were done by adding 1 µl of 10 X T4 ligase buffer and 1 µl of T4 ligase enzyme (Fermentes). Ligation was carried out for 2 hour at room temperature before transformation into DH5-α competent cell (refer section 2.1.6 for details).

2.5 Transformation of ligation mix into DH5-α competent cells

Ligation reaction was added into 50 µl of DH5-α competent cells and kept on ice for 15 minutes. Heat shock transformation was carried out by incubating the cells at 42 °C for exactly 90 seconds, followed by 2 minutes incubation on ice. 950 µl of LB broth were added into the tubes before incubation at 37 °C in shaker for one hour. Cells were spun at 6,000 rpm

for 2 minutes and 950 µl of the supernatant were removed. Cell pellet was resuspended with the remaining medium and plated on LB agar plated supplemented with 0.1 mg/ml ampicillin. Plates were incubated for overnight in a 37 °C incubator.

2.6 PCR screening of transformant

The presence of DNA insert into target plasmid was verified by PCR screening of colonies grown on LB-ampicillin agar plate prior to sequencing. At least five colonies from each plate were selected for the screening. Half of a colony was picked using a sterile pipette tip and resuspended with 100 µl of sterile water in an eppendorf tube. The suspension was boiled for five minutes, and subsequently centrifuged at 13,000 rpm for a minute. One microliter of the supernatant could be used DNA template for PCR reaction.

A PCR reaction cocktail of volume 10 µl was prepared containing 1 X Taq reaction buffer (50 mM KCl, 10 mM Tris-Cl pH 9.0, 1% Triton X-100), 0.75 mM $MgCl_2$, 140 µM of each dATP, dCTP, dGTP and dCTP, 0.5 µM of each upstream primer and downstream primer; and 1.5 U of Taq DNA Polymerase (Promega). One microliter of DNA template was added into the mixture and 30 PCR cycles were carried out with 1 minute denaturation at 94 °C, 1 minute annealing at 52 °C and I minute elongation at 72 °C for each cycle. The PCR products were analyzed on a 1.5% agarose gel for detection of DNA fragment of the appropriate size.

2.7 Isolation of DNA plasmid

Colonies that showed positive PCR screening results were cultured overnight in LB broth supplemented with 100 µg/ml ampicillin in a 37 °C shaking incubator. Cell pellets from 5 ml of overnight culture were recovered by centrifugation at 6,000 rpm for 15 minutes. DNA plasmid was extracted from pelleted cells usingQIAGEN Miniprep Kit (QIAGEN) and eluted with 40 µl of water according to the supplied protocol.

2.8 Plasmid DNA sequencing

Two microliters of plasmid DNA containing about 250 ng of DNA was added with 3 µl of water, 1 µl of T7-promoter sequencing primer (3.2 µM), 2 µl of 5X Big Dye Buffer and 2 µl of Big Dye Terminator V3.1 (Applied Biosystems). Twenty-five cycles of PCR reaction were carried out with denaturation step at 96 °C for 30 seconds, annealing at 50 °C for 15 seconds and extension at 60 °C for 2 minutes. Following the sequencing cycle, a mixture of 3 µl of 3M sodium acetate, pH 4.6, 62.5 µl of 95 % ethanol and 24.5 µl of sterile water was added into each DNA samples for precipitation. After 15 minutes incubation at room temperature, the mixtures were spun at 13,000 rpm for 25 minutes at room temperature. Supernatant was removed, and the pellet was washed twice with 500 µl of 70% ethanol and centrifuged for another 5 minutes between each wash. Supernatant was carefully aspirated and sample was dried in a vacuum centrifuge before sequencing analysis on an automated sequencer, ABI PRISM 3100 (Applied Biosystems).

2.9 Protein expression and purification

2.9.1 Transformation of plasmid into BL21(DE3) competent cells

Plasmid containing DNA insert or mutants was transformed into E. coli BL21 (DE3) cells for the expression of recombinant protein. Transformation procedure was carried out as described in section 2.1.6. BL21 (DE3) competent cells were prepared as discussed in section 2.1.4.

2.9.2 Protein expression

A single colony of E. coli BL21 cells containing the desired plasmid was picked and cultured overnight in 10 ml of LB broth containing 100 µg/ml ampicillin. Ten milliliters of overnight culture were inoculated into 1 liter of fresh LB broth containing 0.1 mg/ml ampicillin. Cultures were grown at 37 °C in a shaker with shaking speed of 200 rpm for approximately 3 hours until the $O.D_{600}$ reached approximately 0.6. Subsequently, IPTG was added at final

concentration of 0.3 mM to induce protein expression. The culture was further grown at 37 °C overnight at 200 rpm before harvesting by centrifugation at 6,000 rpm for 15 minutes at 4 °C. Cell pellets were kept at -20 °C until ready for purification.

Expression of ^{15}N or ^{13}C-labeled protein were carried out with similar conditions as mentioned above, except that the cells were grown in M9 minimal medium (Appendix I) supplemented with ^{15}N-labeled ammonium chloride and/or ^{13}C-labeled glucose. To obtain ^{15}N-labeled sample, cells were grown in 1 X M9 minimal medium in the presence of ^{13}N-ammonium chloride (Cambridge Isotope Laboratories) as the sole nitrogen source. For double labeled ^{15}N and ^{13}C-sample, 1 X M9 minimal medium with ^{15}N-ammonium chloride and ^{13}C-glucose (Cambridge Isotope Laboratories) as the sole nitrogen and carbon source respectively was used.

2.9.3 Protein purification using nickel-affinity chromatography

Cells from 2 liters of culture were resuspended in 30 ml of nickel binding buffer (20 mM Tris-Cl pH 8, 0.5 M NaCl, 5 mM immidazole). The suspension was sonicated for 3 minute each with 38 % sonication amplitude. Sonication was carried out for 4 rounds, and the lysate was centrifuged at 4 °C for 30 minutes at 18,000 rpm. The supernatant was collected for purification. Ni-NTA beads (QIAGEN) were charged with 10 ml of Nickel-charge buffer (50 mM $NiSO_4$), washed with water and equilibrated with 1 X Nickel binding buffer in a chromatography column. All supernatant was slowly loaded into the column and let flow at approximately 1 ml/min. The column was subsequently washed 15 times with 1 X nickel washing (20 mM Tris-Cl pH 8, 0.5 M NaCl, 20 mM immidazole) buffer to remove unbound proteins. His-tagged protein was eluted with 20 ml of nickel elution buffer (20 mM Tris-Cl pH 8, 0.5 M NaCl and 500 mM immidazole). The eluted protein was dialyzed overnight against 50 mM Tris-Cl pH 8, 0.5 M NaCl and analyzed by SDS-PAGE.

2.9.4 Protein purification using glutathione-sepharose affinity chromatography

Cells from 2 liters of culture were resuspended in 30 ml of PBS (140 mM NaCl, 2.7 mM KCl, 10 mM Na_2HPO_4 and 1.8 mM KH_2PO_4, pH 7.4). The suspension was sonicated for 3 minute each with 38% sonication amplitude. Sonication was carried out for four rounds, and the sonication lysate was centrifuged for 30 minutes at 18,000 rpm and 4°C. The supernatant was collected for purification. All supernatant was slowly loaded into a column packed with 10 ml of glutathione-sepharose 4B beads (Amersham Biosciences) equilibrated with 1 X PBS. The column was subsequently washed 15 times with a total of 1 X PBS to remove unbound proteins. GST-tagged protein was eluted with 20 ml of glutathione elution buffer (50 mM Tris-Cl pH 8 and 10 mM reduced gluthathione) and analyzed by SDS-PAGE. Glutathione-sepharose beads were regenerated by washing the column twice with column regeneration buffer 1 & 2 (Appendix II).

2.9.5 Thrombin digestion

Fusion tags (His-tag and GST-tag) attached to the N-terminal of recombinant protein were removed by thrombin digestion. Digestion was carried out in 50 mM Tris-Cl pH 8. Thrombin was added at 2 U/mg of protein and cleavage was carried out for 5 hours at room temperature. Cleaved recombinant proteins were further purified by gel filtration (refer section 2.2.6.)

On column cleavage was carried out immediately after the washing procedure. The same procedure was implemented for both Ni-NTA and GST affinity columns. Thrombin was added at approximately 2 U/mg of protein into the columns and the mixtures were resuspended by placing the columns on the orbital shaker at room temperature for 5 hours. The cleaved recombinant proteins were eluted and immediately passed through the gel filtration column (refer section 2.2.6 for details).

2.9.6 Gel filtration FPLC (Fast Protein Liquid Chromatography)

Gel filtration FPLC was carried out in a HiLoad 16/60 Superdex 75 pg (Amersham Biosciences) size exclusion chromatography column on AKTA FPLC System (Amersham Biosciences) using 50 mM Tris-Cl pH 7.9 with 500 mM NaCl as running buffer. Gel filtration column was pre-equilibrated with at least three column volumes (180 ml) of running buffer before use. Protein sample was concentrated to about 5 ml prior to loading into the column. Chromatography was carried out with a flow rate of 1 ml/min and a total volume of 180 ml. Eluted protein peaks were detected by absorbance at 280 nm and the fractions were analyzed with SDS-PAGE.

2.10 Preparation of NMR sample

Purified protein was concentrated to about 1 mM using an ultra-filtration concentrator (Centriprep YM—3, Millipore) and was exchanged into 50 mM phosphate buffer, pH 7 with addition of 5% deuterium oxide (Cambridge Isotope Laboratories). Concentrated protein (0.8 mM) was centrifuged at 13,000 rpm and 4°C for at least 15 minutes before loading into a 5 mm NMR Shigemi tube.

2.11 Sodium dodecyl-sulphate-polyacrylamide gel electrophoresis (SDS-PAGE)

SDS-PAGE was carried out according to the method described by Laemmli (1970). SDS-PAGE gel was casted according to the table described in Appendix III using the Mini-PROTEAN 3 system (Bio-Rad). Protein sample was mixed with an equal volume of 2 X SDS sample buffer and boiled for 10 minutes. Fifteen microliters of sample was loaded into each wells, and electrophoresis was carried out at 200 V until the marker dye reached the end of the gel (~55 minutes).The gel was stained with Coomassie blue staining solution for about 20 minutes and then destained in destaining solution (Appendix III) for overnight.

2.12 Circular dichroism (CD) spectropolarimetry

Circular dichroism experiments were carried out with 15 μM protein in 1 X PBS buffer. The spectra were acquired with a J-810 Spectropolarimeter (Jasco, Japan) using a quartz cuvette with 1 mm pathlength (Hellma, Germany). The spectra were recorded at wavelength region from 190 nm to 260 nm with 0.1 nm resolutions with a scan speed of 50 nm/min and a response time of 8 seconds, averaged over 5 scans.

2.12.1 Thermal denaturation experiments

Temperature denaturation experiments were carried out for Blo t 21 by recording the molecular ellipticity at 222 nm at which the change was most drastic with the increment of temperature. Spectra were recorded at the temperature slope of 1˚C/min with a resolution of 0.1˚C over the range of 30˚C – 95˚C.

2.13 Sequence alignment

Amino acid sequence alignment was carried out using ClustalW (Higgins et al., 1994) software hosted at European Bioinformatics Institute server (EBI,http://www.ebi.ac.uk/Tools/). Amino acid sequences of all selected allergens from dust mites were acquired from GenBank (http://www.ncbi.nlm.nih.gov/) and Allergome database (www.allergome.com). Aligned amino acid residues were compared based on their distinctly different properties (charged residues/hydrophilic residues versus hydrophobic residues). The sequence of Blo t 21 was aligned with group 5 and group 21 allergens from different species of dust mites.

2.14 Nuclear magnetic resonance and structural determination

2.14.1 NMR chemical shift assignments

3D heteronuclear NMR experiments were carried out to assign the backbone and side-chain chemical shifts using a 2D ^{1}H-^{15}N HSQC as a reference spectrum. All NMR experiments were carried out on a Bruker AVANCE 800 MHz spectrometer equipped with a cryoprobe. Samples were loaded into a 5 mm Shigemi NMR tube and all experiments were carried out at 298K. All data acquired were processed using NMRPipe (Delaglio, Grzesiek et al. 1995) and viewed and analyzed using NMRDraw (Delaglio, Grzesiek et al. 1995) and SPARKY (Goddard and Kneller). Computational processing was carried out on Dell Precision 360 workstation and SGI Origin 300 server.

2.14.1.1 2D ^{1}H-^{15}N HSQC spectrum

2D ^{1}H-^{15}N HSQC spectrum was used as a reference for backbone chemical shifts assignments by other 3D triple resonance experiments. The spectrum was acquired with 1024 complex points over a spectral width of 8012.8 Hz on the amide proton dimension. In the ^{15}N dimension, 256 points were collected over 1774.3 Hz. Carrier frequencies for ^{1}H and ^{15}N were at 4.725 ppm and 117.0 ppm respectively.

2.14.1.2 HNCACB and CBCA(CO)NH

Backbone assignments were carried out by HNCACB and CBCA(CO)NH experiments. The CBCA(CO)NH experiment correlates both the Cα and Cβ chemical shift with the amide from the previous residue while HNCACB provides the intra-residue correlation of its own Cα and Cβ. These two experiments provided sufficient chemical shift information to complete the sequential assignments of all ^{15}N, HN, Cα and Cβ resonances.

In HNCACB (Wittekind and Mueller, 1993), resonances of ^{1}H and ^{15}N of each amide

group were correlated with Cα and Cβ of the same residue, while the Cα and Cβ from the preceding residue would also be observed in the same amide strip but usually weaker. In the acquired F1 dimension (^{1}H) of the experiment, 1024 points were collected over 8012.8 Hz spectral width. In the F2 dimension (^{15}N), 68 points were collected over 1368.7 Hz of spectral width while the F3 dimension (^{13}C) contained 104 points covering 7700 Hz spectral width or 61 ppm. The carrier frequencies for F1, F2 and F3 dimensions were at 4.725 ppm, 119.5 ppm and 43.0 ppm respectively. 3D CBCA(CO)NH experiment (Grzesiek, Vuister et al. 1993) was carried out similarly using the same data points and spectral widths as above, except that the F2 dimension (^{15}N) was recorded with 40 points.

2.14.1.3 C(CO)NH-TOCSY and H(CO)NH-TOCSY

Chemical shifts of all aliphatic ^{13}C were collected from C(CO)NH experiment (Grzesiek, Dobeli et al. 1992) that connected resonance of amide ^{1}H and ^{15}N with ^{13}C from preceding residue's side-chain. A total of 1024 complex points were recorded over a spectral width of 8012.8 Hz in the proton dimension (F1). In the amide ^{15}N dimension (F2), 40 data points were recorded with spectral width of 1368.7 Hz while 104 data points covering 7700 Hz were recorded for the ^{13}C dimension (F3). The carrier frequencies for F1, F2 and F3 dimensions were at 4.725 ppm, 118.83 ppm and 40.38 ppm respectively.

For H(CO)NH experiment (Montelione, Wuthrich et al. 1992), a total of 1024 complex points were recorded over a spectral width of 8012.8 Hz in the F1 proton dimension. In the amide ^{15}N dimension (F2), 40 data points were recorded with a spectral width of 1368.7 Hz while 90 data points covering 3000 Hz were recorded for the proton dimension (F3). Carrier frequencies for F1, F2 and F3 were at 4.725 ppm, 118.83 ppm and 4.725 ppm.

2.14.1.4 HCCH-TOCSY

3D HCCH-TOCSY experiment was utilized to identify side-chain spin system by connecting

aliphatic ^{1}H resonances with their attached ^{13}C resonances (Wang and Zuiderweg 1995). The protein sample used in this experiment was prepared by exchanging ^{13}C-labeled protein with deuterated phosphate buffer at pD 7 in 99.9% D2O. A total of 1024 complex points were collected for F1 dimension (^{1}H) over 8012.8 Hz spectral width, while F2 dimension (indirectly detected 1H dimension) consists of 90 points over 3000 Hz spectral width. F3 dimension (^{13}C) was recorded with 104 data points over 7700 Hz of spectral width. The carrier frequencies for F1, F2 and F3 were at 4.725 ppm, 3.147 ppm and 40.135 ppm respectively.

2.14.1.5 NOE distance restraints and hydrogen-bond restraints

2.14.1.5.1 Hydrogen-deuterium exchange measurement

Hydrogen bond restraints were determined by recording ^{1}H-^{15}N HSQC of ^{15}N-labeled protein exchanged into 100% deuterium oxide buffer using lyophilization technique. The HSQC spectrum was acquired similarly as described in section 2.14.1.1. Peaks that appeared on the spectrum are the amide protons involved in the hydrogen-bonding with carbonyl groups and thus used as hydrogen bond restraints.

2.14.1.5.2 ^{15}N-edited NOESY

Amide proton distance constraints were derived from 3D ^{15}N-edited Nuclear Overhauser Effect spectroscopy (NOESY) with 100 ms mixing time. Each cross-peak in a ^{15}N-NOESY amide strip represents a NOE between amide protons to a nearby proton within around 5 Å distance. 1024 complex points were recorded for the F1 dimension corresponding to the directly detected ^{1}H dimension over spectral width of 8012.8 Hz. For F2 dimension detecting the ^{15}N, 60 complex points were detected over spectral width of 1650 Hz, while 256 complex points were recorded for spectral width of 5500 Hz for F3 dimension (^{1}H). Carrier frequencies for F1, F2 and F3 were at 4.725 ppm, 118.19 ppm and 4.725 ppm respectively.

2.14.1.5.3 ^{13}C-edited NOESY

^{13}C-edited NOESY was recorded using ^{13}C labeled protein in buffer containing 99.9% D_2O with a mixing time of 100 ms. In ^{13}C-NOESY, each cross-peaks represents the NOE between a nearby proton to the particular proton attached to backbone and side-chain ^{13} C. A total of 1024 complex points were recorded for the F1 dimension corresponding to the directly detected 1H dimension over spectral width of 8012.8 Hz. F2 dimension detecting the ^{13}C was recorded with 128 complex points over spectral width of 7000 Hz, while 256 complex points were recorded for spectral width of 4500 Hz for F3 dimension (^{1}H). Carrier frequencies for F1, F2 and F3 were at 4.010 ppm, 47.56 ppm and 4.010 ppm respectively.

2.15 NOE assignments and structure calculation

Some of the NOEs were unambiguously assigned based on the secondary structure information derived from Chemical Shift Index (CSI) obtained using the Cα and Cβ chemical shifts deviation from the random coil values. NOEs from ^{15}N-edited NOESY were particularly useful to identify NOEs between NH-NH and between NH-Hα. For α-helical type secondary structure, strong NOEs could be observed between $NH_{(i+4)}$-$H\alpha_{(i)}$, and $NH_{(i+3)}$-$H\alpha_{(i)}$ and these NOEs were not normally observed in β- strands. For β-strands, strong NOEs were often observed between $H\alpha_{(i)}$-$NH_{(i+1)}$ as well as between amide protons from opposite β-strands that formed β-sheets. These unique NOEs could be used to unambiguously assign most of the NOEs connecting the backbone protons.

Unambiguously assigned NOEs were used to generate initial random structures in CNS (Crystallographic/NMR Refinement Software) version 1.1 developed by Brunger *et al.* (1998) to assist in the manual assignment of the remaining ^{15}N-edited and ^{13}C-edited NOE restraints which were divided into three groups corresponding to the upper-limit distance restraints of 2.9 Å (strong), 3.5 Å (medium) and 5.0 Å (weak). Dihedral angles predicted using the TALOS program (Cornilescu, Delaglio et al. 1999) were included as input data during the structural calculation. The simulated annealing protocols were set at 2000 steps for

the high-temperate annealing stage followed by 5000 steps of cooling stage using torsion angle dynamics. The energy minimization and violated constraints were analyzed and refined using CNS software. An ensemble of 100 structures was generated with which 20 lowest-energy conformers were selected to represent the final 3D-fold of Blo t 21. The quality of the final structure ensemble was validated with PROCHECK (Laskowski, Rullmannn et al. 1996).

2.16 Immunoassay of Blo t 21

2.16.1 Specific IgE binding ELISA experiment

For ELISA experiments, all proteins used were GST-tag fusion proteins for maximum binding on ELISA plate. The volumes of all reagents and sera used in ELISA experiments were at 100 µl per well. Sera from patients were diluted at least 1:10 with PBS and pre-absorbed with 5 mg/ml of GST protein overnight at 4°C. Wild-type Blo t 21 or mutants were coated overnight at 4°C onto Maxisorp ELISA plate (NUNC) at 1 µg protein per well. Plates were washed with PBS-T (PBS, 0.05% Tween 20) and blocked with PBS-1% BSA for half an hour at room temperature. The plates were washed with PBS-T and incubated with pre-absorbed sera for 4 hours at room temperature. This was followed with three washes with PBS-T. Biotin conjugated anti-human IgE monoclonal antibody (BD Pharmingen) diluted 1:250 in PBS-0.05% Tween 20 was added and incubated for another 2 hours. After washing with PBS-T, avidin conjugated HRP (BD Pharmingen) diluted 1:1000 in PBS-0.05%, Tween 20 was added and incubated for half an hour. The plates were then thoroughly washed with PBS-T and then 100 µl of TMB substrate (Sigma Aldrich) was added. The color reaction was detected through absorbance measurements at 655 nm using an ELISA plate reader. All experiments were carried out in duplicates and results were reported as mean values with standard deviations.

2.16.2 End-point inhibition ELISA experiment

In a 100 µl reaction volume, 1 µg of GST-tagged protein was coated onto Maxisorp ELISA

plate (NUNC) overnight at 4°C. Sera were pre-absorbed with 5 mg/ml of GST protein and a single concentration (100 μg) of GST-tagged protein (inhibitors). After overnight incubation at 4˚C, plates were washed with PBS-T and blocked with 4% of full skimmed milk in PBS-0.1% Tween 20 for 30 minutes at room temperature. The plates were washed again with PBS-T and incubated with sera pre-absorbed with GST-tagged protein (inhibitors) for 2.5 hours at room temperature. Subsequent antibodies incubation and colorimetric development were performed as described in section 2.4.1. Results were presented as mean values from duplicates with standard deviations.

2.16.3 Peptide ELISA experiment

All peptides were conjugated with biotin at N-terminal separated by a Acp (Aminohexanoic acid) linker (GL Biochem, Shanghai). The volumes of all reagents and sera used in ELISA experiments were at 100 μl per well. Sera from patients were diluted at least 1:10 with PBS. Wild-type Blo t 21 or mutants were coated 24 hours at 4°C onto Streptavidin coated ELISA plates (NUNC) at 1 μg peptide per well. Plates were washed with PBS-T (PBS, 0.05% Tween 20) and blocked with PBS-1% BSA for one hour at room temperature. The plates were washed with PBS-T and incubated with sera for 48 hours at 4°C. Following by washing 3 times with PBS-T, alkaline phophatase conjugated anti-human IgE monoclonal antibody (BD Pharmingen) diluted 1:250 in PBS-1% Tween 20 was added and incubated for 6 hours at room temperature. The plates were then thoroughly washed with PBS-T and then 100 μl of PnPP substrate (Sigma Aldrich) was added. The color reaction was detected through absorbance measurements at 405 nm using an ELISA plate reader. All experiments were carried out in duplicates and results were reported as mean values with standard deviations.

2.17 Sub-cloning, expression and purification of Der f 7

Using specific primers 5’-CGGAATTCGATCCAATTCACTAT-3’ (Derf7_forward) and 5’-

ATTTTTTTCCAATTCAAGCTTCG-3' (Derf7_reverse), DNA coding for Der f 7 (from residues Asp18 to Asn 213) was amplified by PCR. The first 17 residues of Der f 7 were predicted to be the signal peptide by the SignalP 4.0 server (http://www.cbs.dtu.uk/services/SignalP/)(Petersen, Brunak et al. 2011). The DNA fragment was subcloned between the EcoR I and Hind III restriction endonuclease sites of a modified pET-32a plasmid vector with the S-tag and thioredoxin tag removed and the last two residues of the thrombin cleavage site modified to merge with the BamH I site.

The correct sequence of the DNA insert was confirmed by sequencing before the plasmid was transformed into BL21 (DE3) competent cells for protein expression. Ten milliliter of overnight seed culture was inoculated into 1 liter of Luria Bertani broth (with 0.1 mg/ml ampicillin) and was grown at 37 °C until the OD_{600} reached 0.6. The protein expression was induced with 0.3 mM IPTG and continued to grow a 20 °C overnight. Cell suspension was then harvested by centrifugation (4,000 rpm; 30 min, 4 °C) and resuspended in 30 ml of Ni-binding buffer (20 mM Tris-HCl, pH 8, 5 mM immidazole and 0.5 M NaCl). The cells were lysed by sonication at the amplitude of 38% for 3 minutes (1 second pulse on and 0.1 second pulse off) followed by centrifugation at 18,000 rpm at 4 °C for 30 minutes. The supernatant was then loaded into the Ni-NTA affinity column and let bind for 1 hour at 4 °C. After vigorous washing with 500 ml of washing buffer (20 mM Tris-HCl pH 8, 30 mM immidazole and 0.5 M NaCl), the protein was eluted slowly using 20 ml of elution buffer (20 mM Tris-HCl pH 8, 0.5 M immidazole and 0.5 M NaCl). Subsequently, the protein was dialyzed against buffer containing 50 mM Tris-HCl pH 8 and 0.5 M NaCl at 4 °C for at least 16 hours. The overnight thrombin cleavage was carried out by adding 2U protease/mg of protein at room temperature after the dialysis. The recombinant Der f 7 without His-tag was then passed through a Superdex-200 gel filtration column using the similar buffer used for overnight dialysis. L-selenoMet (SeMet) labeled Der f 7 was expressed using the same bacteria strain grown in M9 minimal medium, in which 25 mg/L of SeMet was added when the OD_{600} reached 0.6. Similar purification protocol for native recombinant Der f 7 was

implemented for the SeMet labeled Der f 7.

2.18 Circular dichroism (CD) spectropolarimetry of Der f 7

Circular dichroism experiments were carried out with 15 μM protein (Der f 7 and Der p 7) in 50 mM Tris-HCl at diffrent pH (pH 4, pH 7 and pH 9). The spectra were acquired with a J-810 Spectropolarimeter (Jasco, Japan) using a quartz cuvette with 1 mm pathlength (Hellma, Germany). The spectra were recorded at wavelength region from 190 nm to 260 nm with 0.1 nm resolutions using a scan speed of 50 nm/min and a response time of 8 seconds, and were averaged over 10 scans.

2.18.1 Thermal denaturation experiments

Thermal denaturation experiments were carried out for Der f 7 and Der p 7 by recording the molecular ellipticity at 220 nm at which the change was most drastic with the increment of temperature. Spectra were recorded at the temperature slope of 1˚C/min with the resolution of 0.1˚C over the range of 55˚C – 95˚C.

2.18.2 Chemical denaturation experiments

Urea-induced denturation was monitored at 220 nm at which the change was most drastic with the increment of urea concentration (M). Each spectrum was represented by and average 10 scans, with the scan rate of 50 nm/min. The transition curve was plotted with the change of molecular ellipticity at 220 nm against urea concentration and subsequently analyzed by a two-state mechanism.

2.19 NMR studies of Der f 7

2.19.1 NMR chemical shift assignments

3D heteronuclear NMR experiments were carried out to assign the backboneand side-chain chemical shifts using a 2D ^{1}H-^{15}N HSQC as a reference spectrum. All NMR experiments were carried out on a Bruker AVANCE 800 MHz spectrometer equipped with a cryoprobe. Samples were loaded into a 5 mm NMR tube and all experiments were carried out at 313K. All data acquired were processed using NMRPipe (Delaglio, Grzesiek et al. 1995) and viewed and analyzed using NMRDraw (Delaglio, Grzesiek et al. 1995) and SPARKY (Goddard and Kneller). Computational processing was carried out on Dell Precision 360 workstation and SGI Origin 300 server.

2.19.2 2D ^{1}H-^{15}N HSQC spectrum

2D ^{1}H-^{15}N HSQC spectrum was used as a reference for backbone chemical shifts assignments by other 3D triple resonance experiments. The spectrum was acquired with 1280 complex points over a spectral width of 11160.7 Hz on the amide proton dimension. In the ^{15}N dimension, 128 points were collected over 1865 Hz. Carrier frequencies for ^{1}H and ^{15}N were at 4.7 ppm and 117.5 ppm respectively.

2.19.2.1 HNCACB and CBCA(CO)NH

Backbone assignments were carried out using HNCACB and CBCA(CO)NH experiments as described earlier in section 2.3.1.2. In the acquired F1 dimension (^{1}H) of the experiment, 1280 points were collected over 11160.7 Hz spectral widths. In the F2 dimension (^{15}N), 92 points were collected over 1865 Hz of spectral width while the F3 dimension (^{13}C) contained 116 points covering 12072.4 Hz spectral width. The carrier frequencies for F1, F2 and F3 dimensions were at 4.7 ppm, 118.5 ppm and 41.7 ppm respectively. 3D CBCA(CO)NH

experiment (Grzesiek, Vuister et al. 1993) was carried out similarly using the same data points and spectral widths as above, except that the F2 dimension (^{15}N) was recorded with 40 points.

2.19.3 Ligand binding and pH titration studies of Der f 7

For ligand binding studies, the highly purified Der f 7 was dialyzed into 50 mM Tris buffer at pH7 and concentrated to 0.5 mM. 2D $^{1}H^{15}N$-HSQC spectrums were acquired at 4 scans using similar parameters as described in section 2.19.2 with and without addition of polymyxin B (PB) at 1:1 dilution. For pH titration studies, the ^{15}N-labeled Der f 7 was prepared in 50 mM Tris pH 7 at 0.25 mM protein concentration. The 2D $^{1}H^{15}N$-HSQC spectrum was acquired similarly as described. Subsequently, the pH was adjusted using 0.1M NaOH solution, with the pH increased by approximately 0.5 for each titration until the final pH reached 9. Peaks perturbation during the pH change from 7 to 9 were estimated using the formula: $\sqrt{(\Delta H)^2+(\Delta N*0.17)^2}$ and plotted against residue numbers.

2.19.4 ^{15}N relaxation studies of Der f 7

The steady-state heteronuclear ^{1}H-^{15}N NOE experiment was carried out in an interleaved manner, with and without proton saturation (NOE_{on}, NOE_{off}). The NOE effect was calculated as an error weighed average ratio of the peak intensities, with an error estimate obtained by propagating the base-plane noise.

2.20 Crystallization of Der f 7

The highly purified protein was dialyzed into 10 mM HEPES pH 7 and concentrated to 8 mg/ml with an Amicon filter (Milipore, 10-kDa molecular weight cut-off) before crystallization. Crystallization screening for the native Der f 7 was carried out using Index Screens (Hampton Research) employing the hanging-drop vapor-diffusion technique at 298 K

with 1 µl protein solution (8 mg/ml) and 1 µl reservoir solution. The initial crystal was obtained after ~24 hours from the reservoir solution containing 0.1 M Bis-Tris pH 7 and 28% Polyethylene glycol monomethyl ether (PEG MME) 2000. The crystallization was further optimized by varying the pH of the reservoir buffer, the concentration of the protein as well as the crystallizing temperature. Preliminary diffraction data using the native Der f 7 crystal were collected with an in-house X-ray machine (Bruker MICROSTAR X-ray generator and PLATINUM135 CCD detector) for screening of the best conditions for crystallization.

Crystallization of the SeMet was optimized based on the conditions used for crystallization of the native Der f 7. The best diffracting crystals of recombinant Der f 7 were grown from a reservoir solution consisting of 0.1 M Bis-Tris pH 7.4 and 28% PEG MME 2000 at 293 K. The SeMet crystal was selected for diffraction data collection using the synchrotron light source.

2.21 Data collection and structure solution of SeMet Der f 7

The best crystal of SeMet labeled Der f 7 was picked up in a clean nylon loop and flash-cooled at 100 K in a nitrogen-gas stream without adding any cryoprotectant solution. Synchrotron data were collected at BL-13B beamline, NSRRC - National Synchrotron Radiation Research Center, Taiwan (NSRRC) Taiwan. X-ray fluorescence spectra recorded for the crystals of SeMet Der f 7 near the Se absorption edge were analyzed with the program *CHOOCH*. Subsequent data set processing was done using the *HKL*-2000 program suite. Structure was solved by molecular replacement technique using PHASER program from the CCP4 suite (McCoy, Grosse-Kunstleve et al. 2007). Der p 7 (PDB code 3H4Z, sequence identity = 86%) was used as the search model. Model building was performed using the COOT program (Emsley and Cowtan 2004) and refinement was carried out using PHENIX (Zwart, Afonine et al. 2008).

2.22 Structure-based alignment and comparison

Class Architecture Topology Homology (CATH) server (http://cathwww.biochem.ucl.ac.uk) developed by Pearl and coworkers was employed for pairwise sequence-based alignment (Pearl, Todd et al. 2005). For multiple 3D structure-based comparison, the DALI program was used (http://www.ebi.ac.uk/dali) (Holm and Sander 1998).

2.23 Immunoassay for Der f 7 and Der p 7

All immunoassays were done using the similar protocol as described in section 2.4.1 and 2.4.2, except that Ni-NTA HisSorb™ ELISA plates (QIAGEN) were used instead of Maxisorp™ plates (NUNC). All proteins were His-tagged and prepared in 1 X PBS buffer. Results were presented as mean values calculated from duplicates with standard deviations.

CHAPTER 3 BLOT21: RESULTS & DISCUSSION

3.1 Resolving Blo t 21 Structure using NMR

3.1.2 2D ^{1}H-^{15}N HSQC spectra of Blo t 21

The two-dimensional (2D) ^{1}H-^{15}N HSQC spectrum showed a good dispersion of amide peaks with most of them having similar intensities (Figure 3.1). We counted ninety four amide peaks out of the predicted ninety six, residues Thr-19 and His-25 (second and eight residues in the modified construct) were missing in the 2D ^{1}H-^{15}N HSQC spectrum. It was later revealed that these residues were actually located near the N-terminus (Thr-19) and the small turn between Arg-23 and Glu-26 (His-25). We were able to locate these residues in other 3D spectrums (CC(CO)NH, HC(CO)NH and ^{15}N-edited NOESY) and included them in the final structure calculation. Five peaks were particularly weak in the HSQC spectrum, i.e. residues Asn-18, Ala 20, Gln-22, Arg-23 and Thr-78. The first four residues were located in the N-terminus region while residue Thr-78 was located in the flexible loop between helices α2 and α3 of the protein. Overall, the overlapping of peaks was minimal in the 2D ^{1}H-^{15}N HSQC, and the overlapped peaks could be easily resolved during assignment of the backbone chemical shifts.

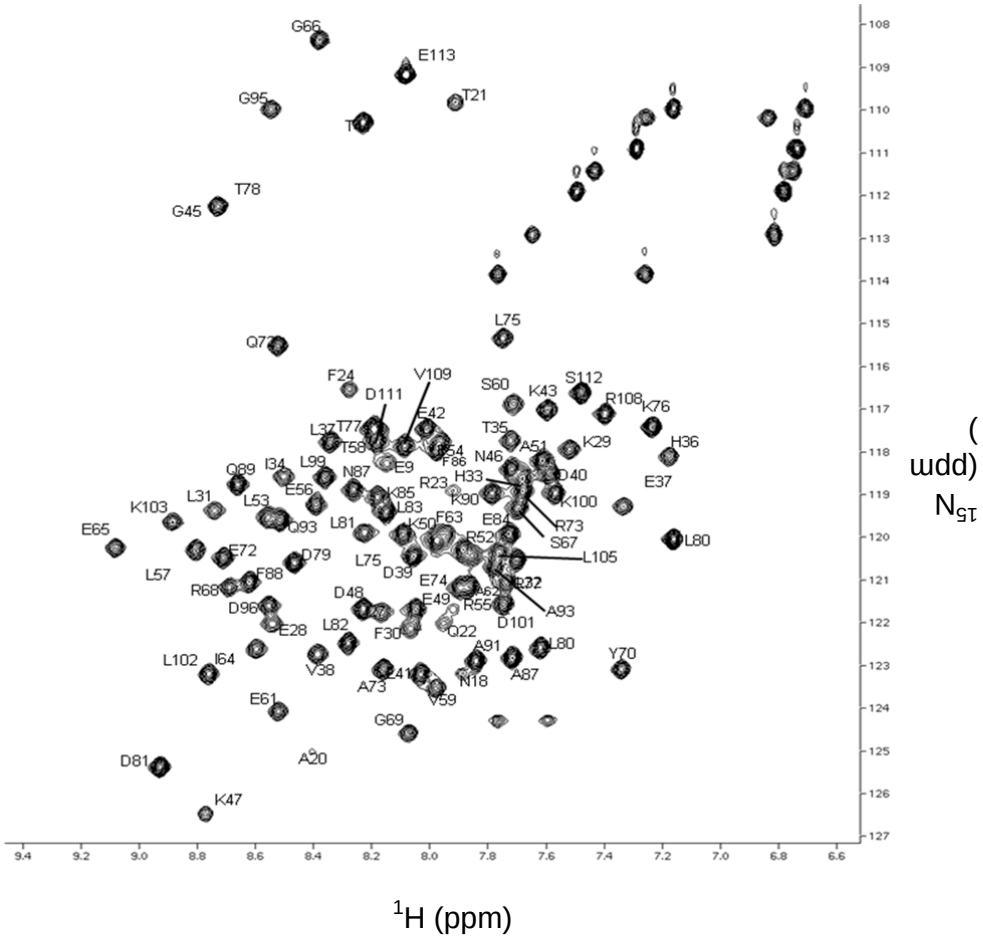

Figure 3.1 Two Dimensional ^{1}H-^{15}N HSQC of Blo t 21. 98% amide cross-peaks of Blo t 21 in the 2D ^{1}H-^{15}N HSQC spectrum were well resolved and have been successfully assigned sequentially. Each peaks represents an amino acid and labeled using the single letter code in sequential order according to the protein sequence.

3.2 Sequence-specific assignment of Blo t 21

3.2.1 Backbone and side-chain assignments

Backbone chemical shifts were assigned using HNCACB and CBCA(CO)NH triple resonance experiments. First, we correlated all the amide peaks with the Cα and Cβ resonances of the same residue using the HNCACB spectrum (Figure 3.2A). Next, CBCA(CO)NH spectrum was used to correlate the amide peaks with the Cα and Cβ of the preceding residue (Figure 3.2B). The amide peaks were then linked together based on the chemical shifts of Cα and Cβ in both spectrum and then fitted into the sequence of Blo t 21

aided by the signature Cα and Cβ chemical shifts values of certain amino acids. For example, Ser and Thr residues have unique Cβ chemical shifts values that are higher than their Cα. In the HNCACB spectrum, Cβ of Ser and Thr cross-peaks are represented as a negative peak, thus, they can be easily identified in the amide strips. Another typical residue used for initial fitting is Ala, owing to its unique Cβ chemical shift values thatusually appeared at ≤20 ppm, much lower than other residues. Finally, Gly residues were also particularly helpful as there was only a Cα cross peak appearing in the HNCACB spectrum.

The backbone amide peaks of Blo t 21 were successfully assigned based on the information provided by the aforementioned experiments as well as the knowledge of the protein sequence. The sequential assignment of the amide peaks in the 2D ^{1}H-^{15}N HSQC was shown in Figure 3.2. The strip plots generated with SPARKY software during the sequential assignment for the backbone amide peaks. Figure 3.2 showed an example of the sequential assignment displayed in the strip plots from residues Leu-41 to Arg-50 in Blo t 21. The Cα and Cβ chemical shift values were assigned for all residues accountable in the 2D ^{1}H-^{15}N HSQC. The assignment for the remaining chemical shifts for side-chain carbon was done using the CC(CO)NH experiment (data not shown).

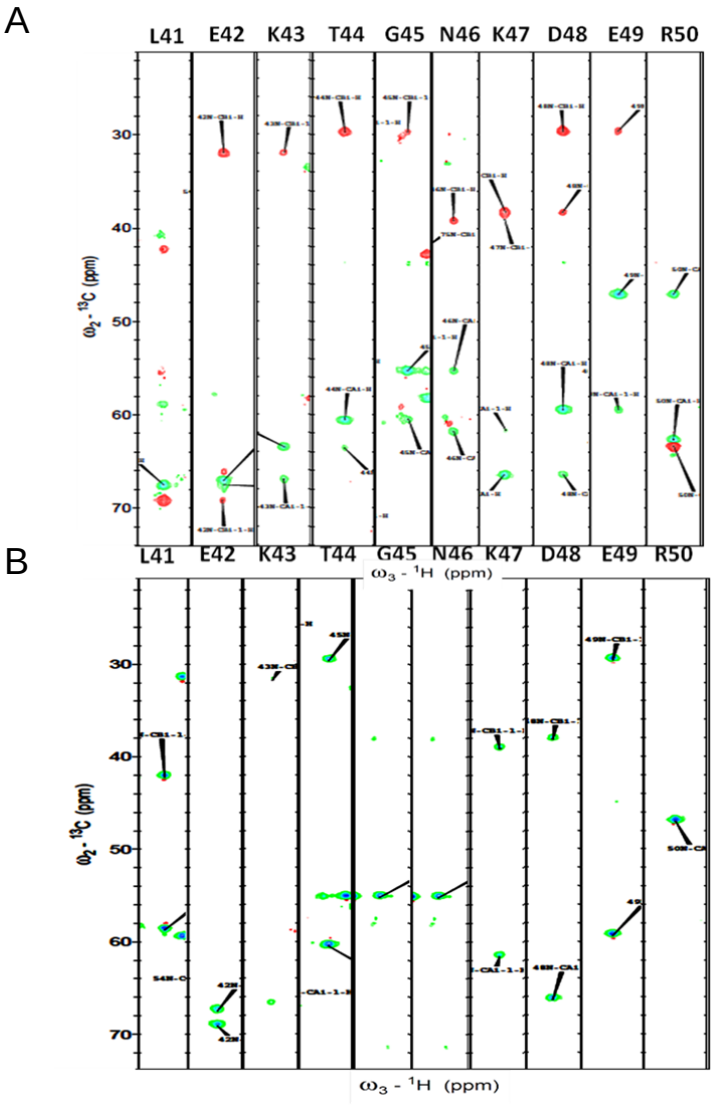

Figure 3.2 Sequential assignment of backbone chemical shifts of Blo t 21. **A)** Strip plots of HNCACB experiment, showing amide strips with Cα and Cβ resonances of the same residue from residues Leu-41 to Arg-50. Negative peaks correlated to Cβ resonances were displayed in red. **B)** CBCA(CO)NH experiment showing amide strips correlating Cα and Cβ resonances of the preceding residue.

In CC(CO)NH experiment, each amide strip correlateed the amide of a residue with all the aliphatic side-chain carbon chemical shifts of the preceding residue. The completeness of the backbone amide, Cα and Cβ chemical shifts assignment for all residues enabled the assignment of the remaining side-chain chemical shifts to be done easily based on the statistically calculated chemical shift values available in the Biological Magnetic Resonence Data Bank (BMRB). This experiment also provided additional information to allow cross-

checking of the sequential assignment for backbone amide. For example, the Cδ chemical shift of Ile and Leu residues usually appears at below 14 ppm; and Thr residue has a Cγ chemical shift which appears at around 20 ppm, distinguishing it from the Ser residue. For side-chain proton chemical shifts assignment, H(CCO)NH experiment was primarily used as it can correlate the amide peak with protons from the preceding residue. Additionally, HCCH-TOCSY experiment was also used to observe the linkage between side-chain carbons to its proton.

3.2.2 Chemical shift index (CSI)

Chemical Shift Index (CSI) employs the chemical shift values of all Cα and Cβ to determine the secondary structure of the protein and their boundaries (Wishart and Sykes, 1994). The deviation of the experimental Cα and Cβ chemical shift values against the random coil values for each specific type of amino acid was calculated based on following formula:

$$\mathbf{CSI = (C\alpha - C\alpha_{RC}) - (C\beta - C\beta_{RC})}$$

Cα = experimental chemical shifts of C-alpha
Cβ = experimental chemical shifts of C-beta
$C\alpha_{RC}$ = standard random coil chemical shift values of C-alpha of the same residue
$C\beta_{RC}$ = standard random coil chemical shift values of C-beta of the same residue

The CSI for each amino acid residues was plotted against the residue numbers in a bar chart. In a typical CSI plot, a positive value represents α-helix secondary structure while a negative value would represent a β-strand region (Wishart, Sykes et al. 1992).

The CSI plot for Blo t 21 is shown in Figure 3.3. Based on the definition of the CSI value as described, Blo t 21 comprised of three α-helices probably connected by two tight turns or loops. The presence of three α-helical secondary structures agreed with the solved structures of the paralogous group 5 allergens, i.e. Blo t 5 (Naik, Chang et al. 2008) and Der p 5 (Mueller et al. 2010), which adopted a triple helical bundle tertiary structure. Based on the

amino acid sequence identity (>31%), Blo t 21 could be sharing the similar folding topology with these proteins.

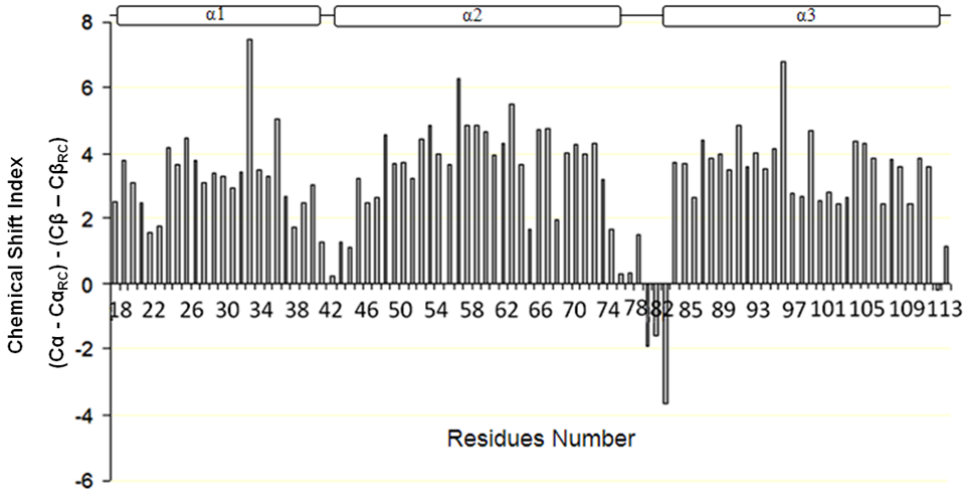

Figure 3.3 Chemical Shift Index of Blo t 21 generated using the chemical shift values of all Cα and Cβ extracted from the triple resonance experiments. The overall plot indicates that at least three α-helices are present in Blo t 21.

3.2.3 NOE assignment by CNS

The NOE assignment of Blo t 21 was completed manually using CNS (Crystallography/ NMR System) developed by Brunger et al (1998). For the initial structure calculation, only the unambiguously assigned NOEs were included, with a majority of short and medium range NOEs, as well as a few long-range NOEs. The long-range NOEs could be identified in both ^{15}N-edited and ^{13}C-edited NOESY as well as the 2D-NOESY spectrums. The ^{15}N-edited NOESY provided the spatial connectivity among the side-chain protons and the backbone amides while the side-chain-to-side-chain protons' connectivity was identified in the ^{13}C-edited NOESY experiments. The 2D-NOESY experiment (using 100% deuterated NMR buffer) was especially useful in identifying the long-range NOEs between the aromatic amino acid residues (six Phe and one Tyr residues were present in Blo t 21) and other spatially connected residues (Figure 3.4A). Interestingly, only one Phe and Tyr residues were present in

Blo t 5. The substitution of Phe residues in Blo t 21 may influence its overall folding as Phe amino acid was known to form important hydrophobic interactions within the core of a protein (Vondrasek, Bendova et al. 2005; Berka, Hobza et al. 2009). Based on the CSI plot as well as the circular dichroism experiments, Blo t 21 should contain predominantly α-helical secondary structure. Therefore, the typical NOE pattern for α-helical structure, i.e. $d_{\alpha N(i, i+3)}$ and $d_{\alpha\beta(i+3)}$ were unambiguously assigned and used for the structural calculation. The initial structure of Blo t 21 that was calculated using the unambiguously assigned NOEs was used as a reference to assist in further assignment of the remaining NOE cross-peaks.

The statistics of the final NMR structure of Blo t 21 are shown in Table 3.1. A total of 1729 NOEs was included for the structure calculation using CNS. Most of the NOEs assigned were intra-residue NOEs and sequential NOEs; about 216 NOEs were belonged to long-range NOEs. Few long-range NOEs were expected as Blo t 21 assumed a relatively simple triple α-helical bundle tertiary structure. We used the CSI plot to aid in identifying the residues that were involved in forming the α-helical secondary structure. For instance, residue His-36 should be located in the α-helical region, and based on the ^{15}N-edited NOESY spectrum, its amide proton shows a typical α-helical NOE cross-peaks pattern, i.e. NH-NH NOEs were observed from residues Thr-35, Glu-37 and Val-38, as well as several other NOEs between NH of His-36 and Hα, Hβ from Thr-35. Some weak NOEs from the Hγ of residues Leu-32, Thr-35 and Glu-37 could be observed as well. The distance constraints were manually included for the structure calculation depends on the intensities of the NOE peaks observed in the NOESY spectra. In the example presented, the NOEs from Thr-35 and Glu-37 amides were considered “strong” while the NOE from residue Val-38 was considered “weak”. All ambiguous protons were considered as pseudo-atoms and labeled with “#” since there was no stereo-specific assignment (Figure 3.4B).

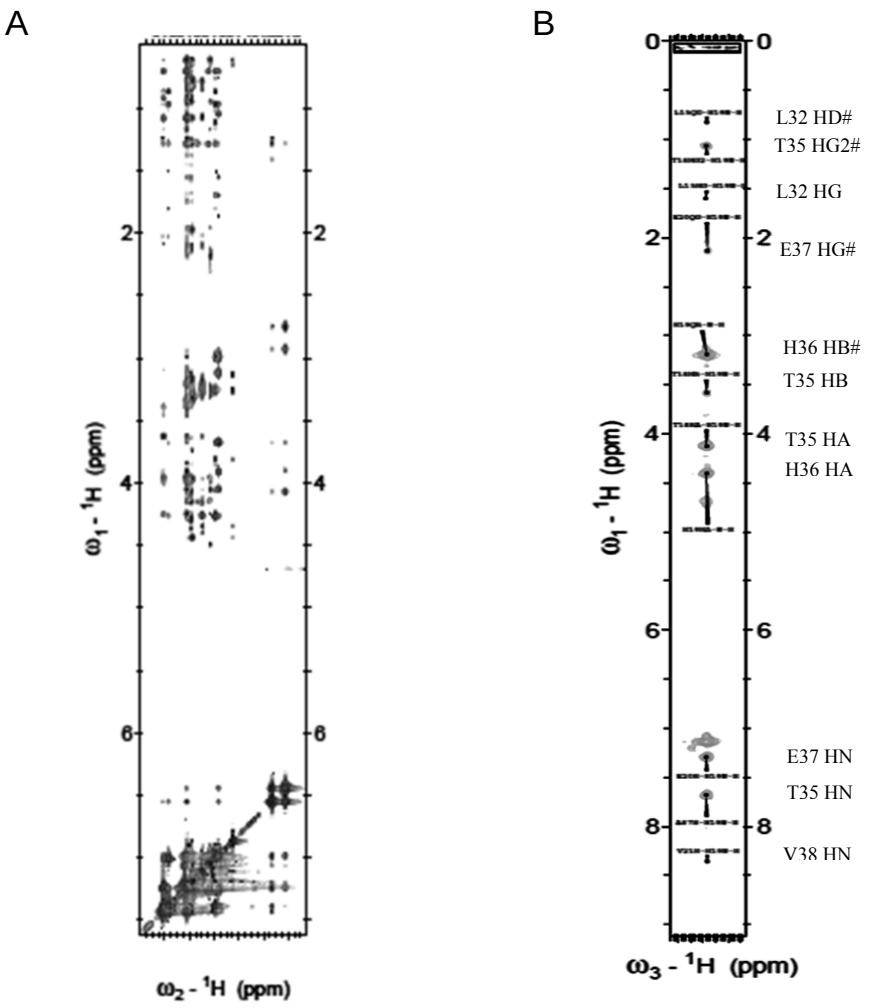

Figure 3.4 Assignment of NOESY spectrums. A) showed aromatic strips from 2D-NOESY spectrum acquired using deuterated NMR buffer. **B)** showed amide strips from ^{15}N-NOESY. Residue His-36 is shown as a representative for residues in α-helix.

3.3 NMR Structure of Blo t 21

The cDNA of Blo t 21 was modified by removing the N-terminus signal peptide (sixteen hydrophobic residues) and an additional seventeen amino acid residues based on the sequence alignment with Blo t 5. The 3D structure of Blo t 5 showed that this region (Leu-1 – Val-17) is unstructured and significant improvement of the 2D ^{1}H^{15}N-HSQC spectra could be achieved by excluding it from the construct of Blo t 21. Similar removal of the N-terminus flexible region based on sequence alignment was conducted on Der p 5 (PDB: 3MQ1), another group 5 allergen isolated from dust mite *D. pteronysinnus*, before the crystallization.

It was also shown that the exclusion of this flexible region did not affect the IgE binding (Mueller, Edwards et al. 2010). The NMR sample of Blo t 21 was prepared as mentioned in the previous chapter and did not show visible precipitation and degradation within 48 hours. Multiple additional peaks were observed in the 2D ^{1}H-^{15}N HSQC indicated that Blo t 21 started to degrade after 48 hours. Therefore, fresh samples were prepared for subsequent experiments to ensure the accuracy of the data collected.

The 3D structure of Blo t 21 was determined by employing the angle and distance restraints derived from a series of heteronuclear multidimensional NMR experiments as described in chapter 2. About 98% of the backbone amides and 97% of the nonlabile and non-aromatic protons were successfully assigned. A total of 1729 NOE restraints and 171 TALOS angle restraints were used to calculate the 3D structure of Blo t 21 using the CNS software. More detailed statistics of the solution structure can be seen in Table 3.1. The final structure wass represented as a 20 lowest-energy CNS conformer with backbone and all R.M.S.D of 0.82 +/- 0.22 Å and 1.61 +/- 0.17 Å respectively (Figure 3.5A). Overall, the 3D structure of Blo t 21 consists of three α-helices aligned in an antiparallel, *clockwise* manner, forming an elongated helical bundle. Individual helices are composed of residues Thr 19 - Thr 44 (α1), Glu 49 – Glu-74 (α2) and Leu 82 - Asp 111 (α3), respectively, connected by two tight turns, encompassing residues Gly 45 – Asp 48 (L1) and Leu 75 – Asp-81 (L2) (Figure 3.5C). Additionally, there is a short “kink” observed in the N-terminus helices, between residues Arg-23 and Glu-26. This peculiar structure was further validated by re-examination of the NOESY spectrum, in which no NOE pattern suggesting the formation of α-helical secondary structure could be observed (Figure 3.5B). Like most of the other inhalant allergens, Blo t 21 contains a fairly high percentage of basic (15%) and acidic (20.4%) residues. The surface of the Blo t 21 is highly charged with predominant distribution of surface exposed acidic residues (Figure 3.5D). An overlay of Blo t 21 with Blo t 5 yielded a Cα R.M.S.D of 3.39 Å, indicating similar folding topology but different local structures, i.e. side-chain orientations.

The 3D structure of Blo t 21 is, not surprisingly, very similar to that of Blo t 5 (PDB: 2JMH). However, some differences could be observed when both structures were analyzed in

detail. For instance, the total number of long-range NOEs that could be unambiguously assigned in Blo t 21 is 216, compared to 156 that were reported by Naik and coworkers (2008). The extra long-range NOEs found in Blo t 21 are most likely contributed by the aromatic side chains. There are six Phe and one Tyr residues found in Blo t 21 compared to only one Phe and Tyr found in Blo t 5. Among six Phe residues, three are located in the hydrophobic core of Blo t 21, which suggests apparent involvement in the contribution of hydrophobic interactions. Indeed, a handful of long-range NOEs could be identified from the aromatic side chains of these residues based on the 2D-NOESY spectrum obtained using the deuterated buffer. A more detailed comparison between the 3D structure of Blo t 21 and Blo t 5 will be presented in the following section.

A. Experimental Restraints	
Total NOEs	1729
Intraresidues (i,j)	523
Interresidue, sequential (|i, j| = 1)	454
Interresidue, medium range (1< (|i-j| ≤ 5)	416
Interresidue, long-range (|i-j| ≥ 5	216
Hydrogen-bond restraints	21
Dihedral angle restraints (φ, ψ)	171
B. Violations (mean ± s.d.)	
Distance constraints (Å)	0.02 ± 4e-04
Dihedral angle constraints (˚)	0.18 ± 0.02
Deviations from idealized covalent geometry	
Bond lengths (Å)	0.002 ± 6e-05
Bond angles (˚)	0.41 ± 0.005
Impropers (˚)	0.33 ± 0.01
Average pairwise r.m.s. deviation	
Back bone (Å):	0.82 +/- 0.22
Heavy atom (Å):	1.61 +/- 0.17
C. PROCHECK Ramachandran plot analysis (%)	
Most Favored Regions (%)	92.3
Additional Allowed Regions (%)	6
Generously Allowed Regions (%)	0.4
Disallowed Regions (%)	1.3

Table 3.1 The Overall Statistics of 20 lowest-Energy Ensemble of Blo t 21 NMR Structure. A total of 1729 NOE restraints and 171 TALOS angle restraints were included in the structure calculation. The overall violations are minimal and most of the residues located in the most favored regions in the Ramachandran Plot (Ramachandran, Ramakrishnan et al. 1963)

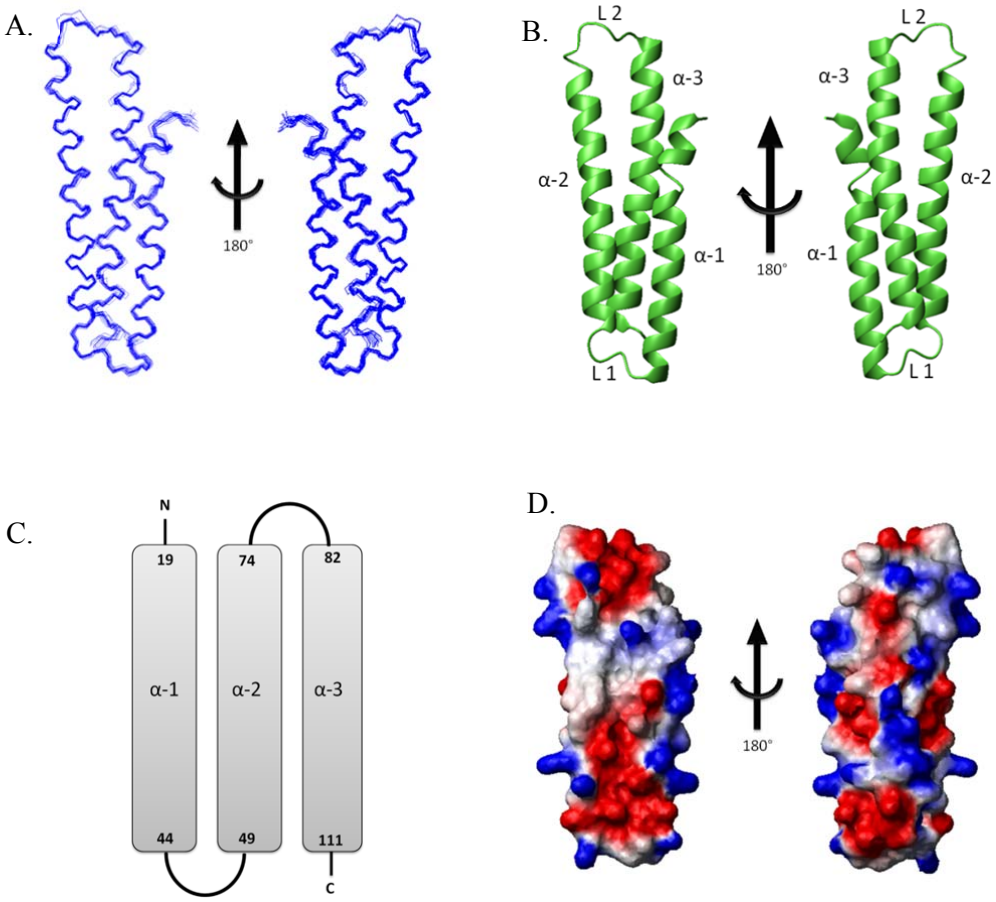

Figure 3.5 NMR Structure of Blo t 21. A) Twenty lowest energy ensembles of NMR structure of Blo t 21. **B)** 3D structure of Blo t 21 shown in ribbon diagram. **C)** Secondary structure topology of Blo t 21. **D)** Surface charge diagram of Blo t 21 generated using software MOLMOL (Koradi, Billeter et al. 1996)

3.4 3D structures comparison of Blo t 21 with Blo t 5 and Der p 5

The 3D structures of Blo t 5 and Der p 5 were resolved using NMR and X-ray crystallography, respectively. (Naik, Chang et al. 2008; Mueller, Edwards et al. 2010). Both proteins consist of three α helices aligned in an antiparallel, *clockwise* fashion. The superimposition of the 3D structures of Blo t 21 with Blo t 5 and Der p 5 yielded the Cα R.M.S.D of 2 Å and 3.39 Å, respectively (Figure 3.6A and 3.6B). The overall folding topology of the two proteins is very similar especially when comparing the α-2 and α-3, but

the N-terminus α-1 is apparently different in these proteins.

In Blo t 5, the N-terminus α-1 is more inclined to α-2, while in Blo t 21, the N-terminus α-1 is aligned in parallel to α-3, with a small "kink" between Arg-23 and Glu-26, which is absent in Blo t 5 (Figure 3.6A). The dimerization of Der p 5 as indicated in the crystal structure was proposed to be concentration and pH dependent. It was confirmed that Der p 5 was predominantly monomeric at neutral pH and low concentration using solution scattering techniques. The N-terminus α-1 of Der p 5 was completely detached from both α-2 and α-3 and interacted with the N-terminus α-1 from another molecule to form a dimer (Mueller, Gosavi et al. 2010). In addition, a study on Der p 21, another group 21 allergen from *D. pteronysinnus* suggested that this protein could also form a dimer, based on the small-angle X-ray scattering experiments (Weghofer, Dall'Antonia et al. 2008). However, there is no experimental evidence suggesting that Blo t 21 is capable of oligomerization, at least at neutral pH. Our NOESY spectrums also did not show any plausible inter-molecular interaction to enable the dimerization of Blo t 21. Instead, many long-range NOEs, especially those from ^{13}C-edited NOESY spectra, could be unambiguously assigned among the three α-helices in Blo t 21, which disprove the possible "splaying" of the N-terminus α-1 in order to accommodate another molecule as indicated by the Der p 5 crystal structure. Nevertheless, the α-2 and α-3 of Der p 5, Blo t 5 and Blo t 21 are very similar. Interestingly, the α-2 and α-3 of Der p 5 and Blo t 21 (Figure 3.6B) seemed to be superimposed much better as compared to Der p 5 - Blo t 5 (Figure 3.6C).

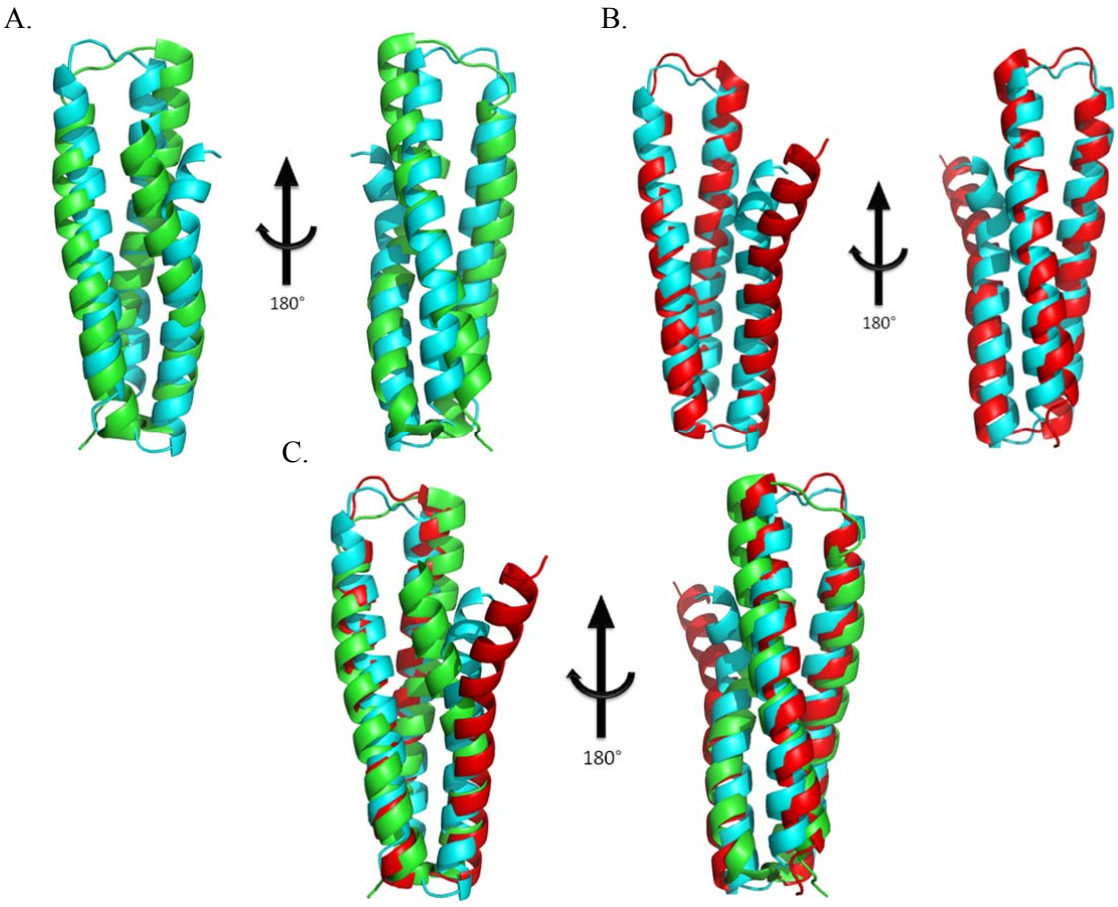

Figure 3.6 Superimposition of the NMR structure of Blo t 21 (Cyan) with **A)** Blo t 5 (Green) and **B)** Der p 5 (Red) yielding the Cα r.m.s.d. of 3.39 Å and 2 Å, respectively. **C)** The α-2 and α-3 of three proteins are very similar but their N-terminus α-1 are oriented in different directions. Diagrams were generated using PyMOL (Delano 2002).

3.5 The Allergenicity of Blot 21 Compared to Blo t 5, Der p 5 and Der f 21

The studies on the allergenicity of Blo t 5 compared to Der p 5 were conducted by Kuo and coworkers in 2003. Direct ELISA experiments conducted on two different populations (Taiwanese and Malaysian) demonstrated low correlation of IgE reactivity between Blo t 5 and Der p 5. In addition, the authors had also investigated the cross-reactivity between these two allergens. Both heterologous absorption and dose-response inhibition studies demonstrated that Blo t 5 and Der p 5 reacted with unique IgE epitopes. Besides the *in*

vitro experiments, *in vivo* skin prick test was also employed to further evaluate the IgE cross-reactivity of these two allergens. The test revealed significant levels of differential reactivity between Blo t 5 and Der p 5 when tested on nineteen asthmatic children, with Blo t 5 elicited the overall bigger diameter of erythema and wheal, which implied higher allergenicity. In conclusion, this study suggested that Blo t 5 and Der p 5 were two distinctively different allergens (Kuo, Cheong et al. 2003).

In this section, we compare the allergenicity among Blot 21, Blo t 5, Der p 5 and Der f 21. As mentioned earlier, the allergenicity and the cross-reactivity of Blo t 5 and Der p 5 were shown to be low and thus, these proteins should use distinct IgE epitopes (Kuo, Cheong et al. 2003). The properties of Der p 21, another group 21 allergen from dust mite *D. pteronysinnus* were reported by Weghofer and coworkers in 2008. Der p 21 shared 69% amino acid sequence identity with Der f 21, and it was shown to highly react to patients' IgE antibodies. This allergen also demonstrated high level of allergenicity based on the basophil activation experiments. Despite the average sequence identity of approximately 40% with group 5 allergens from dust mite (Der p 5, Blo t 5 and Lep d 5), Der p 21 exhibited no relevant cross-reactivity with any of the group 5 allergens tested. The comparison in terms of allergenicity among the group 21 allergens from dust mites has not been reported thus far. It would be interesting to investigate the allergenicity as well as the cross-reactivity between Blo t 21 and Der f 21, which share 32% sequence identity. In our study, Der f 21 was used in place of Der p 21 as the latter was not available.

The allergenicity of an allergen depends predominantly on the distribution of surface exposed residues, which is closely associated to its 3D structure. The structural properties and the sequence identity of Blo t 21, Der f 21, Blo t 5 and Der p 5 were compared in the previous sections. Overall, these proteins consist of three α-helices arranged in an antiparallel fashion separated by two flexible loops; and they share the protein sequence identity ranged from 26 – 39%. However, despite these similarities, they differ significantly in terms of allergenicity. As shown in Figure 3.7, Blo t 5 has the overall highest allergenicity followed by Blo t 21, Der f 21 and Der p 5. There are some exceptional cases such as sera P3 and P12, which

weresignificantly more sensitized against Blo t 21 compared to Blo t 5. Other examples are sera P6 and P10, which demonstrated higher sensitivity to Der f 21 when compared to Blo t 21. In general, these results suggest that all these proteins could interact with the IgE antibodies in different manners, and different sera would present distinct binding profiles to these allergens.

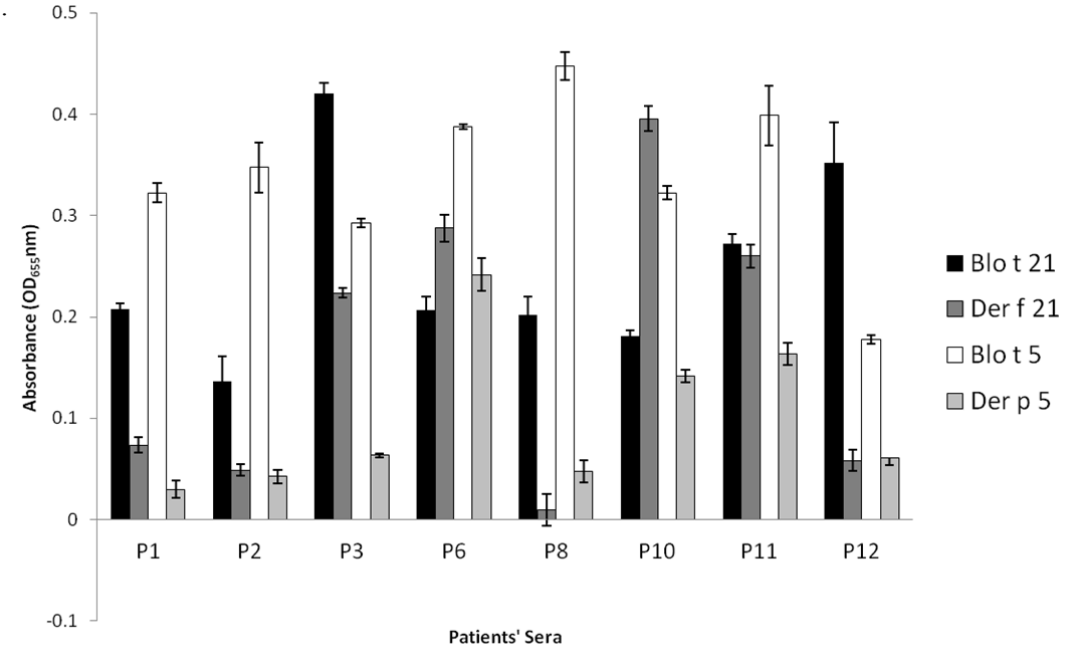

Figure 3.7 The allergenicity of Blo t 21, Der f 21, Der p 5 and Blo t 5. Overall, Blo t 5 (white bars) has the highest allergenicity among all sera, followed by Blo t 21 (black bars), Der f 21 (dark gray bars) and Der p 5 (light gray bars). All proteins were tagged with GST protein at the N-terminus and the Maxisorp™ was used for the experiments.

The low correlation of the IgE reactivity was quite unexpected as the putative IgE epitopes mapped on Blo t 5 are highly conserved in Blo t 21, Der p 5 and Der f 21 as shown in the sequence alignment (refer to section 3.7). The disparity in terms of allergenicity between Blo t 21 and Blo t 5 could be due to the distribution of the IgE epitopes in these proteins based on their 3D structures. Moreover, the additional unique epitope that could be present in Blo t 21 would also contribute to the interaction with different IgE antibodies. The overall lower allergenicity of Der p 5 could be explained by the substitution of residue Glu for Leu at the position corresponding to Glu-76 in Blo t 5. However, the allergenicity profile of

Der f 21 could not be comprehended because even though all the putative IgE epitopes mapped in Blo t 5 are conserved in this allergen, Der f 21 did not seem to behave similarly as either Blo t 5 or Blo t 21. This phenomenon was especially prominent in sera P8, which showed no sensitivity to Der f 21 despite the evidently high reactivity to Blo t 5 and Blo t 21. Based on these results, Der f 21 should be a unique allergen that uses different IgE epitopes to exhibit its allergenicity.

In an attempt to investigate the discrepancies of the allergenicity among Blo t 21, Der f 21, Blo t 5 and Der p 5, we have conducted several experiments including cross inhibition assays and direct ELISA experiments using the whole proteins as well as the peptides derived from these proteins. The details of these experiments will be presented in the late sections.

3.6 Study on the stability of Blo t 21, Der f 21, Blo t 5 and Der p 5

3.6.1 Circular Dichroism

The 3D structures of Blo t 21, Blo t 5 and Der p 5 have been solved and we found that these proteins, despite sharing similar tertiary fold and moderate sequence identity with each other (>31%), are in fact quite different in certain aspects, i.e. the alignment of the helices and side chains orientations. The slight differences in the structures could suggest different properties, including the allergenicity of the proteins. Indeed, in the previous section, we showed that the allergenicity of Blo t 21, Der f 21, Blo t 5 and Der p 5 were very different. Here, we present the CD spectrums and the stability tests on these proteins. These experiments are especially important for Der f 21 as no structural information is available for this protein. Der f 21 shares relatively lower sequence identity with Blo t 21 (32%), Blo t 5 (35%) and Der p 5 (26%), thus, it was probable that this protein possesses different structural properties. Since the 3D structure of Der f 21 is not available, it would be interesting to study the secondary structure and the stability of this protein in comparison with Blo t 21, Blo t 5 and Der p 5 using CD experiments.

All GST-tags were removed from each protein using thrombin and purified by the gel filtration column; the highly purified proteins were dialyzed against 1 X PBS buffer prior to the far-UV CD experiments. The CD spectrums were overlaid as shown in Figure 3.8. In general, all proteins have typical α-helical secondary structures with double minimal peak at ~208 nm and ~222 nm. A closer examination of the spectrums indicated that the minimal peaks of these proteins were not identical, which usually meant that the content of the α-helical structures were different in these proteins (Johnson 1990). Indeed, the 3D structures of Blo t 21, Blo t 5 and Der p 5 were quite different as discussed earlier. The CD spectrum of Der f 21 showed slightly different "dip" in minimal peaks compared to the other three proteins. This result suggested that Der f 21 should be sharing similar secondary structures but slightly different 3D structures as compared to the other three proteins.

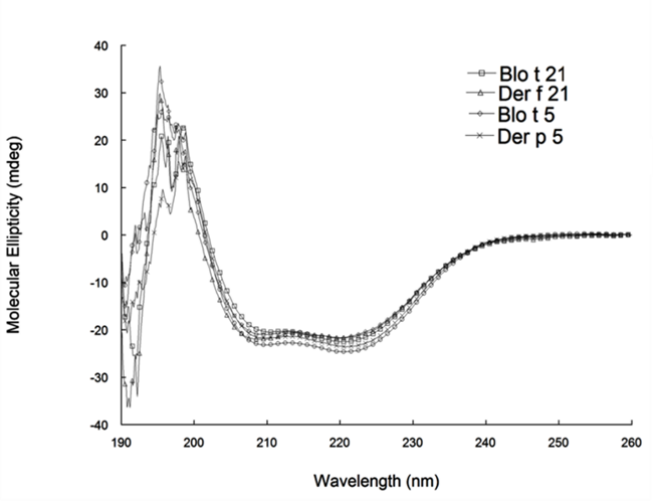

Figure 3.8 The CD spectrum of Blo t 21, Der f 21, Blo t 5 and Der p 5. All proteins showed typical α-helical CD profile with two minimum peaks at wavelength 208 nm and 222 nm. The CD spectrums were acquired using similar parameters and all proteins were buffered with 1 X PBS.

3.6.2 Thermal denaturation experiment

We sought to investigate the stability of Blo t 21 compared to Blo t 5, Der p 5 and Der f 21 using the CD thermal denaturation experiment. All proteins were subjected to heat denaturation at 90°C and subsequently cooled down to 25°C while the spectrums were recorded (Figure 3.9). As it can be seen, all proteins were unfolded at 90°C based on the

increase in the molecular ellipticity (mdeg). However, when the temperature was reduced to 25°C, only Der p 5 and Der f 21 appeared to be fully renatured (Figure 3.9B and 3.9C); Blo t 5 seemed to be able to partially refold while Blo t 21 remained unfolded when the temperature was reduced (Figure 3.9A and 3.9D). The ability of the protein to refold largely depends on its primary sequence (Anfinsen 1973). The content of the solvent in which the protein is subjected to the temperature and the presence of a molecular chaperon are also the crucial factors that govern the protein folding. The sequence identity between Der p 5 and Der f 21 is only 26%, much lower than the 39% shared between Blo t 21 and Blo t 5. The refoldability of Der p 5 and Der f 21 could be due to the content or the arrangement of the hydrophobic residues in their primary sequences, which was obviously different compared to Blo t 21 and Blo t 5 based on their sequence alignment. This phenomenon could be important if the IgE epitopes on Der f 21 and Der p 5 were conformational; such resiliency would be a problem as these proteins remained allergenic even when exposed to extreme temperature.

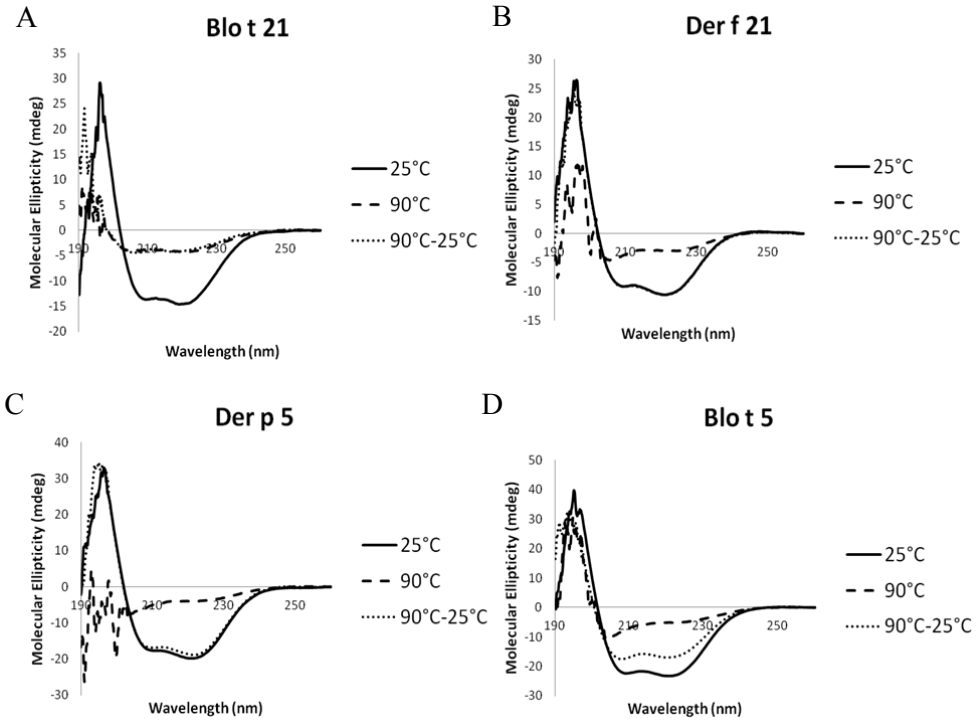

Figure 3.9 The CD spectrum of Blo t 21, Der f 21, Blo t 5 and Der p 5 at different temperatures. All proteins are denatured at 90°C. **B)** Der f 21 and **C)** Der p 5 could be renatured when the temperature is allowed to cool down from 90°C to 25°C. While **A)** Blo t 21 could not be renatured and **D)** Blo t 5 could be partially renatured.

Thermal-induced protein unfolding was monitored by CD approach within the range from 30°C to 95°C. Figure 3.10 showed that the stability of Der f 21 is the highest (Tm = ~87°C), followed by Der p 5 (Tm = ~73°C), Blo t 21 (Tm = ~ 54.5°C) and Blo t 5 (Tm = ~51.4°C). Similarly, Weghofer and coworkers reported high thermal stability of Der p 21, a homologous protein of Der f 21 (Weghofer, Dall'Antonia et al. 2008). In addition, the authors also reported the refoldability of Der p 21 using similar experiments. Der f 21 and Der p 21 shares 69% amino acid sequence identity, which could explain their similar thermal stability. In the same study, it was also demonstrated that Der p 21 and group 5 allergens from dust mite (Der p 5 and Lep d 5) showed limited cross-reactivity. Owing to its high sequence identity with Der p 21, it is possible that Der f 21 share low cross-reactivity with group 5 allergens from dust mites as well. Furthermore, our results indicated that Der f 21 does not highly cross-react with Blo t 21, thus making Der f 21/Der p 21 a distinctively different allergen from dust mite. The details of the cross-reactivity between Blo t 21 and Der f 21 will be presented in the section 3.12.4.

In summary, our results show that Der f 21 and Der p 5 are much more stable than Blo t 21 and Blo t 5. Both proteins exhibit remarkable refoldability that was not observed in Blo t 21 and Blo t 5. The refoldability of Der f 21 and Der p 5 could be important for their allergencity, depends on the nature of their IgE epitopes, which remained elusive thus far. Our results show that the allergencity of Der p 5 is generally lower compared to Blo t 5, which agreeed with the previous finding (Kuo, Cheong et al. 2003); while the allergenicity of Der f 21 was comparable to Blo t 21 in some cases. There seemed to be a correlation between the stability and the allergenicity among Blo t 21, Der f 21, Blo t 5 and Der p 5: Der f 21 and Der p 5 showed higher stability but generally lower allergenicity while Blo t 21 and Blo t 5 were less stable but demonstrated significantly higher allergenicity. Despite the lower allergenicity, a highly stable allergen tends to persist longer in the environment while maintaining its allergenic properties, hence heighten the chances of exposure to the atopic individuals. The remarkably higher stability of Der f 21 and Der p 5 could be one of the factors that allowed these proteins to manifest their allergenicity in the natural environment.

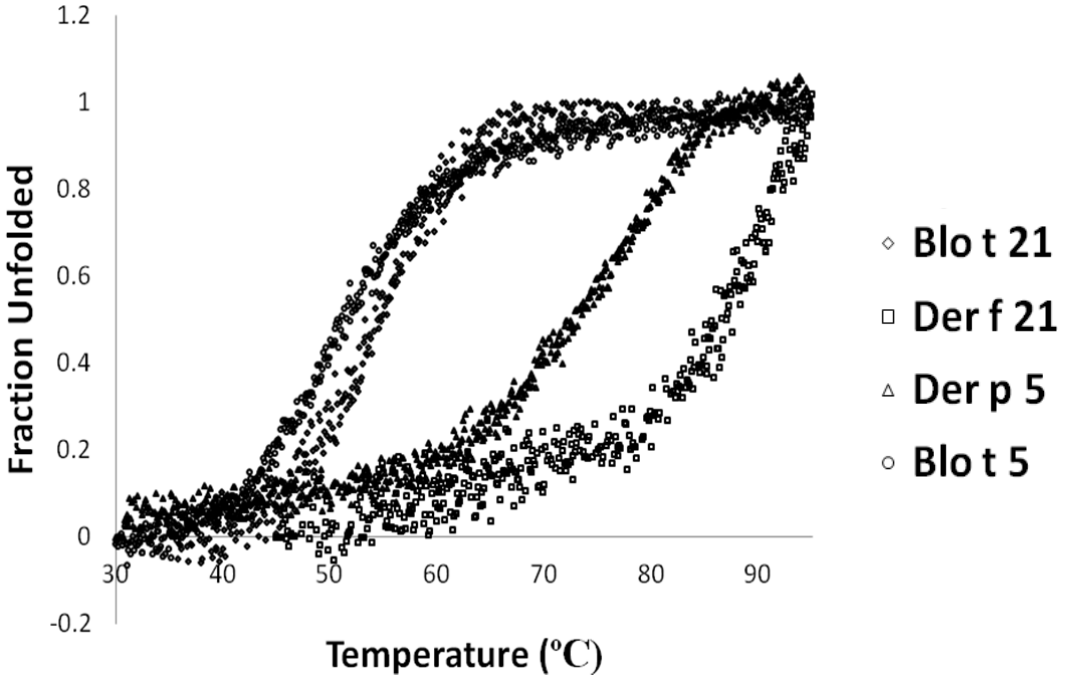

Figure 3.10 Thermal denaturation experiment for Blo t 21, Der f 21, Der p 5 and Blo t 5. Among four proteins, Der f 21 has the highest melting temperature (Tm) of ~ 87°C, followed by Der p 5 with the Tm of ~ 73°C. The Tm of Blo t 21 and Blo t 5 are quite similar, which are ~ 54.5°C and ~51.4°C, respectively.

3.7 Site-directed mutagenesis and IgE epitope mapping of Blo t 21

The multiple sequence alignment was carried out using the group 21 and group 5 allergen from different species of dust mite that are available in the National Center for Biotechnology Information (http://www.ncbi.nlm.nih.gov/) and Allergome (http://www.allergome.org) data bank. There are several isoforms exist for each of these allergens (isoallergen), i.e., allelic polymorphisms that result in substitutions of amino acid at certain positions in the allergen (Christensen, Riise et al. 2010). Only one of each variant that was cited in other publications was selected for sequence alignment analysis. Group 21 allergen isolated from three species of dust mite, i.e. *B. tropicalis* (Blo t 21), *D. pteronyssinus (*Der p 21*)* and *D. farinae* (Der f 21); and group 5 allergens identified in five species of dust mites, i.e. *B. tropicalis* (Blo t 5), *D. pteronyssinus* (Der p 5*)*, *D. farinae* (Der f 5), *Lepidoglypus destructor* (Lep d 5), *Aleuroglyphus ovatus* (Aleo 5), *Suidasia medanensis* (Sui m 5.02) and *Tyrophagus putrescentiae* (Tyr p 5.01) were chosen for the analysis.

Subsequently, multiple sequence alignment was conducted by employing CLUSTALw software (Higgins 1994).

As shown in Figure 3.11**,** residues which share different biochemical properties such as Lys in group 21 allergens compared to Gln, Gly or Ala in group 5 allergens (first boxed residues), are selected for the mutagenesis studies. The selection of these residues was based on the inhibition assay conducted by Gao *et al.* (2007) showing that Blo t 21 and Blo t 5 were cross-inhibiting each other at a low-to-moderate level. Cross inhibition of the allergens is decided by the mutual sharing of IgE epitopes, thus, if both allergens are sharing the residues that interact with the same IgE antibodies, they should highly cross-react to each other. For example, IgE antibodies binding to peanut allergens, Ara h 1, can cross-react with homologous proteins in other legumes like Gly m 1 from soybean (Sicherer and Sampson 2000). Conversely, low cross inhibition is often attributed to the usage of different residues in IgE binding. In general, charged amino acid residues are considered as the most likely candidate for IgE binding as most of them are solvent accessible. Based on these criteria, eighteen amino acid residues were chosen for the subsequent mutagenesis studies. Four amino acid residues that are gray shaded in Figure 3.11 were chosen based on the IgE epitope mapping on Blo t 5 conducted by Chan et al (2008). These residues were described as a linear epitope found in Blo t 5 based on multifaceted immunoassay. Interestingly, all these residues are highly conserved across all group 21 and group 5 allergens except Der f 5 and Der p 5, in which the first Glu is substituted for Leu. Coincidently, it was reported that cross-reactivity between Der p 5 and Blo t 5 were low (Kuo, Cheong et al. 2003). Therefore, the cross-reactivity between Blo t 21 and Blo t 5 was most likely due to these residues.

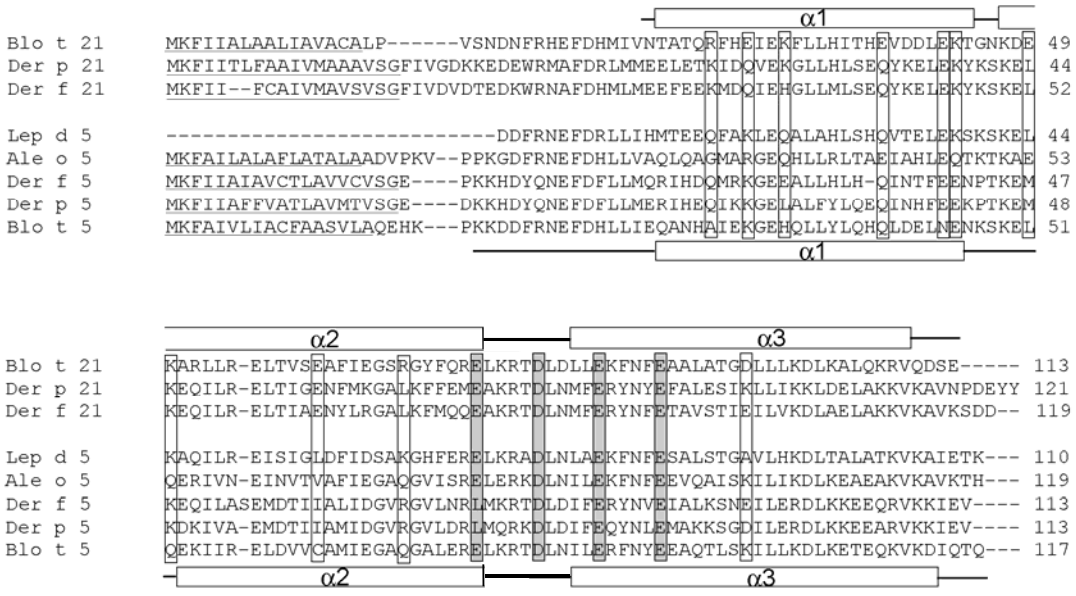

Figure 3.11 Sequence alignment of group 21 and group 5 allergens from dust mites. The boxed residues with distinct properties between group 21 and group 5 allergens are selected for mutagenesis studies. The residues shaded in gray are the IgE epitopes mapped in Blo t 5 (Chan, Ong et al. 2008). Signal peptides predicted using SigalP 3.0 Server (Emanuelsson *et al.* 2007) are underlined. Boundaries of α-helices α-1, α-2, and α-3 are shown as cartoon diagram above (Blo t 21) and below (Blo t 5) the sequences.

Based on the sequence alignment, eighteen charged residues were selected. These residues were either conserved or sharing similar properties of residues among group 21 allergens, but of different properties compared to group 5 allergens. Four residues (Glu-74, Asp-79, Glu-84 and Glu-89) which are conserved across all group 5 and group 21 allergens were chosen as well. Each of these residues was mutated to Ala and the corresponding mutant was tested for its IgE binding reactivity. Skin prick test was conducted on fifteen volunteers with written consents, among which twelve showed positive test results against the wild-type Blo t 21 protein. The initial screening of the wild-type Blo t 21 protein and its single mutants was conducted using the twelve patients' sera, labeled as P1 to P12 and the result is shown in Figure 3.12.

The reduction in IgE binding by the mutated proteins compared to the wild-type protein was observed. Only the mutation of a particular residue that resulted in more than 20% of reduction in IgE binding was scored as significant. As shown in Figure 3.13, out of eighteen residues selected for mutagenesis studies, four indicate a significant reduction of IgE

binding in 50% or more of the patients' sera. Mutation of residue Glu-89 to Ala (E89A) conferred the most drastic IgE reduction, which was demonstrated in 11 of 12 (89.67%) serum samples tested, followed by 8 of 12 (66.67%) in mutant D79A, 7 of 12 (58.33%) in mutant D96A and 6 of 12 (50%) in mutant E84A. All residues appeared to be charged and four residues (Glu-74, Glu-84, Glu-89 and Asp-96) are located in the α-helices while residue Asp-79 was located in the loop region between α-2 and α-3. Coincidently, residues Asp-79, Glu-84 and Glu-89 corresponded to the major epitopes mapped in Blo t 5 previously seemed to be playing an important in IgE binding for Blo t 21 as well.

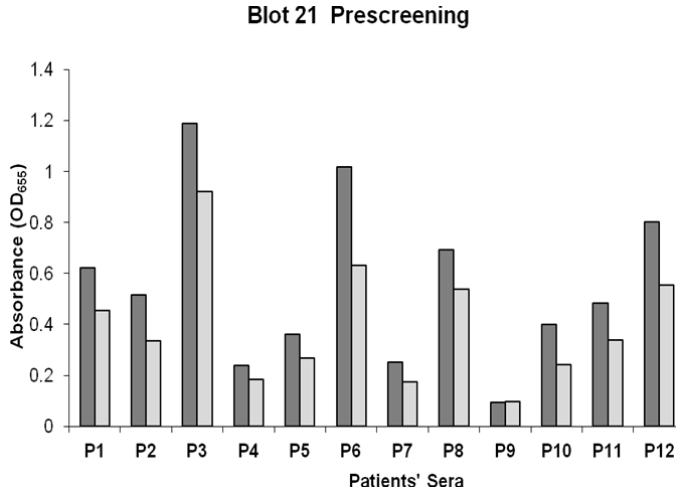

Figure 3.12 The prescreening to evaluate the sensitivity against wild type Blo t 21 was done using sera from twelve volunteers. Two different dilutions of the sera were used, i.e. 1:5 ratio (dark grey) and 1:10 ratio (light grey) to estimate the suitable dilution of sera required for future experiments.

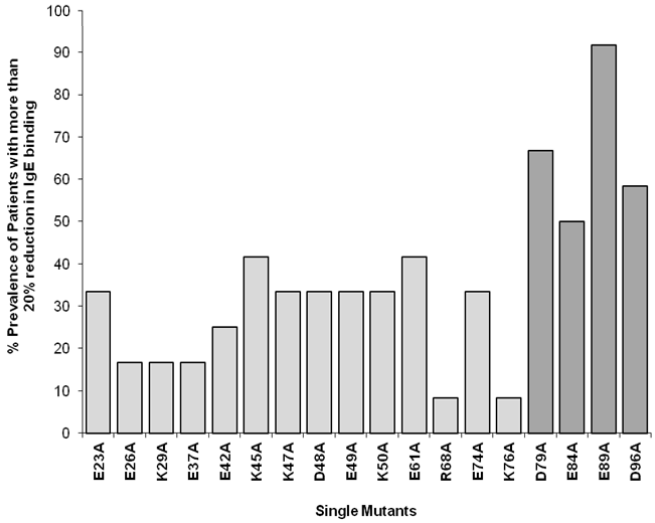

Figure 3.13 Percentage prevalence of volunteers with more than 20% reduction in IgE binding against 18 single mutants of Blo t 21. Among 18 single mutants of Blo t 21, mutants D76A, E84A, E89A and D96A show the highest prevalence (>50%) in 12 volunteers.

It was reported that the IgE epitopes mapped on Blo t 5 were located at the continuous stretch of sequence (loop region between α-2 and α-3) and thus formed a major putative linear epitope (Chan, Ong et al. 2008). However, based on the mutagenesis studies conducted as well as the 3D structure of Blo t 21, at least a part of the putative IgE epitopes on this protein could be conformational. The NMR structure of Blo t 21 revealed that residues Glu-89 and Asp-96 were close to each other and could form a conformational epitope. Additionally, by mutating residues Asp-79, Glu-84 and Glu-89 (corresponding to three major epitopes mapped in Blo t 5 -Asp-81, Glu-86 and Glu-91-) to Ala, significant reduction in IgE binding to Blo t 21 could be achieved. This observation suggests that Blo t 21 and Blo t 5 could be sharing common IgE epitopes, thus explaining the low-to-moderate cross-reactivity between these two allergens.

Even though residue Glu-74 did not show a significant reduction in IgE binding as a single mutant, it was included in the subsequent multiple mutations' studies because it was identified as a major IgE epitope in Blo t 5. We suspected that by combining residue Glu-74 with the nearby residues such as Asp-79 and Glu-84, a more significant reduction in IgE binding could be achieved. We found that residues Glu-74, Asp-79, Glu-84 and Glu-89 (corresponding to Glu-76, Asp-81, Glu-86 and Glu-91 in Blo t 5) are oriented differently based on the structures of Blo t 21 and Blo t 5 (Figure 3.14A and 3.14B, respectively). Based on the surface diagram of Blo t 21, residues Glu-74, Asp-79 and Glu-84 seems to form an IgE binding cluster while residue Glu-89 is forming a separated cluster with residue Asp-96.

These observations imply that there could be at least two IgE binding clusters in Blo t 21, which is different from the proposed single linear IgE epitope identified in Blo t 5. Surprisingly, the surface distribution of these residues on Blo t 21 is very similar to Der p 5 (Figure 3.14C). However, our results show that the allergenicity of Der p 5 is generally low as compared to Blo t 21. Since no information is available for the IgE epitopes of Der p 5, it would be difficult to explain its weak IgE binding based on just the 3D structure. This phenomenon could be attributed to many reasons, such as the Leu substitution at position 73 in Der p 5 compared to the Glu residue found at the corresponding position in Blo t 21.

It is imperative that the overall protein structure is maintained subsequent to the mutations to ensure that the reduction in IgE binding is solely due to the removal of epitope residues. In the next section, the monitoring of the overall folding of the Blo t 21 multiple mutants using circular dichroism (CD) will be presented.

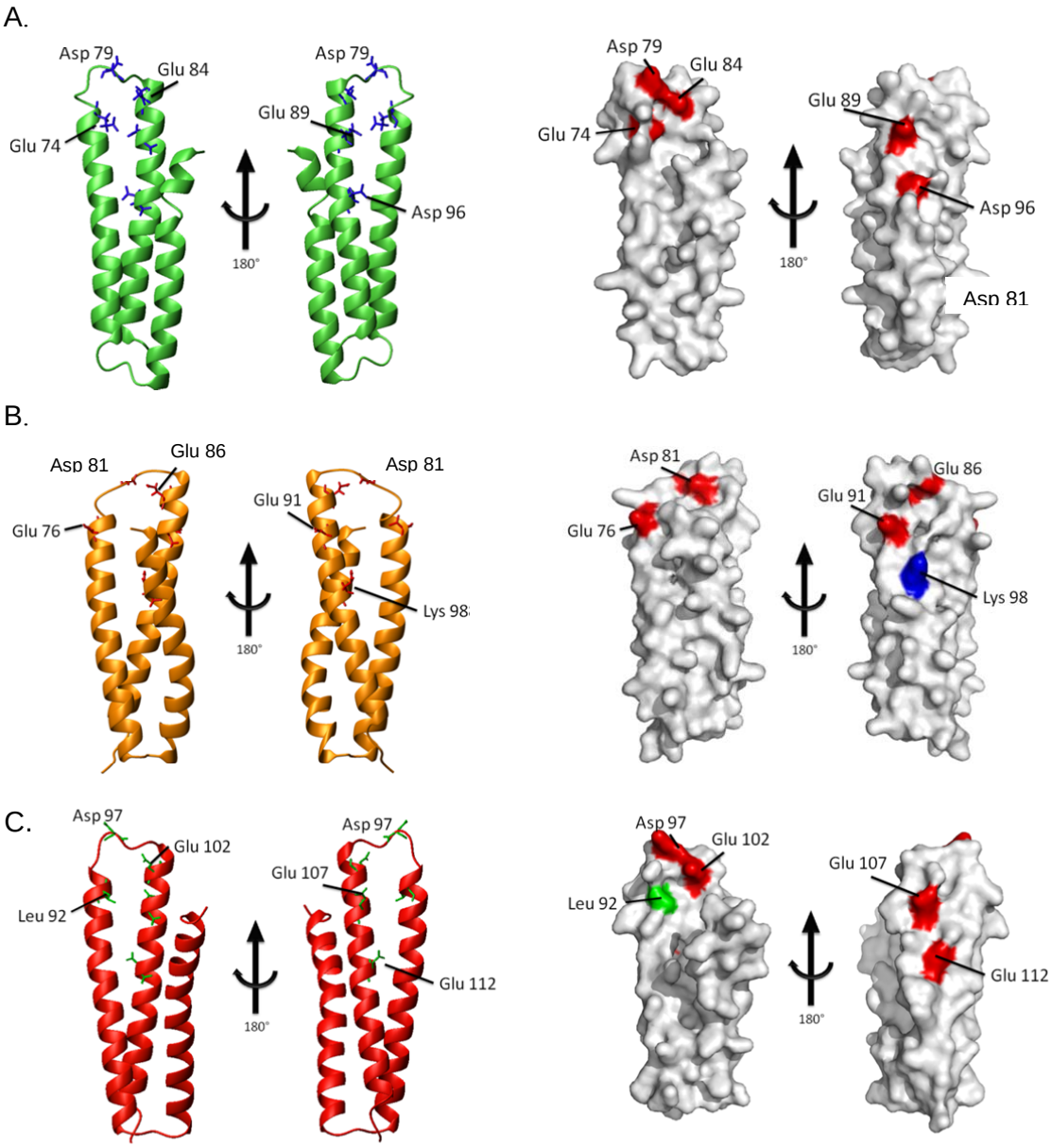

Figure 3.14 Distribution of the residues corresponding to Glu-74, Asp-79, Glu-84, Glu-89 and Asp-96 of Blo t 21 in the 3D structures of Blo t 5 and Der p 5. The distribution of these residues is very similar in **A)** Blo t 21 and **C)** Der p 5 but slightly different in **B)** Blo t 5 based on the ribbon diagrams as well as the surface diagrams. The charged residues are colored red (negative charged) and blue (positive charged) respectively; the hydrophobic residue is colored green in the surface diagrams.

3.8 Circular Dichroism (CD) of Blo t 21 and its mutants

Many publications on the development of hypoallergen emphasized on the maintenance of the overall folding of the mutants compared with the wild-type proteins (Swoboda, De Weerd et al. 2002; Buhot, Chenal et al. 2004) (Chan, Ong et al. 2008). The reduction in IgE binding of the mutants should be contributed by the removal of the unique epitope residues and not due to the conformational changes. In most cases, substitution of a single residue for Ala should not affect the overall folding of the protein (except Gly and Pro due to the unique properties of their side chains). However, when more than one amino acid are involved (multiple mutations), it would be very crucial to examine the secondary fold of the mutants.

The mutagenesis study on Der f 13, a group 13 allergen identified in *D. farinae*, involved the substitution of four charged amino acids for Ala (E41A, K63A, K91A and K103A). The 3D structure of Der f 13 indicated that all putative IgE epitopes were located in the β-strands and solvent accessible. Based on the CD spectra, the multiple mutants (triple and quadruple mutants) showed similar secondary folds as the wild-type Der f 13 (Chan, Ong et al. 2006). The substitution of these charged amino acids for Ala did not alter the overall fold of the protein and therefore were considered as the "real" IgE epitopes. Similar study conducted on Blo t 5 also demonstrated that the substitution of four charged amino acids (E76A, D81A, E86A and E91A) for Ala did not alter its CD profile. The 3D structure of Blo t 5 showed that these amino acids were surface exposed and located in the unstructured loop connecting helix α2 and helix α3, hence, substantial conformational change would be very unlikely (Chan, Ong et al. 2008).

The CD spectrums showed that the overall folding of the Blo t 21 single mutants were similar compared with the wild-type protein (data not shown). However, some multiple mutations such as the double mutant D79A_E84A, quadruple mutants E74A_E84A_E89A_D96A and E74A_D79A_E84A_D96A implied loss in secondary structures based on their CD profile (Figure 3.15). Other mutants including double mutants E84A_D89A and triple mutant E84A_D89A_D96A seem to degrade rapidly upon removal of

the N-terminus GST-fusion tag by thrombin digestion when the SDS-PAGE failed to show visible bands corresponding to the size of the digested mutants. No readable signals were achieved even after concentrating these untagged mutants. Interestingly, the quadruple mutant of Blo t 21 (E74A_D79A_E84A_E89A), which corresponds to the 4A mutant of Blo t 5 (E76A_D81A_E86A_E91A) also demonstrated similar degradation problem, while the latter showed similar CD profile compared to wild-type Blo t 5.

These results consistently show that the substitution of residue Glu at position 84 for Ala together with the similar mutation of either residues Glu-79 or Asp-89 could disrupt the structural integrity of Blo t 21. Sequence alignment shows that this loop region is highly conserved in Blo t 21 and Blo t 5 (>75%), but a closer look at these residues reveal some substitutions of amino acids which could affect the local conformation of these proteins. For example, residue Asp-81 in Blo t 21 which corresponds to position 83 in Blo t 5, is substituted for Asn. Another notable substitution occurs in position 90 in Blo t 21, which is an Ala compared to Glu-92 found in Blo t 5. It is debatable that such substitution could alter the structure of the proteins, but it seems that the structural integrity of Blo t 21 is highly dependent on the charge-charge interaction. The replacement of the negatively charged Asp and Glu with a hydrophobic Ala could disrupt the delicate interaction that maintained the local structure and ultimately unfolds the protein. Nevertheless, it should be noted that the single mutants E79A and D89A indicated similar CD spectrums as compared to the wild-type Blo t 21. In addition, these mutants did show a notable reduction in IgE binding when compared to the wild-type protein

.

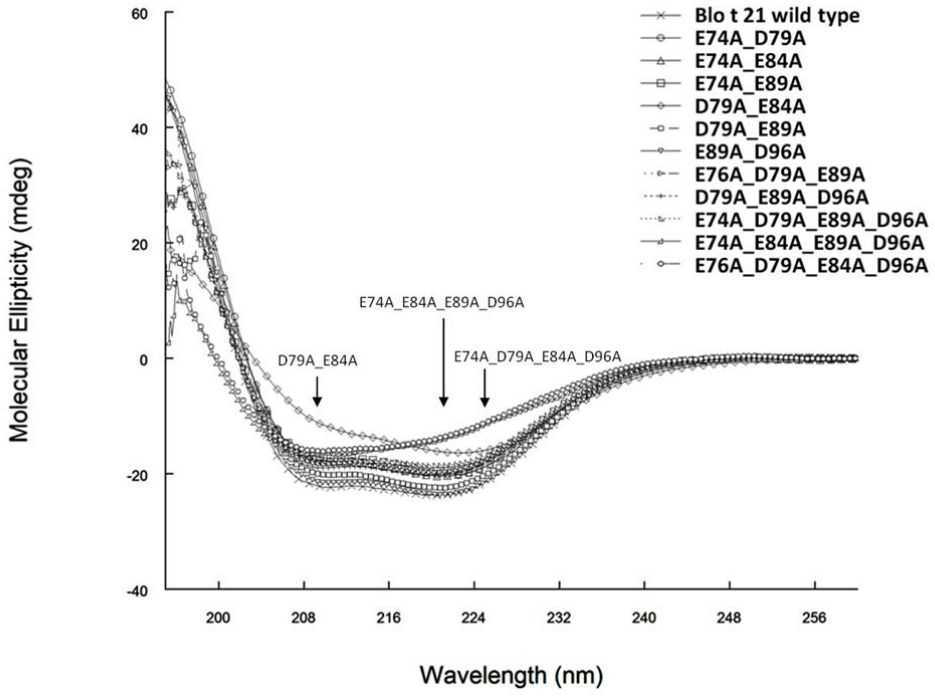

Figure 3.15 Comparison of the CD spectrum of Blo t 21 and its mutants. Most of the multiple mutants are showing similar CD profile with the wild type Blo t 21. However, some mutants: D79A_E84A, E74A_E84A_E89A_D96A and E74A_D79A_E84A_D96A are showing an altered CD profile implying lost in secondary structures (pointed with arrows).

3.9 Multiple mutations of epitope residues further reduce IgE binding

In order to investigate the effect of multiple mutations on the IgE binding to Blo t 21, three double mutants, two triple mutants and one quadruple mutant were chosen. The double mutant 2A (E74A_D79A), 2B (E74A_E84A), 2C (E74A_E89A) and 2D (D79A_E89A) were generated to investigate the combinatorial effect of residue Glu-74 with the neighboring residues in further reducing the IgE binding. In order to investigate the IgE binding of the putative new IgE epitope cluster composing of residues Glu-89 and Asp-96, we have also synthesized the double mutant 2E (E89A_D96A). Two triple mutants 3A (E74A_D79A_E89A) and 3B (E79A_E89A_D96A) were generated to investigate the

combinatorial effect towards the allergenicity contributed by two putative clusters of IgE epitopes according to the 3D structure. The quadruple mutant 4A (E74A_D79A_E89A_D96A) was generated to encompass all combinations of the putative IgE epitopes. Note that some combinations were not included as the mutants showed aberrant CD profiles or degraded after thrombin cleavage. The multiple mutants were then tested for their IgE binding reactivity using eight patients' sera with relatively higher IgE titers.

As shown in Figure 3.16, the double mutants show varying reduction in IgE binding in different patients' sera. Overall, mutant 2A demonstrates the most significant reduction in IgE binding compared to other double mutants. In patients P3, P6, P11 and P12, this mutant shows more than 40% reduction when compared to the wild-type Blo t 21; whereas in patients P1, P8 and P10, this mutant could only reduce the IgE binding by slightly more than 20%. Patient P2 hardly shows any significant reduction for mutant 2A, as well as all other double mutants. Double mutant 2B shows lesser reduction in IgE binding as compared to mutant 2A in general, and mutant 2C shows significant reduction in IgE binding in patients P10 and P11. Mutant 2D shows more than 40% reduction in IgE binding for patient P1, and ≥20% for patients P3 and P6. As for double mutant 2E, significant reduction in IgE binding could be observed in patients P10, P11 and P12 (≥40%), while for the rest of the patients, the reduction is not as significant.

While the triple mutant 3A does not show much reduction when compared to its corresponding double mutant 2A, mutant 3B seems to show further drop in IgE binding compared to all double mutants in all patients except for patient P6. The most significant reduction could be observed in patients P10, P11 and P12 (≥70%). Finally, the quadruple mutant 4A was able to further reduce the IgE binding as compared to the triple mutants in all cases except for patient P12, in which no further reduction could be observed. Remarkably, the reduction was ≥80% as compared to the wild-type Blo t 21 in patients P6, P10 and P11. The average reduction exhibited by the quadruple mutant 4A was about 70% in all patients.

These results indicate that residues Glu-74, Asp-79, Glu-89 and Asp-96 should be the major IgE epitopes in Blo t 21; with residues Glu-74 and Asp-79 forming one epitope cluster

while residues Glu-89 and Asp-96 forming another. Despite the notable reduction in IgE binding observed in the single mutants' screening, residue Glu-84 was excluded from the multiple mutation studies. As mentioned earlier, mutating this residue together with either residue Asp-79 or Glu-89 resulted in the unfolding/degradation of the protein. The exclusion of residue Glu-84 from the 4A quadruple mutant could be the limiting factor that prevented the further reduction in IgE binding for some patients (P1 and P2). Coincidently, residues Glu-74, Asp-79 and Glu-89 were also identified as the major IgE epitopes in Blo t 5 (Glu-76, Asp-81 and Glu-91 in Blo t 5) (Chan, Ong et al. 2008). These residues could be responsible for the partial cross-reactivity between Blo t 21 and Blo t 5. Nevertheless, residue Asp-96, which is a Lys residue at the corresponding position in Blo t 5 (Lys-98), could be a unique epitope identified in Blo t 21. In order to evaluate whether residue Lys-98 is also an IgE epitope in Blo t 5, we mutated it to Ala (K98A). The IgE binding capability of the Blo t 5 single mutant K98A will be presented in the next section.

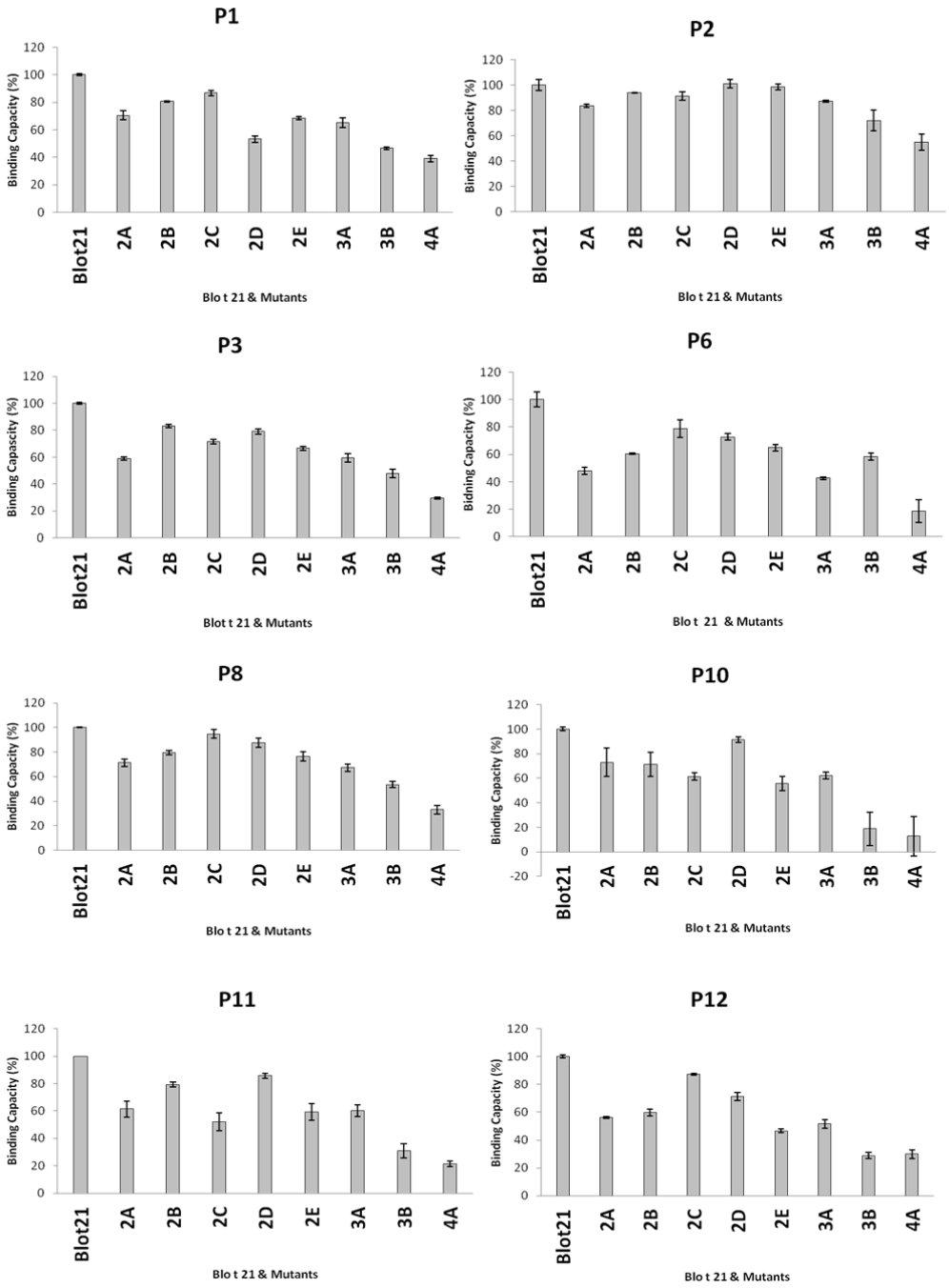

Figure 3.16 Comparing the allergenicity of multiple mutants with the wild type Blo t 21 using ELISA experiment. Overall, the quadruple mutant 4A shows the most significant reduction in IgE binding as compared to the wild type protein as well as the other mutants. Double mutant 2A (E74A_D79A) shows the most significant drop in IgE binding among all double mutants in most sera; triple mutant 3B (E79A_E89A_D96A) shows more significant reduction compared to 3A (E74A_D79A_E89A) in most sera.

3.10 Residue "Asp-96" - A unique IgE Epitopes in Blo t 21?

In an attempt to show that residue Asp-96 is a unique IgE epitope found in Blo t 21, we mutated the corresponding residues in Blo t 5, i.e. Lys-98 to Ala. The single mutant E91A and double mutant E91A_K98A from Blo t 5 were also included in the ELISA experiments. Similar mutants from Blo t 21 were included in this experiment as a positive control (E89A, D96A and E89A_D96A). The Blo t 21 single mutant D96A showed a notable reduction in IgE binding, though not as significant as indicated by the E89A mutant when compared to the wild-type Blo t 21. The double mutant E89A_D96A showed a further reduction in IgE binding in all patients when compared to the single mutants (Figure3.17A). On the other hand, no reduction in IgE binding could be observed for the Blo t 5 single mutant K98A in all sera; while mutant E91A showed a notable drop in IgE binding in most patients when compared to the wild-type Blo t 5. The double mutant E91A_K98A did not show a further reduction in IgE binding when compared to the E91A single mutant (Figure 3.17B).

This experiment shows that residue Asp-96 is a unique IgE epitope in Blo t 21. In Blo t 5, residue Lys-96 bears an opposite charge compared to the negatively charged Asp residue in Blo t 21. The surface charge distributions in the designated region of Blo t 21 and Blo t 5 are also different due to the Lys to Asp substitution (refer to section 3.4). It is highly possible that residue Glu-89 and Asp-96 form a conformational IgE epitope in Blo t 21 that interacts with a unique IgE antibody. Since Blo t 5 lacks of this particular conformational epitope, this could be one of the factors that results in its low cross-reactivity with Blo t 21.

Interestingly, residue Asp-96 is substituted for Glu in Der f 21 at the corresponding position (Glu-99). Glu shares similar properties with Asp, but different properties with residue Lys, which is located at position 98 in Blo t 5. In addition, all the putative IgE epitopes mapped in Blo t 21 are conserved in Der f 21. Therefore, it is possible that Glu-99 is also forming an IgE epitope with Glu-92 in Der f 21, corresponding to Glu-89 and Asp-96 in Blo t 21. It would be interesting to investigate the effect of E99A mutation in Der f 21 to find out whether residue Glu-99 could be an IgE epitope for this protein.

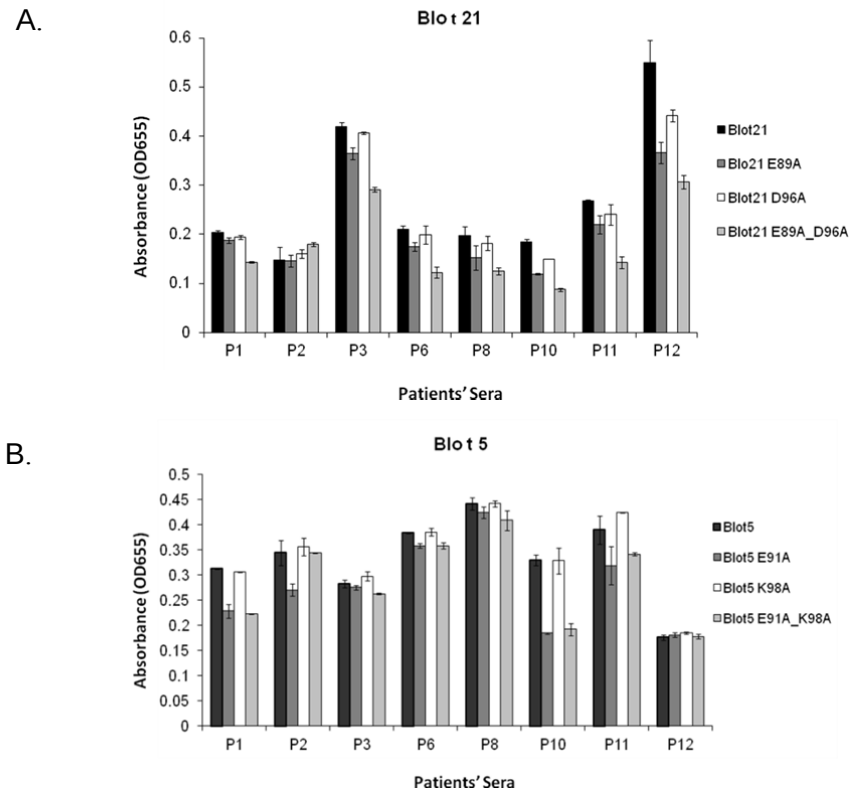

Figure 3.17 Specific ELISA experiment for E89A_D98A (Blo t 21) and E91A_K98A (Blo t 5) double mutants. A) In Blo t 21, the double mutant E89A_ D96A shows notable reduction in IgE binding compared to the single mutants and the wild type protein. **B)** In Blo t 5, only single mutant E91A shows reduced IgE binding compared to the wild type protein, no further reduction is shown by the single mutant K98A and double mutant E91A_K98A.

3.11 Does Der f 21 shares similar epitope with Blo t 21?

In Der f 21, the residue corresponding to Asp-96 in Blo t 21 is substituted for Glu-99; whereas the other major four IgE epitopes are conserved, i.e. Glu-77, Asp-82, Glu-87 and Glu-92 (refer to section 1.7 for sequence alignment). However, the allergenicity test showed that Der f 21 has distinctively different IgE binding capacity compared to Blo t 21 as shown previously. We sought to investigate whether residue Glu-99 is involved in the IgE binding in Der f 21, since the property of Glu is essentially identical to Asp. Two single mutants E92A and E99A as well as a double mutant E92A_E99A were prepared, and the allergenicity of these mutants was observed using direct ELISA experiment. Overall, the Der f 21 double mutant did not show a similar IgE binding pattern as the Blo t 21 double mutant (E89A_D96A), which was consistently less allergenic than the wild-type protein.

As shown in Figure 3.18, the single mutant shows no significant change in the IgE

binding as compared to the wild-type Der f 21. As for the double mutant, only P10 serum showed a significant reduction in IgE binding; P3 and P6 sera shows a slight reduction while P1 serum does not show any difference in IgE binding when compared to the wild-type protein. Interestingly, the double mutant indicates an increase in IgE binding when compared to the wild-type Der f 21 for the rest of the patients' sera. This phenomenon is especially remarkable in serum P8, in which no binding to IgE could be observed for the wild-type protein and single mutants but significantly high binding to IgE is observed in the double mutant. This peculiar increment in the IgE binding was also observed in some of the Blo t 21 mutants (data not shown), and it could be explained by the unfolding of the protein due to the mutations as shown in the CD spectra. However, the CD spectrum of the Der f 21 double mutant was identical to the wild-type protein as well as the single mutants. One possible explanation is that the substitution of the charged residues for hydrophobic Ala would create an interacting surface that favors the binding of an unrelated IgE antibody with complementary paratopes. It is not surprising that the effects of the mutations would vary, depending on the amino acid used for substitution (Frank, 2002). However, there is no extensive study on the effect of different mutations on the allergenicity of an allergen thus far.

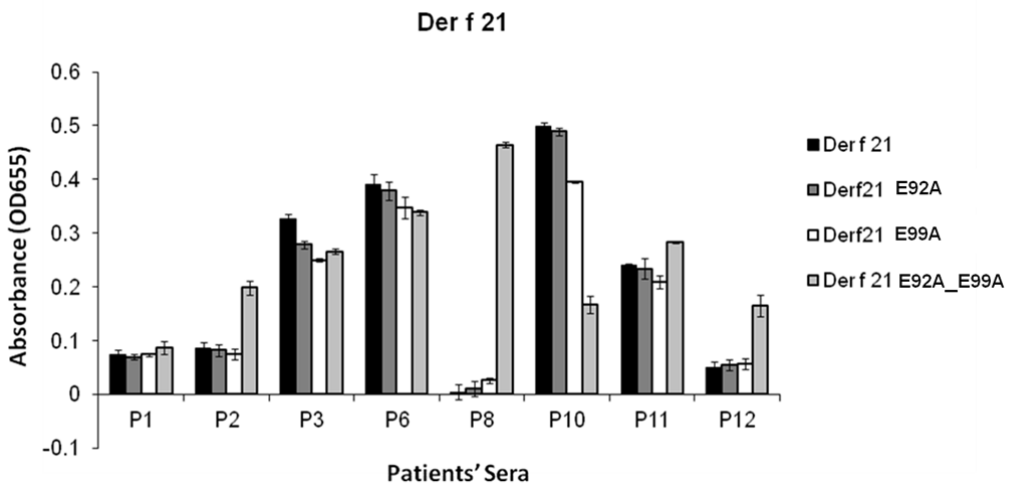

Figure 3.18 Specific ELISA experiment for E92A_E99A in Der f 21. Significant reduction in IgE binding can be achieved in sera P10 by the double mutant E92A_E99A as compared to the wild-type Der f 21, but this mutant shows an increase in IgE binding compared to the wild-type protein in the rest of the patients' sera.

To summarize, Blo t 21, Der f 21 and Blo t 5 should not use the same IgE epitope despite their moderate sequence identity. The IgE epitope mapping experiments suggest that residue Asp-96 is a unique epitope in Blo t 21, and it could be the residue that distinguishes group 21 from group 5 dust mite allergens. However, the result of the study on the double mutant of Der f 21 is not conclusive. In this study, significant reduction of IgE binding by the Der f 21 double mutant when compared to the wild-type protein could only be observed in serum P10, among a total of eight patients' sera; but the increment in binding due to the mutation could also mean that Glu-92 and Glu-99 were interacting with IgE antibodies. Otherwise, the mutation should not affect the binding at all.

3.12 Inhibition Assays

3.12.1 End-point Inhibition assays

The inhibition assay conducted by Gao and coworkers (2007) demonstrated that the cross-reactivity between Blo t 21 and Blo t 5 was low-to-moderate. Similar study was conducted by Kuo *et al* (2003) on Blo t 5 and Der p 5, which demonstrated that these allergens were not cross-reacting to each other, thus, they should use different IgE epitopes to elicit allergic responses. These results suggest that Blot 21, Blo t 5 and Der p 5 are distinct allergens despite their similar 3D structures. A closer look at the protein sequences of these allergens indicates a number of amino acid substitutions that could be the reason underlying their generally low cross-reactivity. We conducted inhibition assay to compare the cross-reactivity among these three allergens using a single point at 100 μg/ml of inhibitors. In this experiment, only six patients' sera that showed significantly higher sensitivity to Blo t 21 were chosen in order to achieve a more reliable data.

Figure 3.19 shows that in most patients' sera, Blo t 21 and Blo t 5 are not able to fully inhibit each other even at 100 ug/mL of protein, which generally agrees with the cross inhibition assay done by Gao *et al.* (2007). Generally, the results suggest that Blo t 21 could inhibit the IgE binding to Blo t 5 much better than the contrariwise. Nevertheless, the cross-

reactivity profile between wild-type Blo t 21 and Blo t 5 is different across the patients. For example, Blo t 5 seems to be able to inhibit the IgE binding to Blo t 21 much better (>28%) compared to the other four patients, which generally show no inhibition at all. In patients P3, P6 and P12, Blo t 21 could inhibit the IgE binding to Blo t 5 at a significantly lower level (<30%) compared to the other three patients. In patient P2, Blo t 21 could inhibit the IgE binding to Blo t 5 up to 70%. The IgE inhibition of Blo t 21 against Der p 5 is generally moderate-to-high except for patient P2, which shows no inhibition at all.

The allergenicity of Der p 5 was generally low when compared to Blo t 21 and Blo t 5 as shown previously in section 3.5. In some cases, it seems that even the wild-type Der p 5 protein could not efficiently inhibit the IgE binding to itself (P1 and P2; <60%). This result was expected, as the IgE binding to Der p 5 was very weak to begin with. Surprisingly, Der p 5 seems to be able to inhibit the IgE binding to Blo t 21 much better than Blo t 5 in most cases. This phenomenon is especially remarkable in patients P2, P8 and P12, in which Blo t 5 is not able to exhibit any inhibition against Blo t 21 but Der p 5 shows an inhibition up to 30%. Overall, Der p 5 is not able to inhibit the IgE binding to Blo t 5 except for patient P3, in which Der p 5 achieves inhibition close to 30%.

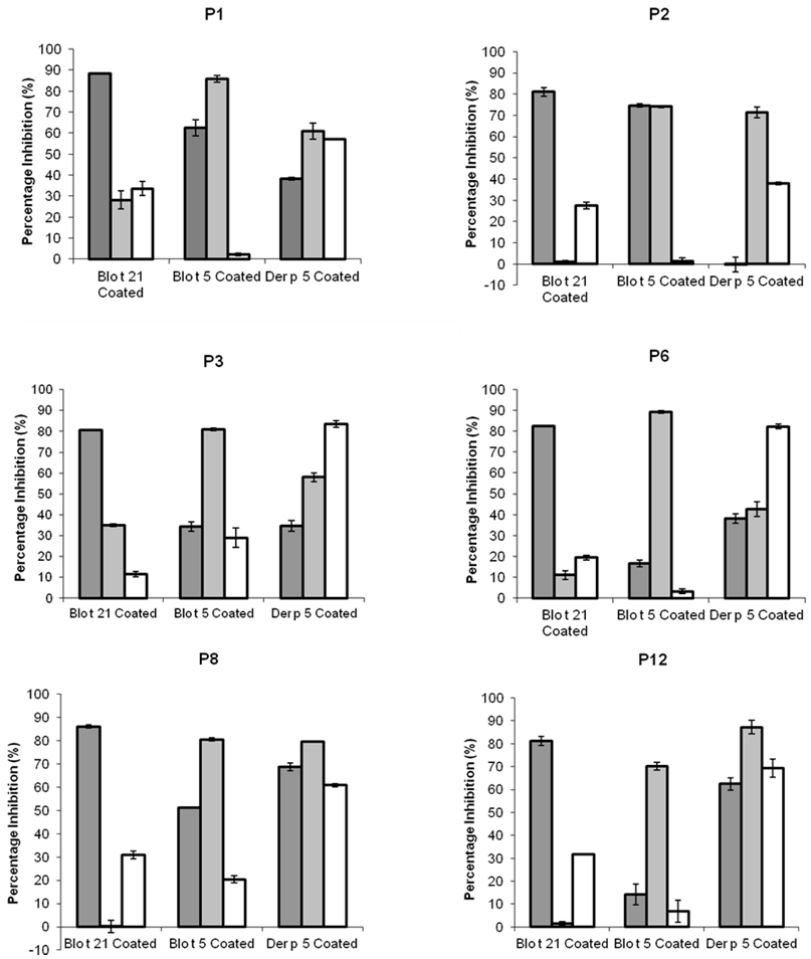

Figure 3.19 The cross-reactivity among Blo t 21, Blo t 5 and Der p 5 were examined by endpoint inhibition assay. The sera are pre-absorbed overnight with Blo t 21 (dark grey bars), Blo t 5 (light grey bars) and Der p 5 (white bars) at 4 °C. Wavelength 655 nm was used to measure the color development after addition of substrate.

This is the first experimental data describing the cross inhibition between Blo t 21 and Der p 5. Based on our data, Der p 5 could inhibit the IgE binding to Blo t 21 up to 30% and in most cases, much better than Blo t 5. A probable inference is that Der p 5 should share some IgE epitopes with Blo t 21 but not with Blo t 5. Moreover, in most patients, Der p 5 could not inhibit the IgE binding to Blo t 5 at all. Both Blo t 21 and Blo t 5 seem to be able to inhibit the IgE binding to Der p 5 very well. We propose that Blo t 21 and Blo t 5 bear the surface epitopes which could interact with the Der p 5-specific IgE antibodies, thus achieving almost full inhibition as shown in the assays. On the other hand, Der p 5 was not able to inhibit the

IgE binding to both Blo t 21 and Blo t 5 even at a high concentration probably because the latter bears extra IgE epitopes that could bind to other IgE antibodies. It should be noted that the cross inhibition of Der p 5 against Blo t 21 and Blo t 5 is very different, which is expected since it was known that Blo t 21 and Blo t 5 should use different IgE epitopes based on their low-to-moderate cross-reactivity.

In summary, this experiment shows that Blo t 21, Blo t 5 and Der p 5 cross-react among one another up to moderate level. According to the sequence alignment of these allergens, most of the putative IgE epitopes mapped on Blo t 5 are also present in Blo t 21 and Der p 5. It is possible that these common charged residues are responsible for the cross-reactivity among these allergens. Different but related IgE epitopes were demonstrated to be able to interact with the same IgE antibody (Frank 2002). In the previous experiment, we showed that Blo t 21 could have a conformational epitope (Glu-89 and Asp-96), which is not found in Blo t 5. In Der p 5, Leu residue at position 73 is substituted for Glu residue in Blo t 21 and Blo t 5 at the corresponding positions based on the sequence alignment. These differences could result in the formation of different IgE epitopes in these allergens. Indeed, most residues in the putative IgE binding site corresponding to that in Blo t 5 are similar in Blo t 21 and Der p 5, but different adjacent residues could affect the overall IgE interacting surface and ultimately, influence the type of IgE antibodies that could bind to it (Frank 2002). In this research, we attempted to identify the major IgE epitopes on Blo t 21, but in reality, there could be more IgE epitopes that are yet to be identified on this protein. Likewise, it was mentioned that Blo t 5 could also have some minor IgE epitopes (Chan, Ong et al. 2008), and the IgE epitope on Der p 5 is unknown thus far. Therefore, more experiments need to be conducted in order to better understand the relationship of the allergenic properties among these allergens.

3.12.2 The effect of L73E mutation in Der p 5

We speculate that the overall lower allergenicity of Der p 5 when compared to Blo t 5

is due to the Glu for Leu substitution at position 73 in this protein. Residue Leu-73 corresponds to residue Glu-74 of Blo t 21 and based on our mutagenesis studies, the latter should be a major IgE epitope in Blo t 21. Coincidently, the corresponding residue in Blo t 5, Glu-76, was also reported to be a major IgE epitope in this protein (Chan, Ong et al. 2008). According to the sequence alignment, all other putative IgE epitopes mapped in Blo t 5 and Blo t 21 are conserved in Der p 5 (Asp-78, Glu-83, Glu-88 and Asp-95). Therefore, it is possible that the L73E mutation of Der p 5 would result in improved allergenicity compared to the wild-type protein.

The replacement was carried out using site-directed mutagenesis approach and the allergenicity of the L73E mutant was compared with wild-type Der p 5 and Blo t 5 using ELISA experiment. Based on the overlaid CD spectrums, the secondary structure of the mutant is identical to that of Der p 5 wild-type (Figure 3.20). As shown in Figure 3.21, mutant L73E shows an improved IgE binding reactivity compared to the wild-type Der p 5. The increase in IgE binding is especially remarkable in patients P11 and P12. In these patients, the IgE binding to the L73E mutant is almost as good as Blo t 5, thus agreeing with our hypothesis that the mutation would "restore" the IgE binding to Der p 5. However, this phenomenon was not observed in the other six patients. In brief, mutant L73E shows a slight increment in IgE binding for patients P1, P3 and P6. For patient P8, even though mutant L73E indicates improvement in IgE binding compared to the wild-type protein, but apparently, the allergenicity is not "restored" as it is still significantly lower compared to that of Blo t 5. Patient P2 does not show any improvement in IgE binding to mutant L73E compared to the wild-type protein while patient P10 shows a slight drop in the binding.

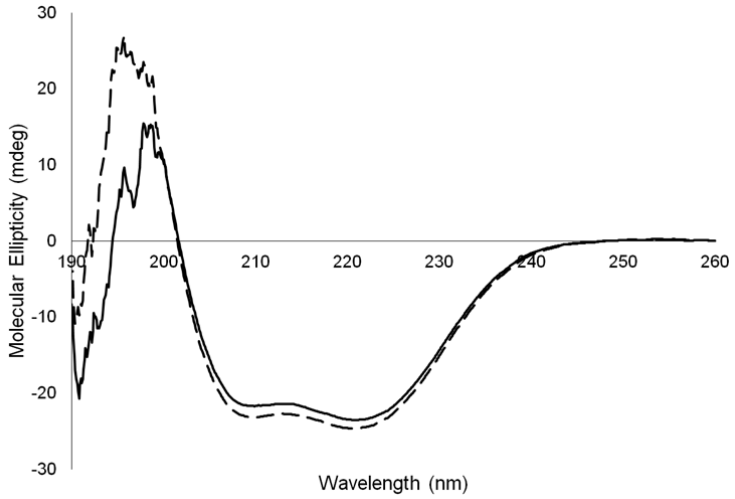

Figure 3.20 The CD spectrum of Der p 5 and its L73E mutant. The overall secondary structure of the L73E mutant (dashed line) is identical to that of Derp 5 wild type (solid line). Both proteins are prepared in 1 X PBS buffer and CD was measured at 25 °C.

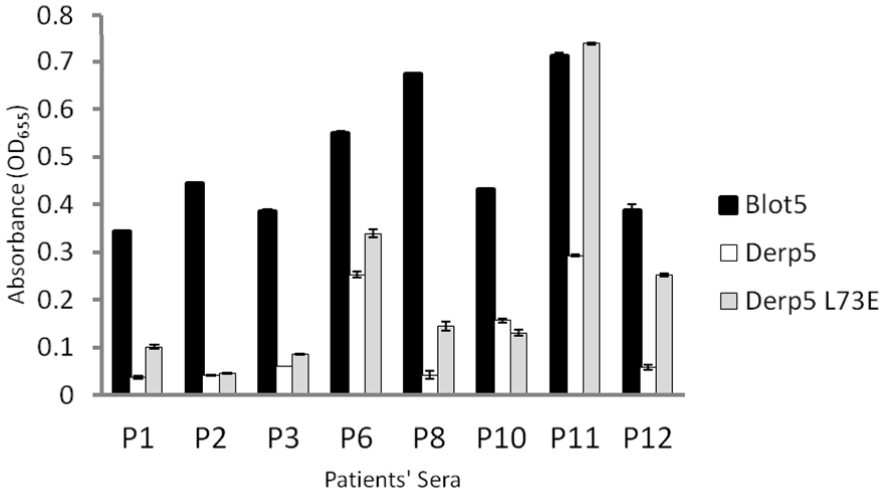

Figure 3.21 The allergenicity of Der p 5 L73E mutant compared to wild type Der p 5 and Blo t 5. Most sera show higher sensitivity to Blo t 5 compared to wild type Der p 5. The single mutant L73E shows significant increase in IgE binding when compared to the wild type Der p 5 in some sera.

To summarize, it appears that the replacement of residue Leu with Glu at position 73 in Der p 5 does improve its allergenicity as shown in most patients' sera. However, the improvements are not uniform and the effects do not seem to be identical in all patients' sera. This mutation does not seem to "restore" the allergenicity of Der p 5 as postulated. We hypothesize that the Der p 5 mutant L73E could mimic the allergenicity of Blo t 5 when all four putative major IgE epitopes are present in this protein. As a result, the IgE binding reactivity of this mutant should be at least similar, if not identical to Blo t 5. Nevertheless, the

improvement in the IgE binding with this mutation is intriguing; it suggests that the IgE binding site of Der p 5 should be in proximity to residue Leu-73, at least in some cases. Otherwise, the mutation should not affect the IgE binding to Der p 5. More experiments need to be done in order to identify the IgE epitopes of Der p 5.

3.12.4 Inhibition assays of Blo t 21 vs Der f 21

It was demonstrated that Der p 21, a homologous protein of Der f 21, showed no relevant cross inhibition with group 5 allergen from dust mite (Weghofer, Dall'Antonia et al. 2008). According to our allergenicity test, Der f 21 seems to have distinct IgE binding activity compared to that of Blo t 21. In addition, this protein also shows different physical properties based on the CD experiments as discussed earlier. These results suggest that Der f 21 could be a unique allergen that uses distinctive epitopes to elicit the allergenicity. We performed inhibition assays to investigate the cross-reactivity between Der f 21 and Blo t 21.

As shown in Figure 3.22, Der f 21 could moderately inhibit the IgE binding to Blo t 21 in all five patients (≤45%). Note that the other three patients were not included in this experiment because they are not highly sensitized to Der f 21 (refer section 3.5). Interestingly, Blo t 21 seems to be able to inhibit the IgE binding to Der f 21 in patients P1 and P11. Coincidently, both patients show stronger binding to Blo t 21 based on our ELISA experiment. This suggests that Blo t 21 could share the same IgE epitopes with Der f 21 while using additional epitopes that could not be recognized by Der f 21 specific IgE antibodies. However, patients P6 and P10 who showed stronger binding activity to Der f 21 compared to Blo t 21 did not exhibit the similar effect. Der f 21 was only able to inhibit the IgE binding to Blo t 21 at 20% and 45% in patients P6 and P10, respectively. For patient P3, Blo t 21 was unable to exhibit inhibition against Der f 21 even though it showed higher sensitivity to Blo t 21. It seems that the cross-reactivity between Blo t 21 and Der f 21 does not correlate with their allergenicity in these patients.

In conclusion, the cross-reactivity between Der f 21 and Blo t 21 is low-to-moderate and thus, Der f 21 should be considered as a unique allergen. Based on the allergenicity test, at least 50% the Blo t 21 sensitized individuals are co-sensitizing to Der f 21. Therefore, it would be necessary to identify the IgE epitopes of this allergen. Based on the sequence alignment, all putative IgE epitopes mapped on Blo t 21 are conserved in Der f 21. However, these epitope residues do not seem to behave similarly in Der f 21 as they do in Blo t 21. In this case, structural information could also be useful in aiding the explanation of the discrepancies in terms of the allergenic properties between Blo t 21 and Der f 21.

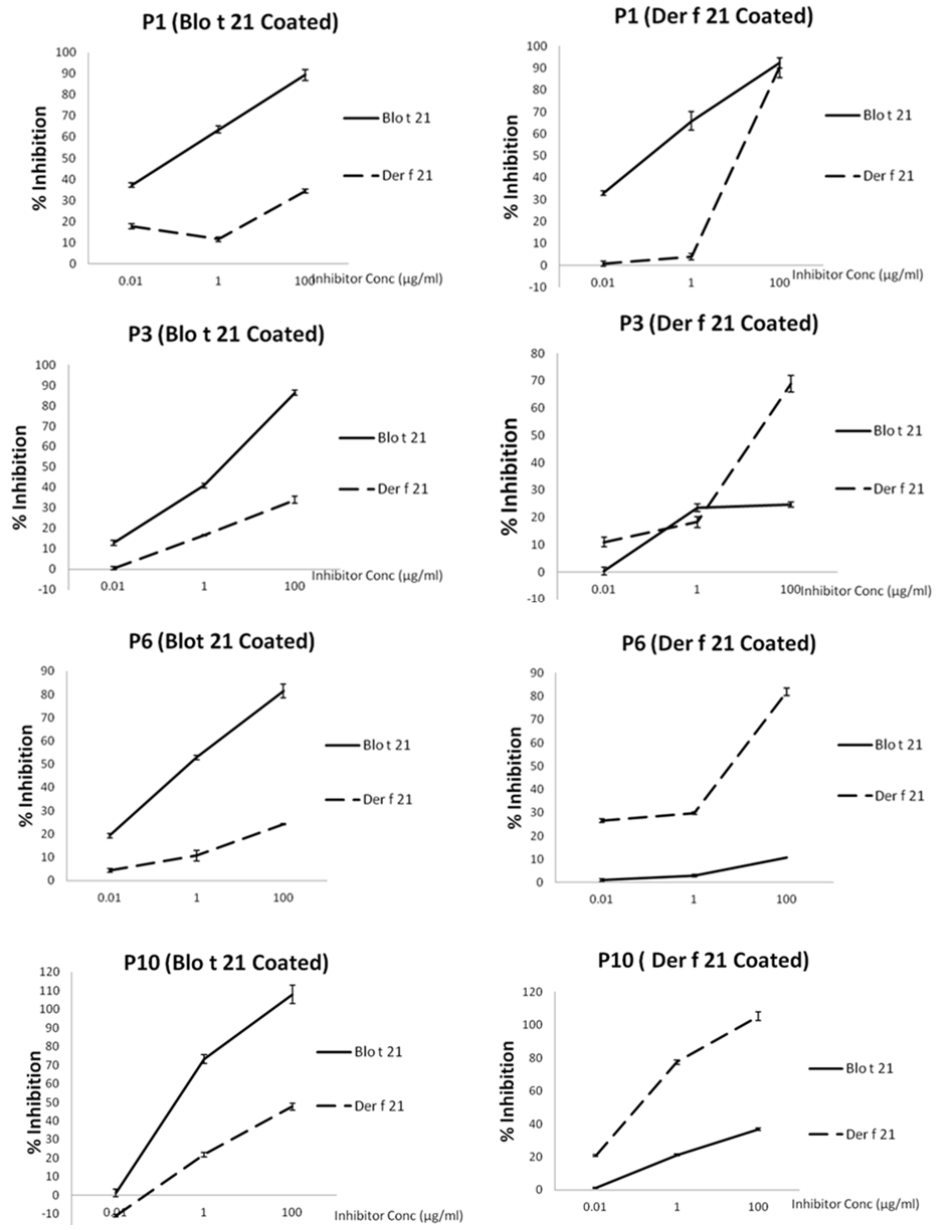

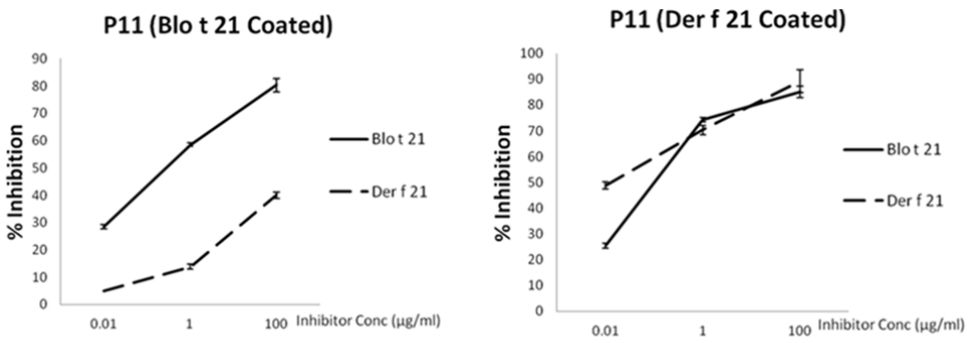

Figure 3.22 The cross-reactivity between Blo t 21 and Der f 21. Der f 21 can inhibit the IgE binding to Blo t 21 at low-to-moderate level in most sera. There is no general trend that can be observed for the inhibition of Blo t 21 against Der f 21. Blo t 21 seems to be able to inhibit the IgE binding to Der f 21 at high level for P1 and P11, but the inhibition is low-to-moderate for the rest of the sera.

3.13 Peptide ELISA

3.13.1 Surface charge distribution at the putative IgE interacting site of Blo t 21, Blo t 5 and Der p 5

In the previous sections, we showed that the cross-reactivity between Blo t 21 and Blo t 5 is generally low, which was consistent with the data reported by Gao et al (2007). Using our samples, we also demonstrated that Blo t 5 and Der p 5 are not highly cross-reactive to each other, coinciding with the published data (Kuo, Cheong et al. 2003). Additionally, we showed that Blo t 21 and Der f 21 are not able to inhibit the IgE binding to each other very well. Together with the allergenicity test on these proteins, we hypothesize that they should be using different IgE epitopes to interact with the IgE antibodies. Based on the peptide ELISA conducted on Blo t 5, Chan and coworkers (2008) showed that the sequence consisting of residues ^{81}DLNILERF^{88} was very important in IgE binding, in which two major IgE epitopes, i.e. Asp-81 and Glu-86 (Figure 3.23D) were involved. Their results also showed that the peptides that did not contain either of these epitopes could not bind to the IgE antibodies from 10 patients' sera. It seems that both residues Asp-81 and Glu-86 are essential for the IgE binding to the peptides derived from Blo t 5. Coincidently, these residues

are conserved in Der p 5, Blo t 21 and Der f 21 as well (Figure 3.23D). Sequence alignment based on these eight residues derived from all four proteins indicates the sequence identity ranged from 37% to 62%.

Figure 3.23 shows the distribution of the charged residues that are included in the peptides used in the subsequent ELISA experiments. Although the amino acid sequences are highly conserved in this region of Blo t 21, Blo t 5 and Der p 5, the overall charge distributions are very different. Note that the putative IgE epitopes mapped in Blo t 21 and Blo t 5 are contributing to the surface charge in different manners as well. Additionally, the surface topology in this region is also unique to all these proteins. These differences might contribute to the formation of a unique interacting surface to accommodate the specific IgE antibodies. Usually, an antibody could interact with an epitope comprised of 10-15 amino acids, of which about five contributed to most of the binding energy, while the adjacent residues would facilitate the accommodation of an antibody to the epitope (Frank 2002). Therefore, it would not be surprising that these proteins are interacting with different IgE antibodies despite having high sequence similarity.

The 3D structures of Blo t 21, Blo t 5 and Der p 5 shows, in consensus, that the first three residues were located in flexible loop region while the subsequent five residues are located in the structured region of these proteins. Theoretically, the peptides should represent the flexible or unstructured regions in the parent proteins, thus, this implies that the IgE antibodies are actually interacting with the unstructured part of the parent proteins. However, as shown in Figure 3.23D, residue Glu-86 which is located in the α-helical region of Blo t 5 seems to play a crucial role in the IgE binding based on the previous peptide ELISA experiment (Chan and Ong et al. 2008). It is possible that the unfolding of this structured region would not affect the IgE recognition as residue Glu-86 is very close to the unstructured region. It would be interesting to investigate the IgE binding to this region derived from all four proteins, as it would aid in explaining the differences in terms of the immuno-properties observed in these proteins.

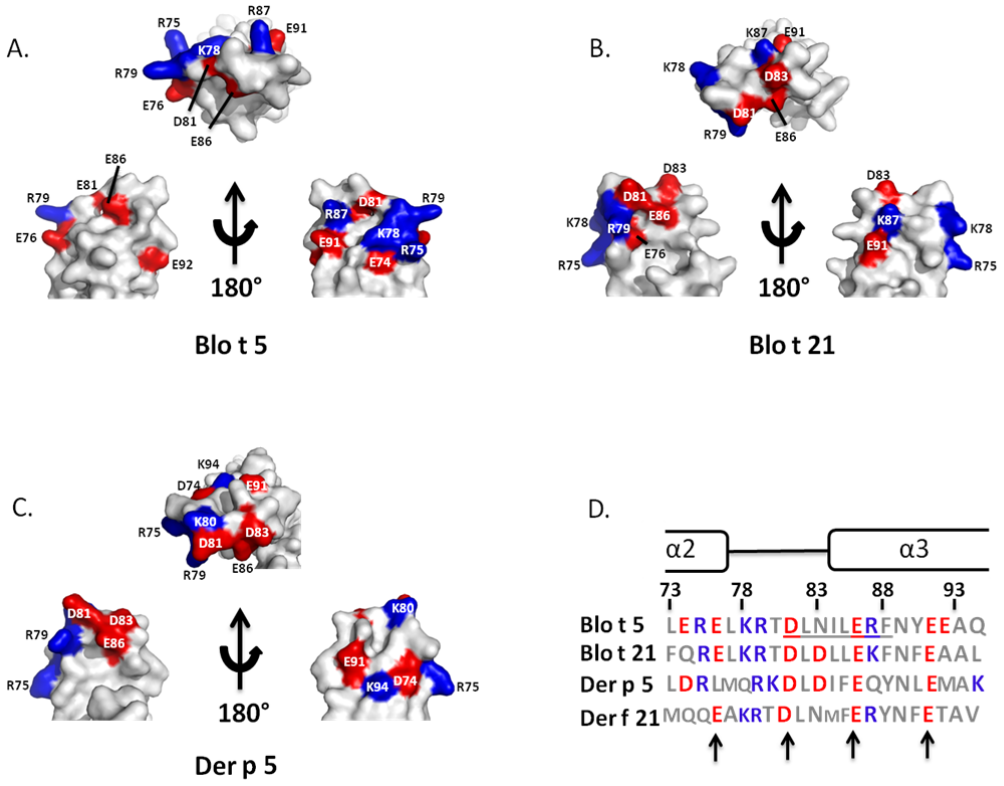

Figure 3.23 3D distribution of charged residues at the putative IgE binding site of A) Blo t 5, B) Blo t 21 and C) Der p 5. D) Sequence alignment of the peptides derived from the proteins used in this study. The charged residues are colored in blue and red representing the positive and negative charges, respectively. Secondary structure diagram is indicated on top of the sequences and the numbering of all residues is corresponding to that of Blo t 5. Der f 21 is only included in the sequence alignment since its 3D structure is not available. Four putative major IgE epitopes which were mapped in Blo t 5 are indicated by arrows. Diagrams are generated using PyMOL (Delano 2002).

3.13.2 Peptides show different IgE binding activities

The peptides were designed based on the sequence alignment of Blo t 21, Der f 21, Blo t 5 and Der p 5, which encompassed four residues corresponding to the putative IgE epitopes mapped in Blo t 5, i.e. Glu-76, Asp-81, Glu-86 and Glu- 91, as well as three additional residues flanking each terminus (Figure 3.23D). An additional peptide derived from Der p 5 with the substitution of Leu-73 for Glu-73 was also included in an attempt to mimic the putative IgE epitopes mapped in Blo t 5. Based on our ELISA results, the L73E substitution in Der p 5 increased the IgE binding of this protein significantly in some cases.

We hypothesize that the similar substitution in the Der p 5 peptide could increase its allergenicity compared to the wild-type peptide. Overall, the results show that the Blo t 21-derived peptide could react better than the other peptides, especially for patients P2, P3, P8 and P11 (Figure 3.24). Coincidently, these patients showed relatively low sensitivity to Blo t 5-derived peptide. Conversely, patients P1 and P12 who reacted better to Blo t 5-derived peptide showed relatively low sensitivity to Blo t 21-derived peptide. The Der f 21-derived peptide had much lower reactivity as compared to the Blo t 21-derived peptide in general. This observation is in sync with the previous ELISA experiments, which showed that Blo t 21 is more allergenic than Der f 21 in most cases. Patient P10 who showed the highest sensitivity to Der f 21 protein in the previous ELISA experiment also registered the highest reactivity to the Der f 21-derived peptide. However, patient P6 who demonstrated higher sensitivity to Der f 21 compared to Blo t 21 reacts similarly to Der f 21 and Blo t 21-derived peptides. Interestingly, Der p 5-derived peptide showed a rather similar trend as Blo t 5-derived peptide, and the L73E substitution in the Der p 5-derived peptide did not appear to improve its allergenicity as indicated in the whole protein ELISA. Previous experiment showed that the L73E mutant of Der p 5 demonstrated significantly higher IgE binding as compared to its wild-type protein. However, this phenomenon was not observed in the peptide ELISA experiment. The Leu-73 to Glu-73 mutation could result in a modified surface topology that might interact with an unrelated IgE antibody. Conceivably, this modified surface epitope might only be allergenic when present in the structured protein by possibly altering the local surface charge distribution.

As shown in the previous section, Blo t 5 could react to most of the patients' sera much better than Blo t 21, similar phenomena would be expected in the peptide ELISA experiments since all residues corresponding to the putative IgE epitopes mapped in Blo t 5 are present in Blo t 21. These residues, i.e. Glu-74, Asp-79, Glu-84 and Glu-89, are also responsible for the IgE binding of Blo t 21 based on our mutagenesis studies. However, the peptide ELISA showed that five patients (P2, P3, P8 P10 and P11) were reacting much weaker to Blo t 5-derived peptide as compared to the Blo t 21-derived peptide, whereas two

patients who were more sensitized to Blo t 5-derived peptides showed weaker reactivity to the Blo t 21-derived peptide**.** These results imply that the IgE antibodies that bind to the Blo t 21 and Blo t 5-derived peptides are different.

The overall higher allergenicity of Blo t 5 could be attributed to the presence of other IgE epitopes in this protein. On the other hand, the relatively lower sensitivity to Blo t 5-derived peptide when compared to Blo t 21-derived peptide could be due to the presence of a unique IgE antibody that recognizes the specific sequence in the Blo t 21-derived peptide. The sequence ^{81}DLNILERF^{88} which was shown to be the important IgE binding site in Blo t 5, was substituted for ^{79}DLDLLEKF^{86} in Blo t 21. The replacement of Asp to Asn at position 81 would probably allow binding to the Blo t 21-specific IgE antibody. In addition, the other two substitution: Leu to Ile and Lys to Arg at position 82 and 85 respectively, could also contribute to the specific interaction with IgE antibodies. In fact, a substitution of even one atom group at the binding site could lead to a significant change in the interaction with the antibodies (Van Regenmortel 1998). It was demonstrated that three Blo t 5-derived peptides bearing the important IgE binding residues were able to react very well to the sera from ten patients, with some of the absorbance exceeding the linear detection range of the spectrometer (Chan, Ong et al. 2008). The overall lower reactivity of the Blo t 5-derived peptide in our study could be explained by the higher dilution of the sera, which was 1:10 instead of 1:1 ratio as stated in the aforementioned publication. The purpose of our peptide ELISA experiment was to compare the allergenicity among the peptides derived from four different proteins, thus, such high concentration of sera would not be necessary. Moreover, in order to investigate the allergenicity of the peptides as compared to their parent proteins, using a same concentration for all the sera would be more appropriate.

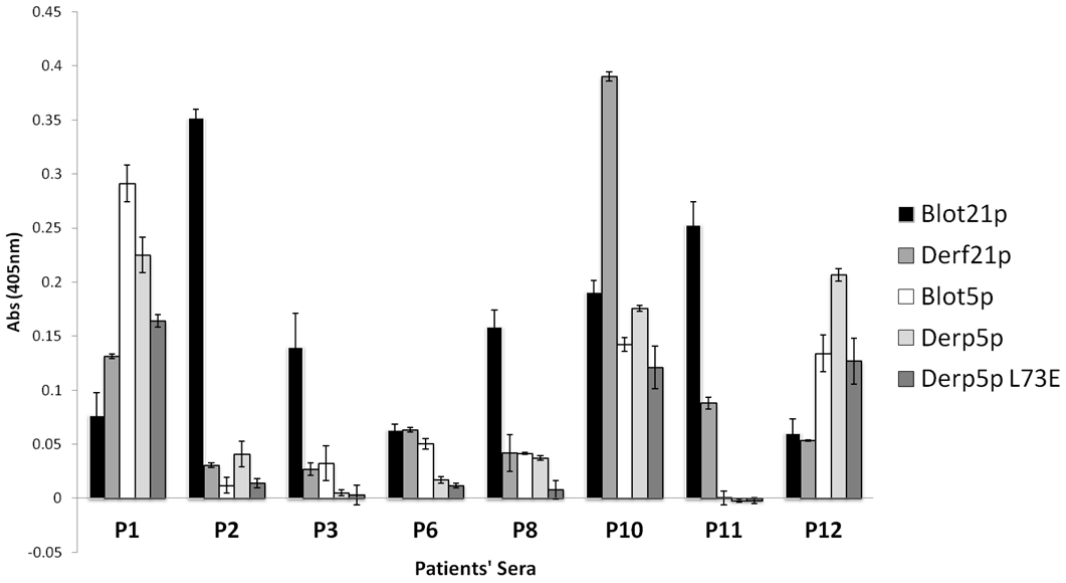

Figure 3.24 Results of the ELISA experiment using peptides derived from Blo t 21, Der f 21, Blo t 5 and Der p 5. Overall, most of the patients' sera show higher sensitivity to Blo t 21-derived peptide. Coincidently, these patients are showing relatively low sensitivity to Blo t 5-derived peptide. Patients P1 and P12 show higher sensitivity to Blo t 5-derived peptide compared to Blo t 21-derived peptide. The sensitivity towards Der f 21-derived peptide is relatively low among all patients except P10. Interestingly, Der p 5-derived peptide is showing a rather similar trend as Blo t 5. However, the L73E modification does not improve the allergenicity of Der p 5-derived peptide.

This experiment suggests that in most patients, the Blo t 21-derived peptide could represent the linear epitope of the protein. In addition, it also unequivocally supports our IgE epitope mapping data, which shows that the major IgE epitopes are indeed located in this part of the protein. As for Der f 21, Blo t 5 and Der p 5, the peptides may not be able to represent the antigenic part of the protein in most cases. Nevertheless, the results demonstrate that even with high sequence identity and the presence of putative major IgE epitopes, the peptides may not necessarily exhibit the same degree of IgE binding. Apparently, other factors such as 3D structure, amino acid constituent in the epitope region and the content of the polyclonal antibodies are also playing a pivotal role in the allergenic manifestation of these allergens.

CHAPTER 4 DER F 7: RESULTS & DISCUSSION

4.1 Characterization of Der f 7

After removing the N-terminal His-tag, the recombinant Der f 7 is 200 residues in length, which includes the full-length recombinant Der f 7 and four residues (Gly, serine, Glu and Phe) from the thrombin cleavage site. The recombinant Der f 7 was shown as a single band in the SDS-PAGE at the molecular weight of approximately 25 kDa. As shown in Figure 4.1A, the purity of the recombinant Der f 7 is very high following the gel filtration and is suitable for crystallization. The gel filtration experiment indicated that the recombinant Der f 7 was a monomer in solution (Figure 4.1B). The purified Der f 7 was subjected to CD experiment to estimate the content of its secondary structure. As shown in Figure 4.2, the CD spectrum indicates that Der f 7 consists of the mixture of α-helices and β-sheets with the minimum peak at 220 nm, which is identical to the CD profile of Der p 7. The crystallization of Der f 7 was conducted before the crystal structure of Der p 7 was available. Therefore, the molecular replacement technique was not possible since there was no homologous protein could be used as the suitable template. We prepared SeMet protein crystal to perform the MAD experiment. The SeMet protein was subjected to MALDI-TOF mass spectrometry to confirm the incorporation of the selenium. As it can be seen in Figure 4.3, the mass shift of 219.59 Da when comparing the mass spectra of the native recombinant Der f 7 with the SeMet recombinant Der f 7 confirmed approximately five selenium Met substitution.

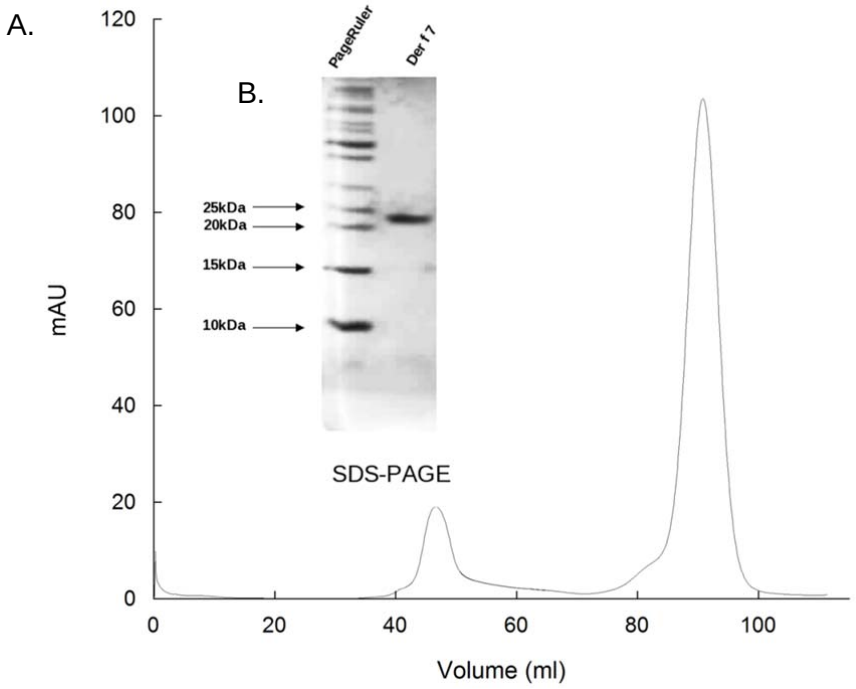

Figure 4.1 SDS-PAGE and gel filtration profiles of Der f 7. The recombinant Der f 7 was subjected to gel electrophoresis using 15% SDS-PAGE followed by Coomassie staining. **A)** The gel-filtration profile of Der f 7 estimates the monomeric state of the protein. **B)** Lane 1, protein markers. Lane 2, purified native recombinant Der f 7. The purified SeMet recombinant Der f 7 shows a similar molecular weight as the native protein.

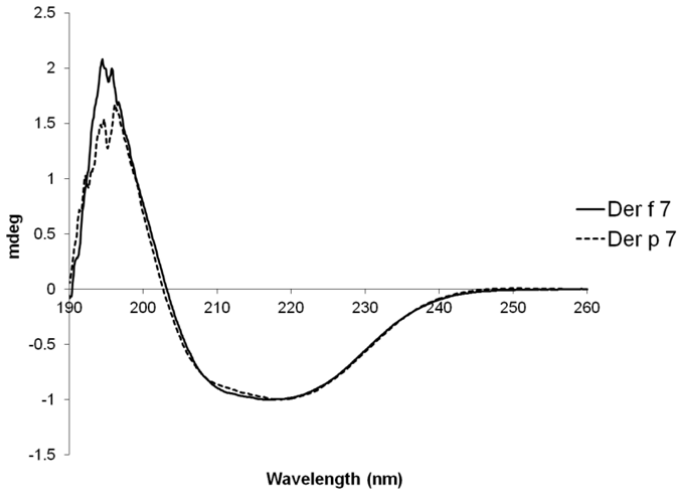

Figure 4.2 Circular dichroism of Der f 7 and Der p 7. Both proteins show similar CD profile with a minimal peak at around 220 nm. The subsequent CD denaturation experiments are carried out using 220 nm as the reference point.

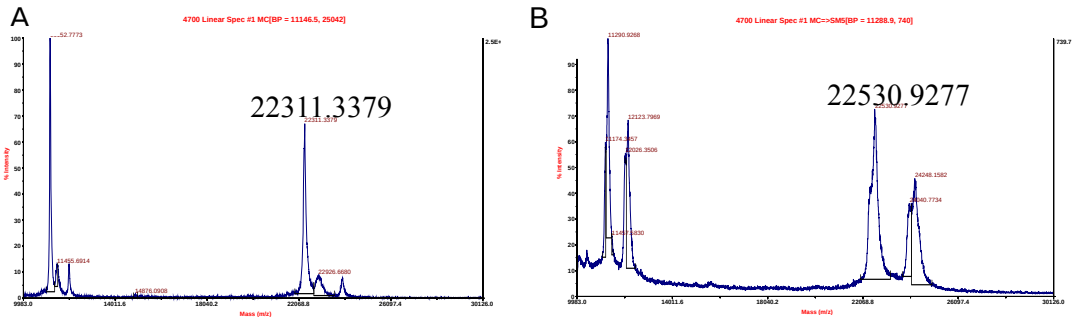

Figure 4.3 Mass Spectrometry of native and SeMet Der f 7. The substitution of Se atoms was confirmed using MALDI-TOF MS experiments. The mass shift of approximately 219.59 Da from the native recombinant Der f 7 **A)** and SeMet recombinant Der f 7 **B)** indicates the substitution of five L-Selenium atoms.

4.2 Crystallization and data collection of SeMet recombinant Der f 7

The initial crystals of Der f 7 were too small and fragile for the diffraction studies, despite the observable polarization (Figure 4.4A). The crystallization was further optimized by varying the pH of the reservoir buffer, the concentration of the protein as well as the crystallizing temperature. The best diffracting crystals of recombinant Der f 7 were grown from a reservoir solution consisting of 0.1 M Bis-Tris pH 7.4 and 28% PEG MME 2000 at 20°C. The SeMet crystals of recombinant Der f 7 were grown to approximately 0.34 * 0.25 * 0.2 mm within 1 week (Figure 4.4B).

A high-resolution data set was collected to 2.24 Å using the best crystal of SeMet recombinant Der f 7 (Figure 4.5**)**. The crystals of recombinant Der f 7 belonged to the space group $P2_12_12_1$ with two molecules in one asymmetric unit. The unit cell parameters were a = 50.2 Å, b = 58.7 Å, c = 123.8 Å and the solvent content was ~ 43.7% with Matthews constant of 2.16 $Å^3$/Da (Kantardjieff & Rupp, 2003), assuming the presence of two molecules in one asymmetrical unit. The detailed statistics for the SeMet crystal of recombinant Der f 7 can be seen in Table 4.1. Overall, the quality of the data collected using SeMet crystal was better than that of the native crystals (data not shown). Therefore, the subsequent structural determination was carried out using the data collected from the SeMet crystal.

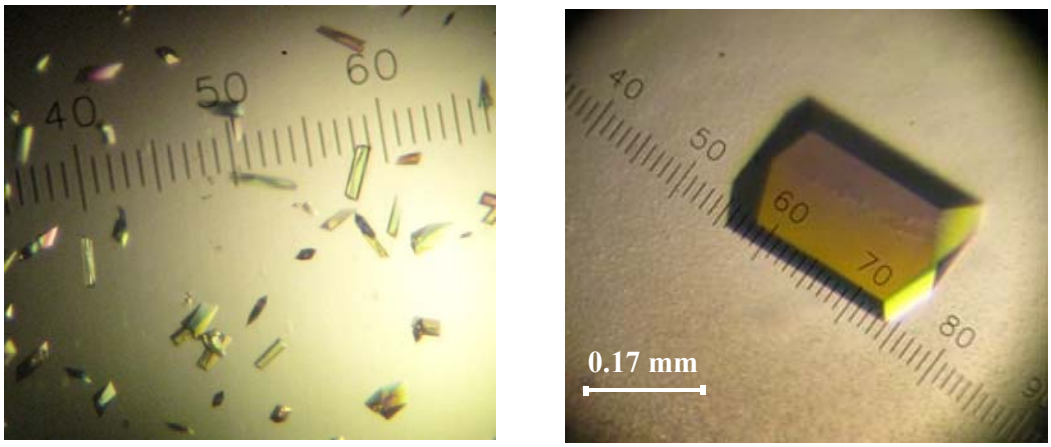

A **B**

Figure 4.4 Crystals of recombinant Der f 7. A) Initial crystals formed by native recombinant Der f 7. **B)** Optimized crystal formed by SeMet recombinant Der f 7.

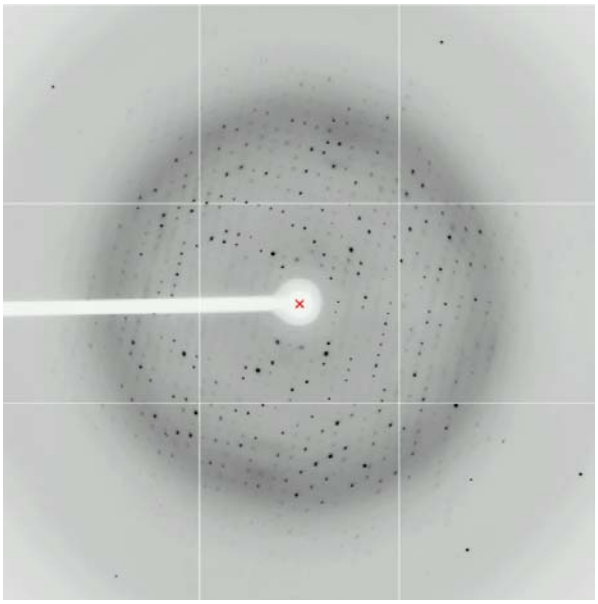

Figure 4.5 Diffraction pattern of SeMet Der f 7. The best SeMet recombinant Der f 7 crystal was diffracted to 2.24 Å resolution. Data collection was done on beamline BL-13B at National Synchrotron Radiation Research Center (NSRRC), Taiwan.

Table 4.1 Refinement statistics for Der f 7

	Peak	Inflection	High Resolution
Beamline (BNL)	BL-13B	BL-13B	BL-13B
Wavelength (Å)	0.97920	0.97939	0.96360
Oscillation angle (°)	0.5	0.5	0.5
Space group	$P2_12_12_1$	$P2_12_12_1$	$P2_12_12_1$
Unit-cell parameters			
a (Å)	50.26	50.19	50.19
b (Å)	58.81	58.66	58.67
c (Å)	123.94	123.81	123.81
Resolution limits (Å)	30.0-2.27 (2.35-2.27)	30.0-2.27 (2.35-2.27)	30.0-2.24 (2.32-2.24)
Observed *hkl*	163589	96729	100187
Unique *hkl*	17333	17373	33587
Redundancy	9.4 (6.5)	5.6 (5.1)	3.0 (2.6)
Completeness (%)	97.8 (87.7)	98.1 (90.9)	97.9 (90.9)
Overall $I/\sigma(I)$	33.42 (3.66)	19.98 (4.78)	22.38 (3.08)
R_{sym} (%)	4.6 (39.4)	5.0 (31.7)	3.1 (27.6)

Rsym = Σ |*Ii* - <*I*>| / Σ |*Ii*|, where *Ii* is the intensity of the *i*th measurement and <*I*> is the mean intensity for that reflection.

4.3 Crystal Structure of Der f 7

The final model of Der f 7 was solved and consisted of two molecules in one asymmetrical unit, in which one molecule was interacting with another in an inverted fashion (Figure 4.6). This model agreed very well with the Matthew's constant of 2.16 $Å^3$/Da as described earlier. There are 63 well-defined water molecules added in the model, and refinement was continued until the R-value converged to 0.24 (R_{free} = 0.29) for reflections I>σ (I) to 2.8 Å resolution. The model had good stereochemistry, with all residues within the allowed regions of the Ramachandran plot (Table 4.2) analyzed by PROCHECK (Laskowski *et al.* 1993). The structure of Der f 7 has a "super-roll" conformation as described in the CATH database (Pearl, Todd et al. 2005). The N-terminal consisted of an α-helix, followed by eleven β-sheets that wrap around the C-terminal α-helices. The first two β-sheets separated by a flexible loop (Lys-7 to Gln-25 and Met-32 to Val-34) were aligned in an antiparallel manner

with the third β-sheet (Gly-52 to Arg-62). Following the third β-sheet, there was a short α-helix (Leu-64 to Gln-66) and two short β-sheets (Met-67 to Arg-69 and Asn-74 to Lys-76). There were six antiparallel β-sheets discontinued by flexible loops (Val-82 to Val-90, Val-95 to Leu-105, Thr-111 to Gln-119, Val-122 to Ile-129, Thr-136 to Val-142 and Asn-147 to Ile-152) before the protein ended with a long C-terminal α-helix (Pro-160 to Leu-193) (Figure 4.10). The N-terminal helix seems to form a cleft together with the end of the C-terminal helices as well as the adjacent β-sheets. Based on the analysis of several homologous proteins, which will be discussed in further detail in the next section, this cleft could interact with an unknown ligand that could be important for the biophysical function of Der f 7 (Figure 4.7A).

The overall structure of Der f 7 is very similar to Der p 7, as they shared 86% sequence identity. When superimposed, these proteins showed a backbone R.M.S.D. of 0.577Å (Figure 4.8). The surfaces of both proteins were highly charged with predominantly negative charges (Figure 4.9). In general, the structure of Der f 7 shows low-to-moderate B-factor as depicted in Figure 4.7B. A few regions showed particularly high B-factor: from residues E24 to T28, R43 to D49, H91 to D93 and P130 to I135. Coincidently, Mueller and coworkers also reported that residues from R43 to I47 were missing in chain B of Der p 7 structure. The first five residues are untraceable in both chains of Der f 7 structure, but all chains of Der p 7 show complete set of residues at the N-terminus. When superimposed, both chains of Der f 7 structure yield the R.M.S.D. 0.005 Å for 191 Cα atoms.

Table 4.2 Refinement statistics for Der f 7

Data set	Der f 7 (6-196)
Mosaicity range	0.42 – 0.76
Refinement statistics:	
Rcryst (%)	24
Rfree	29.8
No. of waters	63
Overall mean B value (Å^2)	51.94
Average for molecule A	50.52
Average for molecule B	53.35
r.m.s. deviation from ideal values	
Bond length (Å)	0.003
Bond angle (°)	0.96
Dihedral angle (°)	16.16
Ramachandran statistics	
Residues in most favored regions (%)	89
Residues in additionally allowed regions (%)	8.4
Residues in generously allowed regions (%)	2.6
Residues in disallowed regions (%)	0

r.m.s. Root mean squared.
Rcryst = Σ ||Fo| - |Fc||/ Σ|Fo| calculate from the working data set.
Rfree was calculated from 5% of data randomly chosen not to be included in refinement.
Ramachandran results were determined using PROCHECK

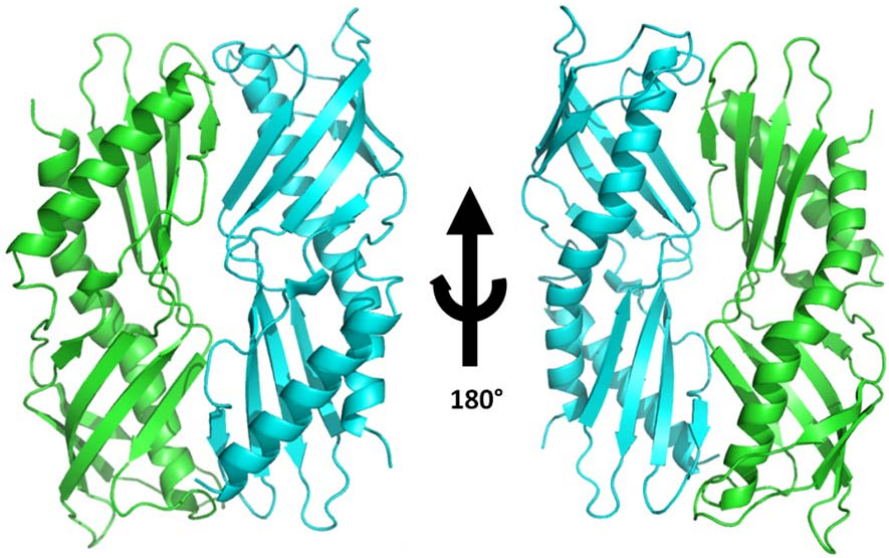

Figure 4.6 The final model of Der f 7 crystal structure. There are two molecules in one asymmetrical unit, in which one molecule is interacting with another in an inverted fashion. This model agrees with the Matthews constant of 2.16 Å^3/Da (Kantardjieff & Rupp, 2003). Models are generated using PyMOL (Delano Scientific) software.

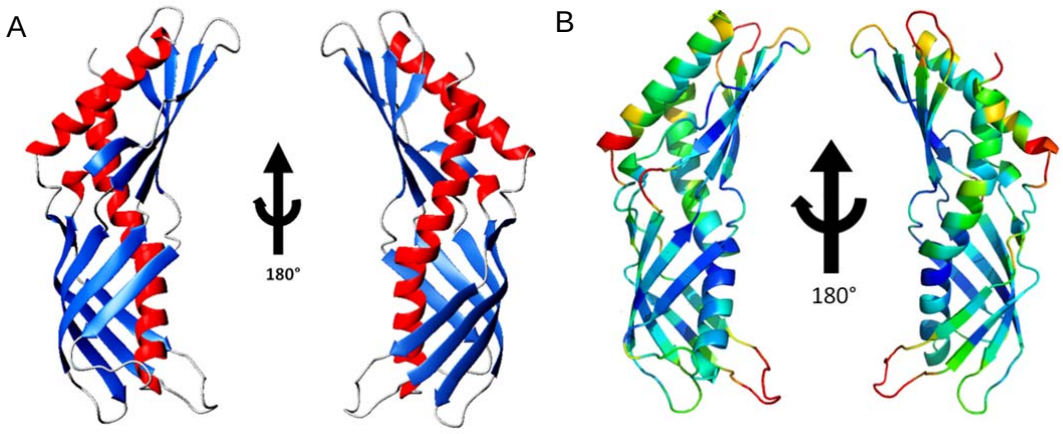

Figure 4.7 Ribbon diagram of Der f 7 crystal structure. A) Der f 7 consists of both α-helices (red colored) and β-sheet (blue colored) secondary structures. The N-terminal helices seemed to form a cleft together with the end of the C-terminal helices as well as the adjacent β-sheets which could be a ligand binding site for Der f 7. Models are generated using MOLMOL software (Koradi, Billeter et al. 1996). **B)** shows the Der f 7 structure from chain A colored by relative B factor, where red is high (>80) and blue is low(<30). Models are generated by PyMol (Delano Scientific).

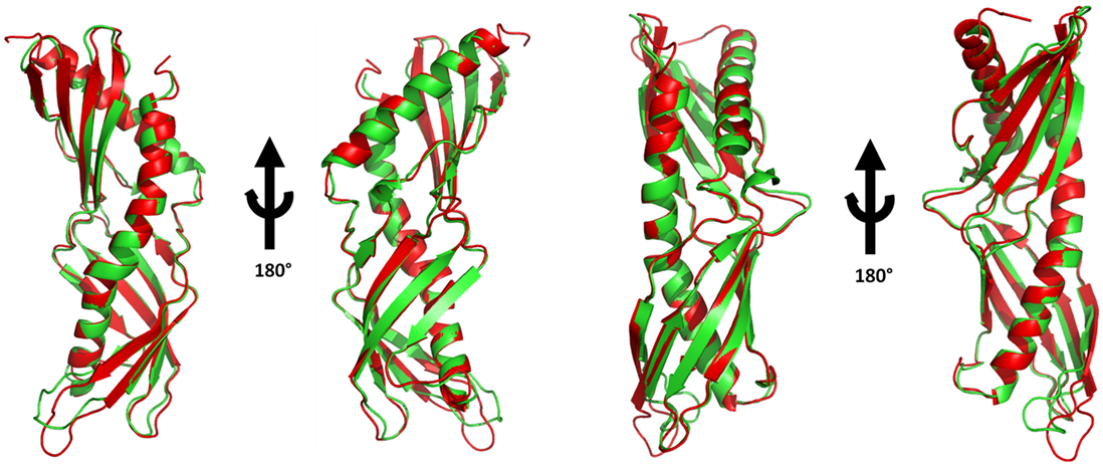

Figure 4.8 Superimposition of Der f 7 and Der p 7. The overall structure of Der f 7 (green colored) is very similar to Der p 7 (red colored), its homologous protein sharing 86% sequence identity. When superimposed, these proteins showed a backbone root means square deviation (r.m.s.d) of 0.577 Å. Models are generated using PyMOL (Delano Scientific) software.

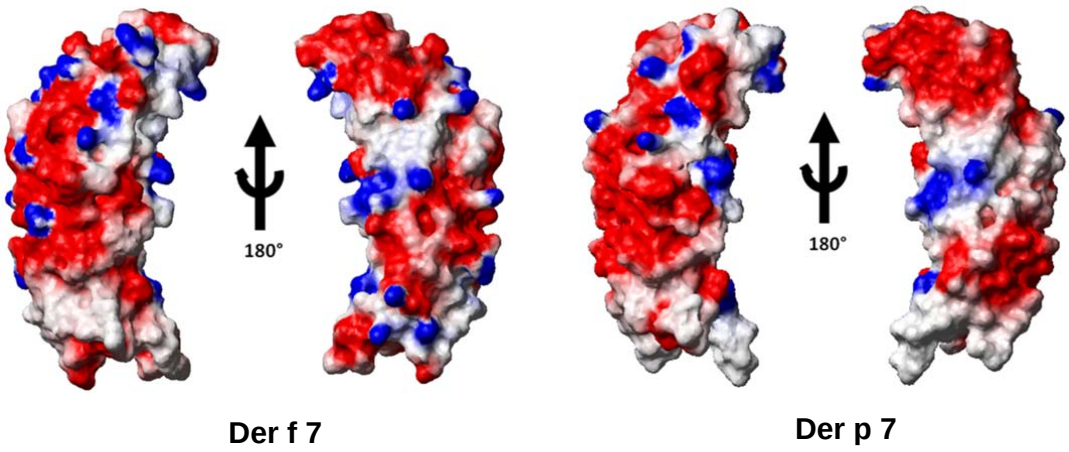

Figure 4.9 Surface charge distribution of Der f 7 and Der p 7. The surface of both proteins is highly charged. It seems that negatively charged patches (red colored) dominate both proteins, and Der f 7 seems to bear slightly more positive charge patches (blue) compared to Der p 7. Surface charged diagrams are generated using MOLMOL software (Koradi, Billeter et al. 1996).

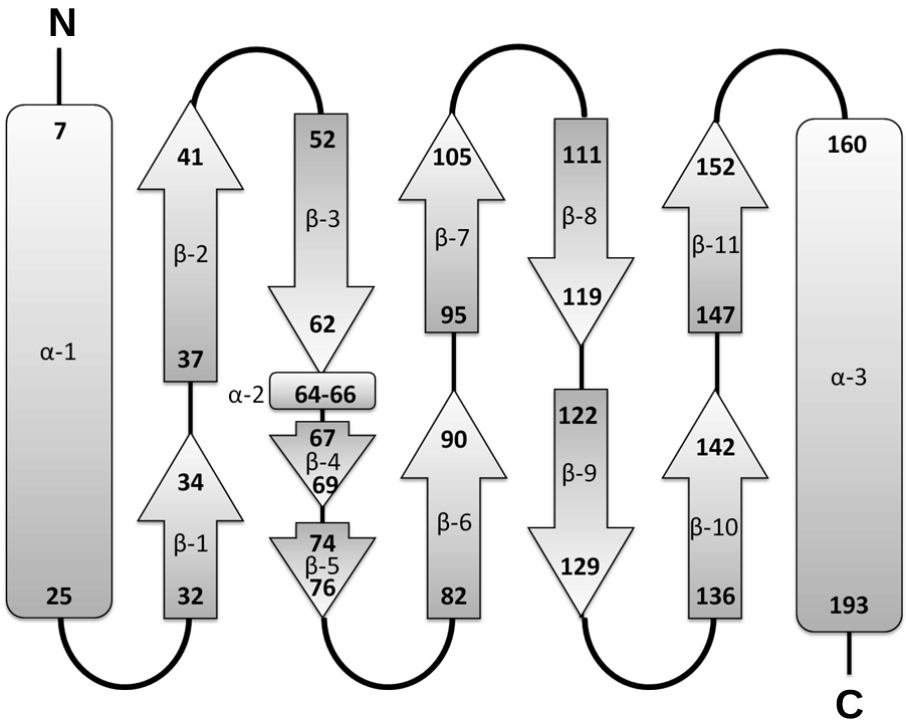

Figure 4.10 Secondary structure topology of Der f 7. There are altogether three α-helices (cylinders) and eleven β-sheets (block arrows) in Der f 7. The numbers of the residues are labeled marking the beginning and the end of the secondary structures. Loops and unstructured regions are represented by black solid curves and lines respectively.

4.4 Structural homology

Despite its high sequence identity with Der p 7, there is no clue regarding the possible function of Der f 7. It was reported that Der p 7 could be related to a family of proteins involved in human innate immune recognition of bacterial lipid products. However, there was no direct experimental evidence that supports the hypothesis. Even though Der p 7 was shown to bind to polymyxin B (PB), the binding was very weak and therefore, implying that PB was not a natural ligand for Der p 7 (Mueller, Edwards et al. 2010). Since Der f 7 shows such a high sequence and structural homology with Der p 7, it is conceivable that Der f 7 could also interact weakly with PB and possibly, with another similar natural ligand binding to Der p 7.

The software DALI (Holm and Rosenstrom 2010) was employed to identify the proteins which are likely to be related to Der f 7 based on the overall protein folding. More than 500 hits were returned from the search and the top fifteen hits with the marginal match scores (z-score) of more than 10 were chosen for analysis (Table 4.3). Not surprisingly, the top matches are the maltose-binding periplasmic protein tagged Der p 7, followed by juvenile hormone binding protein (JHBP), bactericidal/permeability-increasing protein (BPI), takeout-like protein and cholesterol ester transfer protein. Interestingly, some major allergens also appear in the list, i.e., major pollen allergen Bet v 1, major cherry allergen Pru av 1 and major carrot allergen Dau c 1. The structure of these allergens belongs to the fold superfamily known as steroidogenic acute regulatory protein (StAR) related lipid transfer domain (START), which is initially identified as a lipid binding domain.

The striking similarity between Der f 7 and the JHBP from insects may imply similar functions shared by these proteins. JHBP is essential for transporting the juvenile hormone (JH) in the hemolymph of butterflies and moths (Kolodziejczyk, Bujacz et al. 2008). In insects, juvenile hormone is crucial in ensuring the growth of larvae, while preventing the metamorphosis cycles (Nijhout 1994). It is known that dust mites, albeit distinctively different from insects, also have the juvenile (larvae) stage. Hence, it is possible that the group 7 allergens from dust mites, owing to their high structural homology with JHBP, could be

involved in regulating the development of dust mites. The other insect-related protein that shows high homology with Der f 7 is the takeout-like protein, which was postulated to be involved in various aspects of the physiology and behavior of insects (Hamiaux, Stanley et al. 2009). The superimposition of Der f 7 with JHBP and takeout-like protein yielded an R.M.S.D. of 3.6 Å over 173 Cα atoms and 4.4 Å over 171 Cα atoms, respectively (Figure 4.11A and 4.11B). Coincidently, JHBP and takeout-like protein are known to bind to hydrophobic ligands, which is similar to the allergens composed of START domains.

Similar to Der p 7, Der f 7 shows significantly high structural homology to the N-terminal domain of bactericidal/permeability-increasing protein (BPI). BPI is a protein with potent killing activity against gram-negative bacteria by interacting with the surface lipopolysaccharide. An R.M.S.D. of 3.4 Å over 173 Cα atoms was achieved by overlaying the 3D structure of Der f 7 with the N-terminal domain of BPI protein (Figure 4.11C**).** Figure 4D shows the whole structure of the BPI protein. As it can be seen, the ligand (red sticks) is bound to the cleft similar to the one described in Der f 7 as well as Der p 7. The similar cleft found in JHBP from silkworm was also demonstrated to be interacting with the juvenile hormone III (Suzuki *et al.,* unpublished data). Therefore, it is possible that Der f 7 would employ the same cleft to interact with its natural ligand.

Table 4.3 Selected DALI matches to Der f 7.

No.*	PDB ID	Z-Score	R.M.S.D.	Length align	No.of residues	ID (%)	Name
1	3h4z-A	27.2	1.1	191	568	84	MBP-Der p 7
4	2rck-B	13.4	3.6	173	208	12	JHBP
7	2rqf-A	12.0	4.1	174	227	11	BPI
8	3a1z-C	11.8	4.8	173	212	11	Hemolymph JHBP
12	1ewf-A	11.3	3.4	173	456	15	BPI
13	3e8w-A	11.1	4.4	171	219	11	Takeout-like protein
15	2obd-A	10.5	3.9	174	472	11	Cholesteryl ester transfer protein
367	1h2o-A	3.5	4.1	105	159	11	Pru av 1 allergen
383	1fm4-A	3.4	3.9	103	159	8	Bet v 1 allergen
525	2wql-A	2.6	4.5	104	152	10	Dau c 1 allergen

* The omitted numbers represent different chains from the same proteins (1-15)

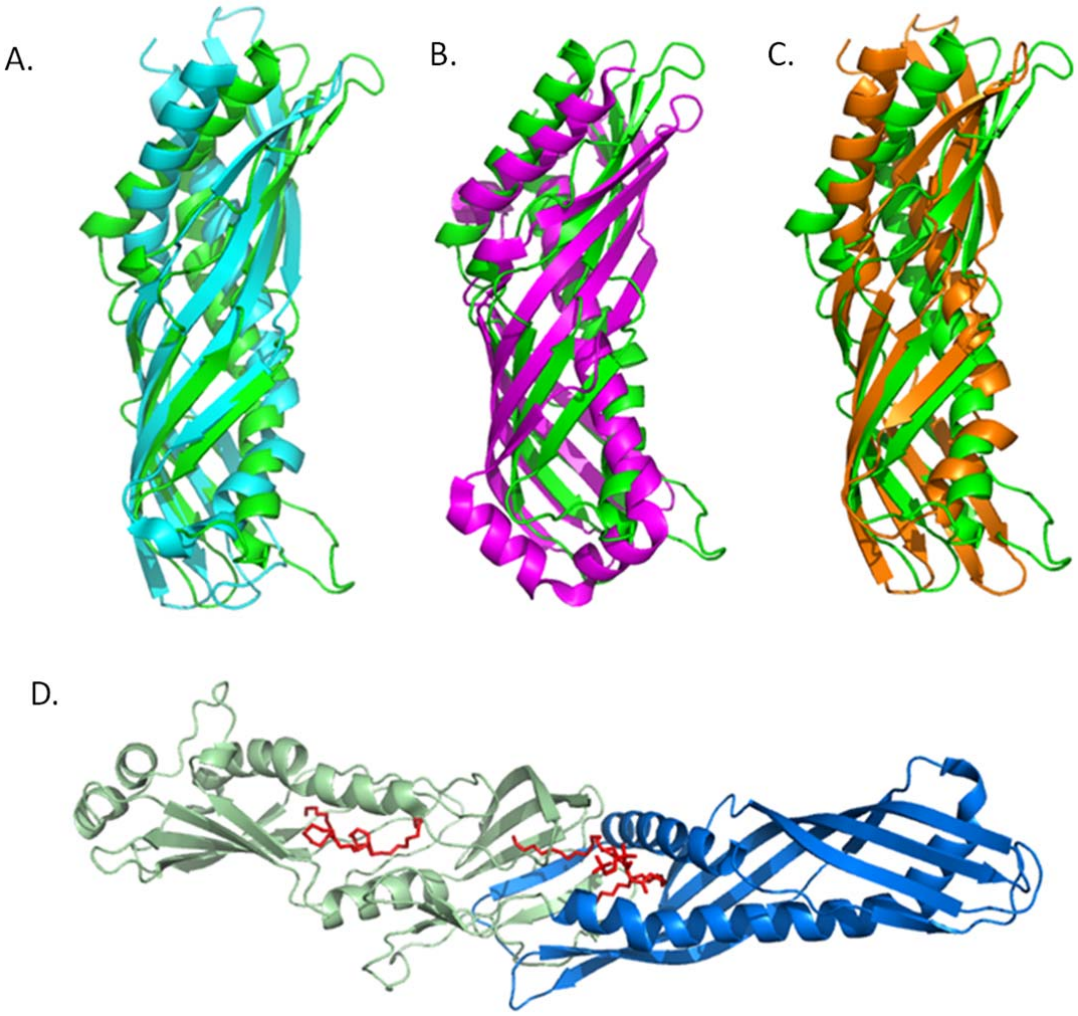

Figure 4.11 Superimposition of Der f 7 with its homologous structures. Der f 7 is colored green in all panels. **A)** Der f 7 overlaid with takeout-like protein (cyan), **B)** JHBP (magenta) and **C)** BPI protein (orange). **D)** The crystal structure of BPI protein with two domains colored differently; the ligand 1,2-diacyl-sn-glycero-3-phosphocholine is portrayed as red coloured sticks.

4.5 NMR Studies on Der f 7

The cDNA of Der f 7 was subcloned into a modified pET-32a expression vector and was expressed at a high level in *E. coli* BL21 cells as a soluble His-tagged fusion protein at about 26 mg/L of His-tagged fusion protein in M9 minimal medium. Overnight thrombin digestion was carried out to remove the N-terminal His-tag, and the protein was purified to homogeneity using gel filtration column. The highly purified protein was dialyzed against 20

mM phosphate buffer at pH 7 and remained highly soluble at the concentration of 1 mM with no visible precipitation for seven days.

CD spectra showed that the secondary structure of Der f 7 was a mixture of α-helices and β-sheet, consistent with the CSI which showed that Der f 7 consisted of at least seven β-sheets flanked by two α-helices (Figure 4.13). A complete set of NMR spectra were acquired for Der f 7 as mentioned in the previous sections. The two-dimensional $^{1}H^{15}N$-HSQC is reasonably well with 185 countable amide resonance excluding the prolines and side chains (Figure 4.12). The completeness of the backbone assignment is about 86% (160 out of 185 residues assigned) but the overall side chains' assignment is less than 60%. Attempts to improve the completeness of the side-chain assignment by including the HCCH-TOCSY experiment were unsuccessful. Even though more side-chain protons could be assigned using HCCH-TOCSY spectrum, there were still about 20% of the side-chain protons which remained unresolved. The side-chain proton assignments were completely missing in two regions of the protein (Lys-40 to Gly-52 and Tyr-103 to Pro-110). It was later revealed that these regions are highly flexible based on the crystal structure of Der f 7. The solution structure of Der f 7 using NMR was extremely challenging as most of the side-chain atoms were missing in the spectrums. Coincidently, Mueller and coworkers had also reported similar problem while attempting to solve the structure of Der p 7 using NMR (Mueller, Edwards et al. 2010). As a result, we attempted to crystallize Der f 7 and solved its 3D structure using X-ray crystallography method. Even though the data acquired from the NMR experiments were not used for the structure determination of Der f 7, it proved to be useful in the subsequent experiments, including ligand binding and dynamics studies. The backbone assignment was not complete but it was sufficient for the aforementioned experiments with an aid of the crystal structure of Der f 7. The ligand binding study was conducted on Der p 7 using NMR experiments, and it was demonstrated that this allergen could bind weakly to polymyxin B. Similar studies had been carried out on Der f 7 using PB as well as other ligands, and the results will be presented in the later sections.

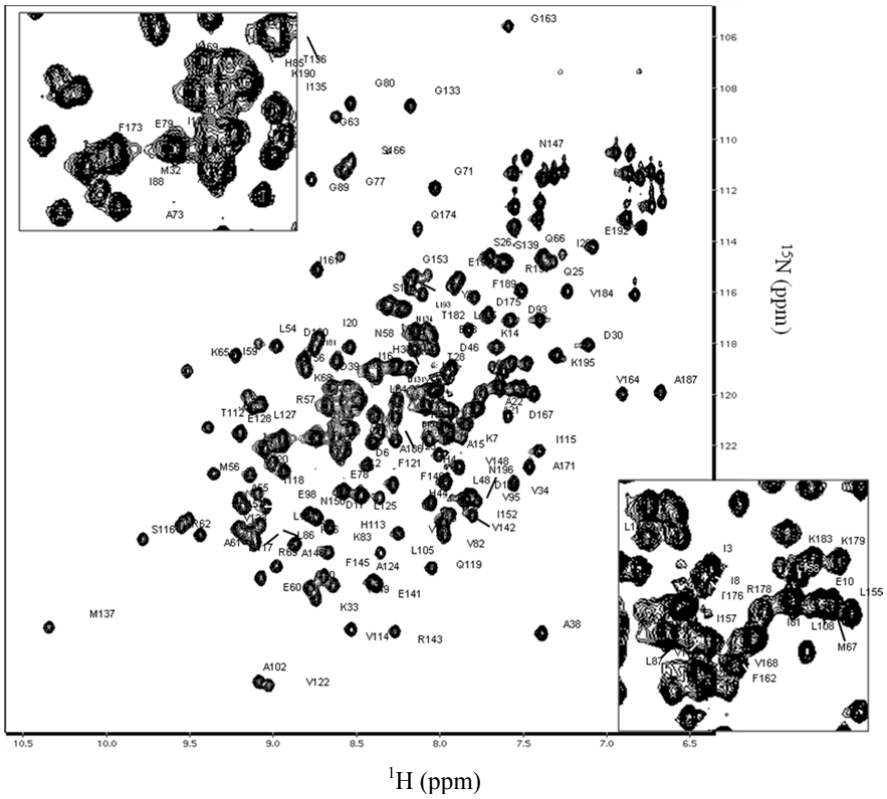

Figure 4.12 The two dimensional $^{1}H^{15}N$-HSQC of Der f 7 with backbone assignment shows that this protein is well-folded with generally well-dispersed amide resonances. The NMR spectrums were processed using NMRPipe software and the peaks assignment was done using SPARKY software.

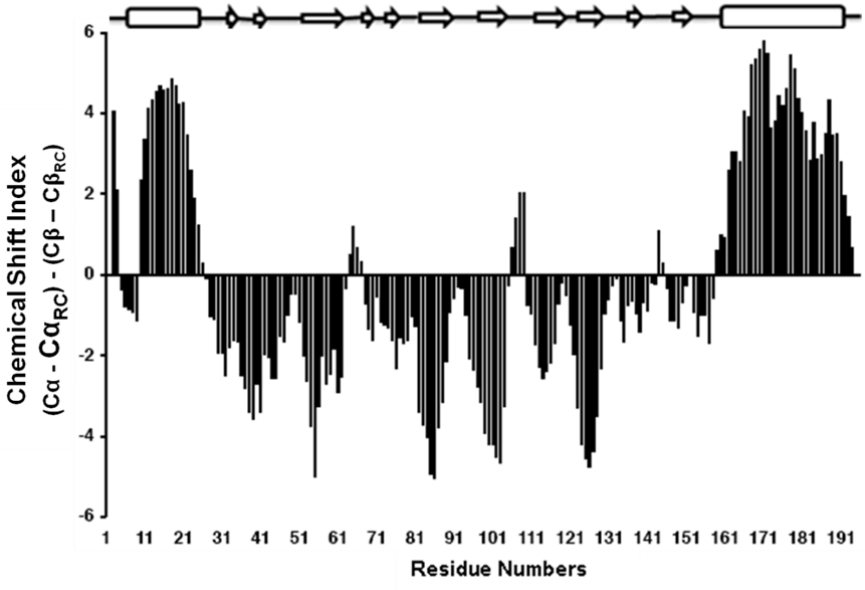

Figure 4.13 Chemical Shift Index (CSI) of Der f 7. Both terminus of Der f 7 consist of two α-helices which are separated by at least 10 β-sheets, agreeing with the crystal structure of this protein. Therefore, the NMR data should be reliable for the subsequent functional studies.

4.6 IgE Epitope mapping of Der f 7

Ever since the discovery of the group 7 allergen from dust mites by Shen and coworkers (Shen, Chua et al. 1993), numerous immunological characterizations had been conducted on the two representative proteins: Der f 7 and Der p 7, isolated from house dust mite *D. farinae* and *D. pteronysinnus*, respectively. Initially, the allergenicity of group 7 allergens from dust mite was characterized by means of immunoassay such as radio-immuno assay (RIA), immunoblots and skin prick test. All these experiments demonstrated that the group 7 dust mite allergens were clinically important and therefore, should be considered as a major source of allergen. Despite the relatively low prevalence of reactivity against the allergic sera (~50%), Der p 7 was, in some cases, shown to elicit a much higher IgE response when compared to Der p 2 protein, a major group 2 allergen from dust mites (Shen, Chua et al. 1996). Several monoclonal antibodies (mAbs) were also raised against Der f 7 and Der p 7 and were subsequently used to study their allergenicity and cross-reactivity (Shen, Chua et al. 1995; Shen, Chua et al. 1996; Shen, Lin et al. 1997).

Recently, there were updates on the putative IgE epitopes on the Der f 7. Using twenty overlapping peptides, Shen and coworkers showed that the binding activity of one of the mAbs, HD12, was inhibited by the peptides bearing common residues Leu-48 and Phe-50 in Der f 7. These residues were located at the flexible region between β-2 and β-3 of Der f 7 crystal structure (Figure 4.26). Since HD12 was shown to be able to inhibit the IgE binding up to 26%, it was also proposed that Leu-48 and Phe-50 could be the IgE binding residues as well. The authors suggested that the aforementioned residues were responsible for the specificity of HD12 mAbs against Der f 7 since the corresponding peptides derived from Der p 7 were not able to inhibit the HD12 antibody binding to Der f 7 (Shen, Tam et al. 2011). These results implied that Der f 7 and Der p 7 were using different epitopes to interact with HD12 mAbs and possibly, IgE antibodies.

According to their earlier studies, there were four mAbs that could specifically interact with Der f 7 - HD2, HD4, HD10 and HD12 - (Shen, Lin et al. 1997). It was shown that HD10 and HD12 antibodies were cross inhibitory, but HD2 and HD4 antibodies, which were cross inhibitory to each other, were not cross inhibiting with HD10 and HD12 antibodies. It is possible that the HD2 and HD4 mAbs were interacting with different part of the Der f 7, thus explaining the lack of cross-reactivity with HD10 and HD12 antibodies. Indeed, the binding of both HD2 and HD4 antibodies to the wild-type Der f 7 were not inhibited by any of the peptides tested. Perhaps the HD2 and HD4 antibodies were interacting with the conformational epitopes in the Der f 7. In the same report, the authors had also mentioned HD19, a mAb that could specifically interact with Der p 7. It was demonstrated that the peptides derived from Der f 7 were unable to inhibit the binding activity of this antibody. Additionally, the corresponding sequence in Der p 7 was ^{46}GIIDL^{50} with substitution of Ile and Leu at position 48 and 50, respectively. Both data suggested that Der p 7 could be using unique epitopes to interact with different antibodies.

In this section, we attempt to investigate the IgE binding to residues Leu-48 and Phe-50 in both Der f 7 and Der p 7 using different approaches. As mentioned earlier, Shen and coworkers employed multiple peptide ELISA experiments to study the HD12 mAbs binding to Der f 7. This method proved to be effective in identifying the linear IgE epitopes as the peptides could at most represent the flexible and continuous regions in a protein. In some cases, even the flexible loop in a protein could be subjected to steric hindrance due to its proximity to the neighboring residues. As it can be seen in Figure 4.26, the position of residue Phe-50 near the hydrophobic core of Der f 7 could hinder its accessibility to the antibodies. In this case, the peptide derived from this region may not represent the real situation in the whole protein. In addition, there is no direct evidence showing that residues Leu-48 and Phe-50 are able to interact with the IgE antibodies.

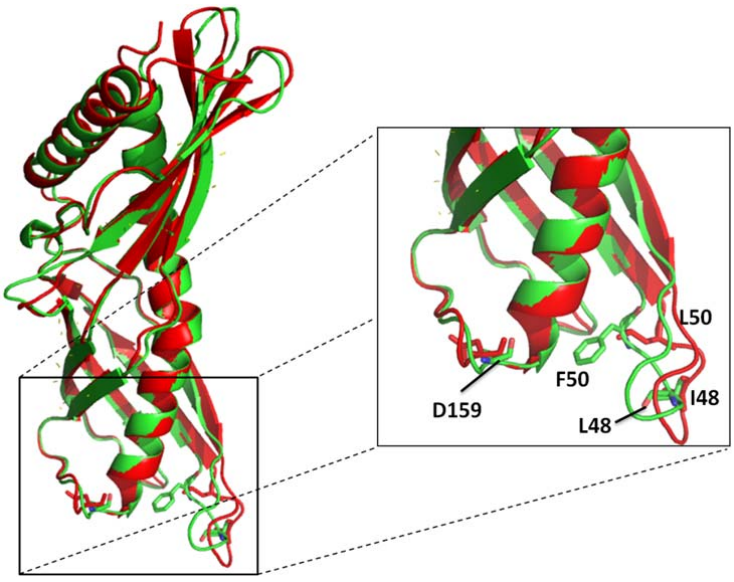

Figure 4.14 Locations of residues 48, 50 and 159 in Der f 7 and Der p 7 3D structures. The putative IgE epitopes are shown as sticks and labeled in the magnified diagram. As it can be seen, residue Leu-48 and Phe-50 in Der f 7 (green colored) are substituted for Ile-48 and Leu-50, respectively in Der p 7 (red colored), while residue Asp-159 is conserved in both proteins. Diagram generated using PyMOL software (DeLano Scientific).

4.6.1 Single mutant D159A & double mutant L48A_F50A

Using site-directed mutagenesis, we mutated both residues Leu-48 and Phe-50 to Ala in Der f 7. Similarly, residues Ile-48 and Leu-50 were mutated in Der p 7 and both double mutants were expressed and purified using the protocol described in chapter 2. The experimental procedure for ELISA was similar as described in the previous sections except that the Ni-NTA HisSorb™ ELISA plate (QIAGEN) was used. Maxiosorp™ ELISA plates (NUNC) showed inconsistent results even for the wild-type proteins (high standard deviations), probably due to the inconsistent binding of the proteins onto the plates. The Ni-NTA HisSorb™ ELISA plate could be a more reliable choice as it was reportedly designed for optimal binding to His-tagged proteins (QIAGEN).

Figure 4.27 shows that all patients are responding well to the wild-type proteins, though with different sensitivities. Even with the same dilution (1:10 ratio), patient P6 was almost twice as sensitive as patient P3. Briefly, Patient P3 showed slightly higher sensitivity to the Der f 7 compared to Der p 7. The Der f 7 double mutant showed reduced IgE binding

compared to the wild-type protein. In contrast, the Der p 7 double mutant did not show any reduction in IgE binding when compared to the wild-type protein. On the other hand, patient P6 showed almost equal IgE binding to wild-type Der f 7 and Der p 7 as well as their double mutants. Based on the results, it seems that residues Leu-48 and Phe-50 were probably the IgE epitopes for patient P3 but not P6. Consistently, the Der p 7 double mutant did not show any reduction in IgE binding in both patients' sera. This result agreed with the peptide ELISA experiment conducted by Shen et al (2011), which demonstrated the lack of inhibition of HD12 antibody by the peptides comprised of residues Ile-48 and Leu-50 from Der f 7. Our results showed that residues Leu-48 and Phe-50 could be involved in IgE binding in Der f 7 for certain individuals; larger sample size would be needed in order to further study their IgE binding reactivity.

In a separate account, Chou and coworkers described the critical role of residue Asp-159 in the IgE binding as well as the cross-reactivity between Der f 7 and Der p 7 (Chou, Tam et al. 2011). This residue is located in the loop region between β-11 and α-3 based on the 3D structure of the proteins (Figure 4.26). The authors performed dot-blot inhibition experiments by pre-absorbing the sera with the same set of peptides derived from Der f 7 (Shen, Tam et al. 2011). Their results showed that only the peptides with common sequence ^{156}SILDP^{160} were able interact with IgE antibodies in 2 out of 30 patients' sera tested. They later mutated residues Ile-157, Leu-158, and Asp-159 to Ala in the Der f 7 using site-directed mutagenesis and showed that these mutants have reduced IgE binding activities. Subsequently, using the dot-blot inhibition assay, the authors showed that only D159A mutant was unable to inhibit the IgE binding to the wild-type Der f 7 and Der p 7, thus concluded that Asp-159 was a core amino acid responsible for the IgE binding in these proteins.

A closer examination of the results provided by Chou and coworkers revealed several questionable points. Firstly, it was shown that the single mutants I157A, L158A, and D159A demonstrated drastic reduction in IgE binding compared to the wild-type Der f 7 based on the dot-blot assay in two patients' sera. Curiously, only D159A mutant was unable to inhibit the IgE binding to the wild-type protein. Theoretically, if a mutation resulted in a drastic

reduction in IgE binding compared to the wild-type protein, its inhibition of IgE binding to the wild-type protein should be reduced as well. However, based on their results, the IgE inhibition activity of I157A and L158A single mutants seemed to be as good as the wild-type protein itself. Secondly, the peptide derived from Der p 7, Dp7-16 (^{151}HIGGLSILDPIFAVL^{165}) which was essentially identical to the corresponding peptide derived from Der f 7, Df7-16 (^{151}HIGGLSILDPIFGVL^{165}), except for the Ala to Gly substitution at position 163, was showing much higher inhibition to the wild-type Der f 7 (89%) compared to the peptide Df7-16 (62%). Since the proposed antigenic determinant triad "ILD" was conserved in both peptides, it was rather peculiar that these peptides have such different inhibition activities. Thirdly, out of 30 patients' sera, only 2 (patients 990 and 1045) were exhibiting results consistent with the author's hypothesis, in which only one set of data was presented.

We mutated residue Asp-159 to Ala in both Der f 7 and Der p 7 using site-directed mutagenesis and prepared the mutants similarly as the wild-type proteins. As shown in Figure 4.27, the D159A single mutant does not show any reduction in IgE binding in both patients when compared to the wild-type proteins. Patient P3 showed a slight increment in IgE binding for the D159A mutant when compared to the wild-type Der f 7. A similar phenomenon was observed in the Der p 7 as well. Our results contradicted with the previous study that described Asp-159 residue as a critical amino acid involved in IgE binding of Der f 7 and Der p 7. Of course, it is very hard to derive any meaningful conclusion based on such a small sample size. Nevertheless, together with the data provided by Chou and coworkers, in which they showed that merely ~7% (2/30) of the samples were supporting their hypothesis, it would be reasonable to conclude that residue Asp-159 is not a major IgE epitope in both Der f 7 and Der p 7.

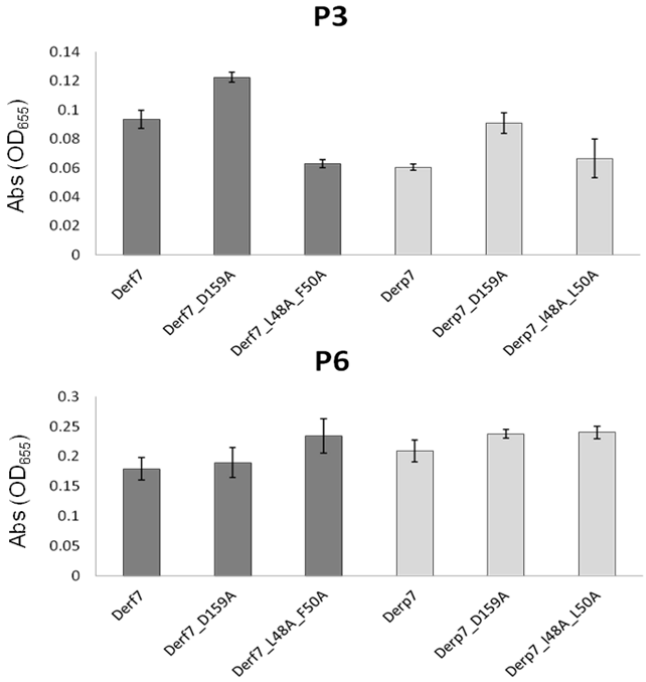

Figure 4.15 Specific IgE ELISA experiment comparing the allergenicity of Der f 7 and Der p 7 as well as their mutants. Dark gray bars represent the Der f 7 and its mutants while light gray bars represent Der p 7 and its mutants. All experiments were done using Ni-NTA HisSorb Plates (QIAGEN) and results are presented as the average values.

4.6.2 Cross inhibition between Der f 7 and Der p 7

The high sequence and structural homology shared by Der f 7 and Der p 7 prompted us to believe that the immunological properties of these proteins were similar, if not identical. However, based on the RIA experiment conducted on 41 asthmatic sera by Shen and-coworkers, it turned out that Der p 7 seemed to be much more allergenic than Der f 7 (Shen, Chua et al. 1995). Out of 41 samples, it was reported that 17 (41%) were reactive to both proteins, in which 76.5% (13/17) showed much higher sensitivity to Der p 7. In most cases, sera with high binding activity to Der p 7 were showing only one third (30%) reactivity to Der f 7. Clearly, the patients were co-sensitized to both allergens, but there was a distinct difference in terms of their reactivity towards these allergens. Owing to their similarities, it is very likely that they shared some IgE epitopes, thus explained their cross-reactivity (Chou, Tam et al. 2011). However, based on the RIA experiment, it is highly possible that Der p 7 has more IgE epitopes than Der f 7. Therefore, it is conceivable that these proteins would have limited cross-reactivity.

The end-point inhibition assay using 100μg/ml of the inhibitor (Der f 7 or Der p 7) was performed in order to examine the cross-reactivity between Der f 7 and Der p 7. As shown in Table 4.5, the Der p 7 can inhibit the IgE binding to Der f 7 very well for both patients' sera, whereas the IgE inhibition of Der f 7 against Der p 7 seems to be slightly weaker. Note that even the positive controls were showing only moderate inhibition (45.8-59.5% inhibition) in almost all cases except for the Der p 7 control in patient P6 (82.3% inhibition). Interestingly, the similar results were observed previously using the Maxisorp™ plates, although with high standard deviations (data not shown). The consistently moderate inhibitions as shown by the positive controls in our results implied that either the concentration of the inhibitor was not sufficient, or the affinity of the inhibitors towards the IgE antibodies was low. Either way, our results showed that the cross-reactivity between the Der f 7 and Der p 7 was generally high; with Der f 7 having slightly lower inhibition against Der p 7, at least for these two patients. Again, such a small sample size was hardly sufficient to represent the real cross-reactivity between these two proteins. More experiments need to be done with larger sample size.

Patients	**% Inhibition**		**% Inhibition**	
	Inhibitors		**Inhibitors**	
	Der f 7 (+)	**Der p 7**	**Der f 7**	**Der p 7 (+)**
P3	46.8	57.2	45.8	52.1
P6	53.4	59.5	67.7	82.3

Table 4.5 Endpoint inhibition assay for De f 7 and Der p 7. The Ni-NTA HisSorb plate was coated with 1μg/well of Der f 7 or Der p 7. Both sera were pre-absorbed with 100μg/ml of proteins for 24 hours at 4°C. Results are presented as an average values in percentage.

4.6.3 Putative IgE epitopes on Der f 7 and Der p 7

The cross-reactivity between pairs of highly homologous proteins had been studied in other groups of allergens isolated from dust mites. Chapman and coworkers showed that two group 1 major allergens from dust mites, Der f 1 and Der p 1 sharing 81% sequence identity were highly cross-reacting to each other. However, the anti-Der p 1/Der f 1 murine

monoclonal antibodies was shown to be unable to inhibit the binding of the specific human IgE to Der p 1, thus suggesting that Der p 1 and Der f 1 have different epitope binding sites for IgE and monoclonal antibodies (Chapman, Heymann et al. 1987). When the 3D structures of Der f 1 and Der p 1 were resolved later, the non-conserved residues were mapped on the surface diagrams in an attempt to explain the species-specific phenomenon as described by Chapman et al (1987). Chruszcz and coworkers showed that there were four non-conserved patches on the surface of Der f 1 and Der p 1, which could aid in identifying the residues responsible for the cross-reactivity and species-specificity of these proteins (Chruszcz, Chapman et al. 2009).

Likewise, Der f 2 and Der p 2, two major group 2 dust mite allergens were shown to be highly cross-reactive to each other. Interestingly, studies on the IgG binding to various isoforms of these proteins revealed different cross-reactivity. Der p 2 isoform, namely Der p 2.0101, showed low cross-reactivity with the natural Der p 2 (nDer p 2) compared to other isoforms tested (Der p 2.0102 and Der p 2.0103). The cross-reactivity of Der p 2.0101 isoform with nDer p 2 was restored by mutating residue D114 to N114, based on the sequence alignment with other isoforms. The authors concluded that the cross-reactivity of Der f 2 and Der p 2 was the result of conserved antigenic surface; substitution of even a single residue (D114N) could also result in a dramatic change in the cross-reactivity (Smith, Benjamin et al. 2001).

We attempted to identify the surface epitope of group 7 dust mite allergen by mapping the non-conserved residues between Der f 7 and Der p 7 on the crystal structure. This approach could help to identify the non-cross-reacting IgE epitopes between Der f 7 and Der p 7. As shown in Figure 4.28, 23 out of 29 non-conserved residues could be labeled on the surface diagram of Der f 7. Note that one of the postulated IgG/IgE epitopes Phe-50 was buried based on the surface diagram, so as other unlabeled non-conserved residues. Several surface patches were quite different between Der f 7 and Der p 7. A few patches which comprised of residues Q25K, A55D, E60Q, A124E and K179A on the Der f 7 structure were particularly interesting. These substitutions from charged for non-charged residues or vice-

versa could be a plausible explanation for the significant difference in terms of the allergenicity between these proteins. The rest of the residues were sharing similar properties, such as D18E and T111N. Nevertheless, it is still possible that these residues could be unique IgE epitopes in either protein, as the L48 for I48 substitution in the Der p 7 peptides indeed negated their interaction with the Der f 7-specific mAbs (Shen, Tam et al. 2011).

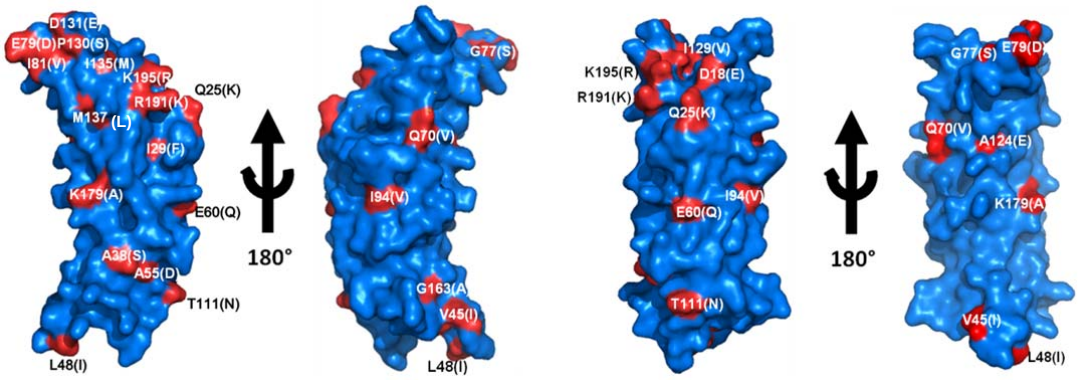

Figure 4.16 Surface diagram of Der f 7 in four different orientations. The conserved and non-conserved residues between Der f 7 and Der p 7 are colored in blue and red, respectively on the surface diagrams. The non-conserved residues are labeled and the bracketed labels represent the corresponding residues in Der p 7. Diagram generated using PyMOL software (DeLano Scientific).

To summarize, the IgE epitopes on Der f 7 and Der p 7 should be very similar based on their sequences and structural identities. However, Der p 7 seems to possess more IgE binding epitopes compared to Der f 7 since its allergenicity was much higher according to the data provided by Shen and coworkers (Shen, Chua et al. 1995). Residues Leu-48 and Phe-50 in Der f 7 might not be the major IgE epitopes, which is not surprising as they were only shown to bind to mAbs, even though it was reported that the particular mAbs was cross inhibitory with IgE antibodies up to 26% (Shen, Tam et al. 2011). On the other hand, residue Asp-159 was very unlikely to be a major IgE epitope in Der f 7 and Der p 7 based on our results and the published data (Chou, Tam et al. 2011). By comparing the non-conserved residues between Der f 7 and Der p 7 aided by the crystal structure, we proposed that residues Lys-25, Asp-55 and Glu-124 could be the unique IgE epitopes in Der p 7. More experiments need to be done in order to determine the IgE binding sites in these proteins.

4.7 Ligand binding studies

Thus far, the function of group 7 allergen from dust mites still remained a mystery. Even though the structure-based comparison using DALI server indicated a few homologous structures with known functions and ligands, but the previous studies on the ligand binding of Der p 7 failed to provide meaningful information (Mueller, Edwards et al. 2010). According to the authors, the attempts to bind Der f 7 to various types of lipid such as lipopolysaccharide (LPS), distearoyl phosphotidyl choline (DSPC), lyso- palmitoyl PC and N-octyl-glucoside were not successful based on the 2D $^{1}H^{15}N$-HSQC experiments. Surprisingly, the addition of polymyxin B that was known to sequester the LPS showed peak perturbations in the 2D $^{1}H^{15}N$-HSQC. Based on the mapping of the strongly perturbed residues in the Der p 7 crystal structure, the interaction site of PB resembled the ligand binding site of the homologous proteins, which was the cleft formed by the N and C-terminus of the protein. The striking resemblance led the authors to believe that the Der p 7 could be interacting with an unknown lipid, which was the common feature of several allergens (Thomas, Hales et al. 2005). It was suspected that these natural lipid adjuvants could be important in eliciting allergenicity for some allergens (Trompette, Divanovic et al. 2009).

In this section, the search for a possible ligand that could interact with group 7 allergens continues. It was shown that juvenile hormone III could complex with the homologous protein of Der f 7 - Juvenile hormone binding protein (JHBP) - from silk worm (Suzuki et al., unpublished data). Juvenile hormones are commonly known to be responsible in ensuring the growth of the larva, while preventing metamorphosis in insects (Nijhout 1994). Although dust mite belongs to a distant family from insect (Arachnid), it is known to undergo a larvae stage (Colloff 2009). The striking structural similarity of group 7 dust mite allergens and the insects JHBP prompted us to study the binding of JHIII to Der f 7. In addition, an analogue of JHIII -methoprene- was also included in the ligand binding studies. Methoprene was shown to be effective at suppressing the population growth of *D. farinae* (Downing, Wright et al. 1990), hence, it is a viable candidate as a ligand for Der f 7. Lastly,

the binding of PB to Der f 7 was also examined using the 2D $^{1}H^{15}N$ HSQC.

The 2D $^{1}H^{15}N$ HSQC spectrums indicated no peak perturbation with the addition of JHIII and methoprene at 1:1 ratio into the Der f 7 samples (data not shown). Similar results were obtained regardless of the extension of incubation time or increased ligand concentration (up to 1:5 ratio). These results showed that JHIII and methoprene were not interacting with the Der f 7. On the other hand, the addition of PB into the Der f 7 sample resulted in conspicuous peak shifts at 1:1 ratio (Figure 4.29). Subsequently, the peak shifts were analyzed and plotted against the residue number as shown in Figure 4.30. Several residues were showing significant perturbation, i.e. Ala-15, Ile-16, Ile-129, Leu-64, Ile-135, and Lys-194. These residues, together with the other ten residues with moderate perturbations were mapped on the 3D structure of Der f 7 (Figure 4.31).

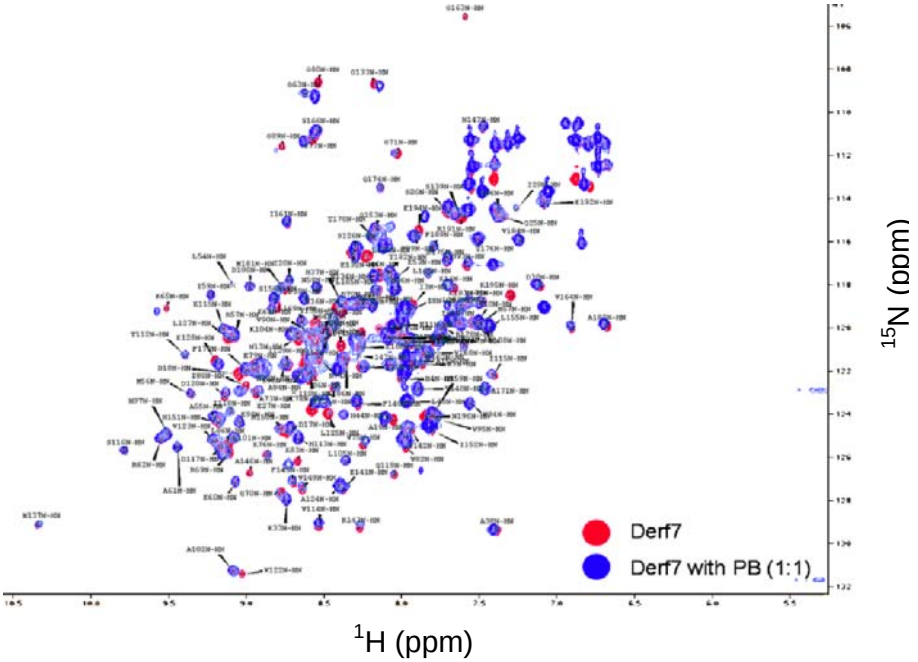

Figure 4.17 Peaks perturbation in the 2D-$^{1}H^{15}N$ HSQC of Der f 7 upon addition of Polymyxin B (PB). A number of peaks are perturbed upon addition of PB at 1:1 ratio. Red peaks represent apo-Der f 7 while blue peaks represent PB-bound Der f 7.

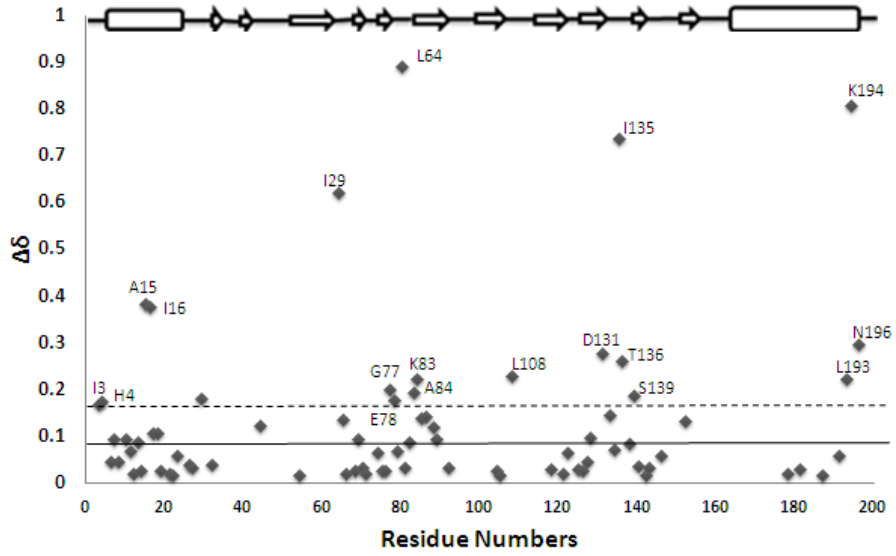

Figure 4.18 Chemical shift perturbation plot of Δδ versus residues of Der f 7 for the PB titration experiment. Solid line represents the mean value and the dashed line represents the mean +1 standard deviation

Figure 4.31 shows the comparison of the possible ligand interacting residues between Der f 7 and Der p 7. As it can be seen, the interaction site is similar between these proteins, but it seems that there are differences in the residues involved in the binding. The common residues that could be involved in the binding were Glu-78 and Asn-196, both located in the flexible regions. The other putative interacting residues were considerably different in these proteins. For example, residues Glu-11 and Ile-12 at the N-terminal α-helix were mapped on the Der p 7 crystal structure, but these residues were only weakly perturbed in Der f 7. Instead, residues Ala-15 and Ile-16 were the only two residues that were shown to be strongly perturbed in the N-terminal α-helix of Der f 7 structure. There is little information that can be obtained from this data, since PB is not a natural ligand for the group 7 dust mite allergens. Nevertheless, the comparison between the PB binding to Der f 7 and Der p 7 revealed that these proteins were using mostly different residues to interact with PB. Interestingly, \ some substitutions occurred in this region of thetwo proteins, such as the substitution of Ile-16, Ile-29, Gly-77 and Ile-135 in Der f 7 for Val-16, Phe29, Ser-77 and Met-135 in Der p 7.

Coincidentally, these residues were not mapped in the Der p 7 structure, probably due to their weaker perturbations.

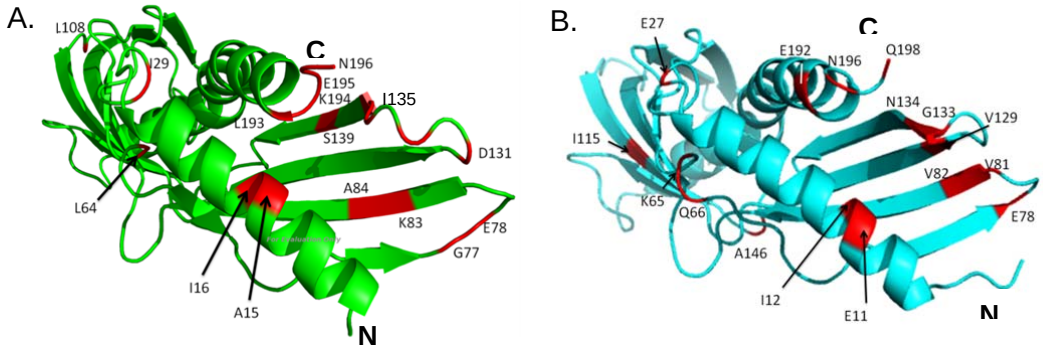

Figure 4.19 The 3D structure of Der f 7 and Der p 7 showing the possible residues involved in PB binding. A) The residues that have significant chemical shift perturbation as shown in Figure 4.32 are colored red in Der f 7. **B)** Similar experiment was conducted on Der p 7 by Mueller and Chang et al. (2010).

In conclusion, there is still no known ligand that could show better binding than PB to both Der f 7 and Der p 7 thus far. However, the binding to PB was weak and most likely unspecific. According to all the ligand binding data, it seems that Der f 7 and Der p 7 showed better affinity to a more hydrophilic substrate: PB is cationic, basic and acts like a surfactant with an estimated octanol-water partition coefficient of -5.62 (Molinspiration Cheminformatics, Slovensky Grob, Slovak Republic). Other ligand candidates which were more lipophilic in nature: DSPC (8.339), JHIII (4.27), methoprene (4.065), lyso- palmitoyl PC (-1.303) and N-octyl-glucoside (-1.432) did not show decent interaction with these proteins. A broader spectrum screening would be required to identify the natural ligand(s) for these proteins.

CHAPTER 5 CONCLUSION & FUTURE WORK

5.1 Structural studies and imuno-characterization of Blo t 21

Earlier studies showed that most dust mite-sensitized patients were co-sensitized to Blo t 21 and Blo t 5. Several publications demonstrated that allergens sharing high protein sequence identity usually would share similar IgE epitopes. The key question of our study is whether the generation of hypoallergen for Blo t 21 is necessary since it is sharing relatively high protein sequence identity with Blo t 5 (39%). Even though the cross-reactivity between these allergens were shown to be limited, but the underlying factors associated with this phenomenon was unknown. Therefore, we sought to explain the disparities between Blo t 21 and Blo t 5 with aids from the 3D structures, as well as means of immunological approaches.

In this thesis, we present the high-resolution three-dimensional structure of Blo t 21, a novel major allergen isolated from *B. tropicalis*. The 3D structure of Blo t 21 was successfully determined using NMR techniques with a backbone R.M.S.D. of 0.51 Å and heavy atom R.M.S.D. of 1.35 Å. The overall structure of Blo t 21 consists of a three antiparallel α-helical bundles arranged in a clockwise manner that resembles that of the Blo t 5. Despite sharing similar folding topology, the 3D structure of Blo t 21 is quite different from Blo t 5. When superimposed, these proteins yield the Cα R.M.S.D. of 3.39 Å. In addition, the surface charged diagram also shows that the distribution of charged residues of these two proteins is very different.

The differences in the 3D structure could contribute to the low-to-moderate cross-reactivity between Blo t 21 and Blo t 5. The IgE epitopes on Blo t 21 which were identified and confirmed using various functional assays are forming at least two epitope clusters as shown in its three-dimensional structure, in which one of them is a conformational epitope. This characteristic is significantly different from that in Blo t 5, which was shown to use a putative linear epitope in IgE binding. The two epitope clusters on Blo t 21 are considerably far apart from each other. Hence, there should be more than one IgE molecule binding to Blo t 21 at the same time. One of the epitope clusters which consists of residues Glu-74 and Asp-

79, could be interacting with the same IgE molecule that also binds to Blo t 5, thus explaining their cross-reactivity. However, another epitope cluster that comprised of residues Glu-89 and Asp-96, may bind to an IgE molecule that is unique to Blo t 21. Residue Glu-89 and Asp-96 are located close to each other based on the 3D structure of Blo t 21, thus, could form a conformational epitope. These observations indicate that Glu-89 and Asp-96 are two unique IgE epitopes found in Blo t 21.

Previously, Chan and coworkers (2008) showed that the sensitized sera could react to the peptides derived from the immunodominant region of Blo t 5, thus concluding that Blo t 5 bears a putative linear epitope. The sequence identity between Blo t 21 and Blo t 5 in this particular region is quite high (62%), and all the putative IgE epitopes determined in these proteins are present in this stretch of amino acids. We performed ELISA to compare the allergenicity of the peptides derived from this region of Blo t 21 and Blo t 5, with the initial hypothesis that their IgE binding activity should be similar. Surprisingly, the results show that most sera react much better to the Blo t 21-derived peptide compared to the Blo t 5-derived peptide. Similar peptides derived from Der f 21 and Der p 5 show distinct binding activities as well. These results show that the IgE antibodies interacting with this part of the protein are highly sequence dependant. The presence of the putative major epitopes in the homologous peptides derived from Blo t 21 and Blo t 5 does not seem to be the determining factors for the IgE binding. Rather, it seems that the adjacent amino acids are playing a major role in defining the IgE epitopes as well. This experiment also implies that the limited cross-reactivity between Blo t 21 and Blo t 5 is not just due to the presence of a unique conformational epitope, but also a linear epitope that recognizes unique IgE antibodies in Blo t 21.

We have also included Der f 21 and Der p 5 in this thesis. The physical and immunological studies reveal that these two allergens are distinctively different from Blo t 21 and Blo t 5. Most of our patients' sera react weakly to Der p 5, but respond fairly well to Der f 21. Based on the limited cross-reactivity between Der f 21 and Blo t 21, we propose that Der f 21 might be using a different set of IgE epitopes. Additionally, the generally weak

allergenicity exhibited by Der p 5 suggests that the IgE epitope of this protein should be different as well.

5.2 Future directions: Blo t 21

1) It has still remained uncertain whether our 4A mutant can be used as a hypoallergen for immunotherapy purposes. The potential of this mutant as a hyproallegen will be examined using means of *in vivo* approaches, including skin prick test, cytokine releasing profile and mouse immunization.
2) It would be interesting to identify the residues that confer a higher allergenicity to the Blo t 21-derived peptide. A set of peptides will be designed using the same boundaries with replacement at specific positions based on the sequence differences between Blo t 21 and Blo t 5. For example, residue Asp at position 81 in the Blo t 21-derived peptide will be replaced with Asn, matching the Blo t 5 sequence. Subsequently, the allergenicity of these peptides will be tested using ELISA. The replacement of a critical residue should reduce the IgE binding drastically compared to the original Blo t 21 peptide. Using this method, we should be able to pinpoint the residue(s) responsible for the higher allergenicity exhibited by Blo t 21.
3) Previously, Naik and coworkers (2008) studied the monoclonal antibodies' binding site of Blo t 5 using NMR approaches. Based on their studies, the mAbs binding sites are different from the IgE epitopes mapped later by Chan and coworkers (2008). It would be interesting to study the mAbs binding to Blo t 21. For instance, can the Blo t 21-specific mAbs inhibit the binding of Blo t 21 to IgE antibodies?
4) Our results show that Der f 21 and Der p 5 have limited cross-reactivity with Blo t 21 and Blo t 5. Identifying the IgE epitopes of these proteins could help to explain their distinct allergenic properties compared to Blo t 21 and Blo t 5. In addition, determining the 3D structure of Der f 21 would be interesting as it will help to locate the IgE epitopes.
5) The studies on the IgE epitopes mapping and cross-reactivity can be expanded to the

other group 5 and 21 allergen from different mite species (Lep d 5, Sui m 5, Sui m 21, Ale o 5 etc.). Sequence alignment shows that all four putative major IgE epitopes mapped in Blo t 5 and Blo t 21 are conserved in these allergens. However, there is limited data on the level of sensitization and cross-reactivity among the group 5 and 21 allergen from other mite species. Identifying the IgE epitopes and level of cross-reactivity in other mite species will provide us with a better picture on the allergenic properties of these proteins.

5.3 Crystal structure and IgE epitopes of Der f 7

Der f 7 was identified as a major allergen based on its IgE binding reactivity with 46% of sera from asthmatic children assayed by RIA technique (Shen, Chua et al. 1995). Besides that, the same authors also examined its interaction with mAbs extensively. Mueller and coworkers determined the crystal structure of its homologous protein, Der p 7 and it was shown to bind with polymyxin B (PB). Nevertheless, the weak binding implied that PB was not the natural ligand of Der p 7. The peptide immunoblot experiment conducted by Shen and Chou in the separate accounts suggested that residues Leu-48, Phe-50 and Asp-159 were the IgE epitopes in Der f 7. However, their data were not conclusive. Solving the structure of Der f 7 would be necessary to aid in identifying the major IgE epitopes in this allergen.

Here, we present the 3D structure of Der f 7 determined using X-ray crystallography technique. The initial attempts using NMR approaches were not successful due to the lack of NOEs that can be unambiguously assigned in order to obtain the final structure. The best crystal was diffracted to 2.24Å resolution using the synchrotron beamline. The final model was refined to the R-value converged to 0.24 (R_{free} = 0.29) for reflections $I>\sigma$ (I) to 2.8 Å resolution, and comprised of two molecules in an asymmetrical unit, with generally good stereochemistry. The 3D structure of Der f 7 consists of two α-helices forming the N and C-terminus, with the latter wrapped around by eleven β-sheets. This structure is essentially identical to that of Der p 7, with slight differences in the flexible regions when superimposed. The structure-based homology search using DALI server retrieved a list of lipid binding

proteins, which suggested that Der f 7 could interact with a lipid-like compound.

Der f 7 and Der p 7 were migrating in a non-conventional manner in SDS-PAGE. At pH 7, Der f 7 runs as 26 kDa, 25 kDa and 18 kDa bands while Der p 7 runs as 28 kDa, 25 kDa and 18 kDa bands. On the other hand, Der f 7 runs as a single band (25 kDa) while Der p 7 runs as two bands (28 kDa and 25 kDa) in SDS-PAGE at pH 9. It was later revealed that the band "splitting" was not due to protein degradation, rather, the aberrant mobility in SDS-PAGE seems to be affected by the composition of the charged residues. Our current data are not sufficient to explain these phenomena, but it led us to further study the stability of Der f 7 and Der p 7 at different pHs. We found that both proteins were much more stable at pH 7 compared to pH 9, with the Tm differed by at least 7°C. The factors underlying the higher stability of Der p 7 remain elusive. Attempts to stabilize Der f 7 via replacing charged residues mimicking that of Der p 7 were unsuccessful. Nevertheless, there could be a correlation between the physical properties of these proteins and their respective allergenicity. Shen and coworkers (1995) showed that Der p 7 is significantly more allergenic than Der f 7 in all sensitized test subjects. Furthermore, these allergens were shown to be interacting with different mAbs.

Based on the ELISA experiments, we showed that by replacing residues Leu-48, Phe-50 and Asp-159 to Ala in Der f 7, no significant reduction in IgE binding can be observed when compared to the wild-type protein. Therefore, these residues are unlikely to be the major IgE epitopes in Der f 7. The mapping of the non-conserved residues between Der f 7 and Der p 7 on the 3D structure of Der f 7 revealed that residues Lys-25, Asp-55 and Glu-124 could be the unique epitopes in Der p 7. The corresponding residues share different properties in Der f 7: Gln-25, Ala-55 and Ala-124, respectively, while the rests of the non-conserved residues are sharing similar properties, i.e. Ile to Val, etc.

The absence of peak shifts in the 2D-$^{1}H^{15}N$ HSQC spectrums upon the addition of JHIII or methoprene into the Der f 7 NMR samples indicated that these are not the probable ligands for Der f 7. Not surprisingly, Der f 7 shows notable peak perturbations with the addition of PB, but the affected residues are quite different from those reported previously in

Der p 7. We found that there are some substitutions of amino acids in the mutual binding sites of Der f 7 and Der p 7, i.e. Ile-16 and Ile-29 in Der f 7 are substituted for Val-16 and Phe-29 in Der p 7. Nonetheless, the information is inconclusive since PB is not a natural ligand for these proteins. Identifiation of the natural or homologous ligand for these proteins can be interesting since the bound forms could have different allergenic properties.

5.4 Future direction: Der f 7

1) The formation of a 18 kDa component in the SDS-PAGE is still a mystery. As mentioned, Shen and coworkers detected a similar component in the natural extract that interacts with specific mAbs. However, the identity of this component is unknown, though it was assumed to be a degraded form of Der f 7. It would be interesting to find out whether the 18 kDa component formed by the recombinant protein at pH7 also shows selective binding to the mAbs. This may help to explain the "splitting" phenomenon in SDS-PAGE. Similar experiment can be done based on Shen and coworkers' work, but the recombinant protein instead of natural extracts will be used.
2) There are only two sensitized sera used in our immunological work, therefore, the results are not conclusive. More samples will be needed to study the IgE binding to the Der f 7 mutants Q25K, A55D and A124E. In addition, cross-reactivity between Der f 7 and Der p 7 will be tested as well.
3) Broader screening of lipid-like compounds will be carried out to identify the natural or homologous ligand for Der f 7. Subsequently, the IgE binding reactivity of the bound form will be compared to the apo-form.
4) The major IgE epitopes of Der f 7 is still unknown. More residues will be chosen for mutagenesis studies based on the crystal structures of Der f 7 and Der p 7. A more comprehensive sequence alignment analysis, including the group 7 allergens from other mite species (Blo t 7, Lep d 7, Sui m 7, etc.) will be helpful in serving this purpose.

References

Abbas, A. K. and A. H. Lichtman (2003). Cellular and molecular immunology. Philadelphia, Saunders.

Akdis, C. A. and K. Blaser (2001). "Role of IL-10 in allergen-specific immunotherapy and normal response to allergens." Microbes and infection / Institut Pasteur **3**(11): 891-898.

Akinbami, L. (2006). "The state of childhood asthma, United States, 1980-2005." Advance data(381): 1-24.

Anfinsen, C. B. (1973). "Principles that govern the folding of protein chains." Science **181**(96): 223-230.

Banerjee, B., V. P. Kurup, et al. (2002). "C-terminal cysteine residues determine the IgE binding of Aspergillus fumigatus allergen Asp f 2." Journal of immunology **169**(9): 5137-5144.

Berka, K., P. Hobza, et al. (2009). "Analysis of energy stabilization inside the hydrophobic core of rubredoxin." Chemphyschem : a European journal of chemical physics and physical chemistry **10**(3): 543-548.

Bousquet, J., P. G. Holt, et al. (2008). Allergy and allergic diseases. Oxford ; Hoboken, NJ, Wiley-Blackwell.

Buhot, C., A. Chenal, et al. (2004). "Alteration of the tertiary structure of the major bee venom allergen Api m 1 by multiple mutations is concomitant with low IgE reactivity." Protein science : a publication of the Protein Society **13**(11): 2970-2978.

Chan, S. L., S. T. Ong, et al. (2006). "Nuclear magnetic resonance structure-based epitope mapping and modulation of dust mite group 13 allergen as a hypoallergen." Journal of immunology **176**(8): 4852-4860.

Chan, S. L., T. C. Ong, et al. (2008). "Nuclear magnetic resonance structure and IgE epitopes of Blo t 5, a major dust mite allergen." Journal of immunology **181**(4): 2586-2596.

Chan, S. L., T. C. Ong, et al. (2008). "Nuclear magnetic resonance structure and IgE epitopes of Blo t 5, a major dust mite allergen." J Immunol **181**(4): 2586-2596.

Chapman, M. D., P. W. Heymann, et al. (1987). "Epitope mapping of two major inhalant allergens, Der p I and Der f I, from mites of the genus Dermatophagoides." Journal of immunology **139**(5): 1479-1484.

Chapman, M. D., A. Pomes, et al. (2007). "Nomenclature and structural biology of allergens." The Journal of allergy and clinical immunology

119(2): 414-420.

Chew, F. T., D. Y. Goh, et al. (1999). "The economic cost of asthma in Singapore." Australian and New Zealand journal of medicine **29**(2): 228-233.

Chou, H., M. F. Tam, et al. (2011). "Asp159 is a critical core amino acid of an IgE-binding and cross-reactive epitope of a dust mite allergen Der f 7." Molecular immunology **48**(15-16): 2130-2134.

Christensen, L. H., E. Riise, et al. (2010). "Isoallergen variations contribute to the overall complexity of effector cell degranulation: effect mediated through differentiated IgE affinity." Journal of immunology **184**(9): 4966-4972.

Chruszcz, M., M. D. Chapman, et al. (2009). "Crystal structures of mite allergens Der f 1 and Der p 1 reveal differences in surface-exposed residues that may influence antibody binding." Journal of molecular biology **386**(2): 520-530.

Colloff, M. (2009). Dust mites. Collingwood, Victoria

Dordrecht, CSIRO Pub. ;

Springer.

Colloff, M. J. (2009). Dust Mites. New York, Springer**:** 448 p. ill 426.000 x 019.300 cm.

Cornilescu, G., F. Delaglio, et al. (1999). "Protein backbone angle restraints from searching a database for chemical shift and sequence homology." Journal of biomolecular NMR **13**(3): 289-302.

de Halleux, S., E. Stura, et al. (2006). "Three-dimensional structure and IgE-binding properties of mature fully active Der p 1, a clinically relevant major allergen." The Journal of allergy and clinical immunology **117**(3): 571-576.

De Marino, S., M. A. Morelli, et al. (1999). "An immunoglobulin-like fold in a major plant allergen: the solution structure of Phl p 2 from timothy grass pollen." Structure **7**(8): 943-952.

Delaglio, F., S. Grzesiek, et al. (1995). "NMRPipe: a multidimensional spectral processing system based on UNIX pipes." Journal of biomolecular NMR **6**(3): 277-293.

Denepoux, S., P. B. Eibensteiner, et al. (2000). "Molecular characterization of human IgG monoclonal antibodies specific for the major birch pollen allergen Bet v 1. Anti-allergen IgG can enhance the anaphylactic

reaction." FEBS letters **465**(1): 39-46.

Derewenda, U., J. Li, et al. (2002). "The crystal structure of a major dust mite allergen Der p 2, and its biological implications." Journal of molecular biology **318**(1): 189-197.

Downing, A. S., C. G. Wright, et al. (1990). "Effects of five insect growth regulators on laboratory populations of the North American house-dust mite, Dermatophagoides farinae." Experimental & applied acarology **9**(1-2): 123-130.

Emsley, P. and K. Cowtan (2004). "Coot: model-building tools for molecular graphics." Acta crystallographica. Section D, Biological crystallography **60**(Pt 12 Pt 1): 2126-2132.

Enrique, E., T. Malek, et al. (2008). "Sublingual immunotherapy for hazelnut food allergy: a follow-up study." Annals of allergy, asthma & immunology : official publication of the American College of Allergy, Asthma, & Immunology **100**(3): 283-284.

Fedorov, A. A., T. Ball, et al. (1997). "The molecular basis for allergen cross-reactivity: crystal structure and IgE-epitope mapping of birch pollen profilin." Structure **5**(1): 33-45.

Fernandez-Botran, R., V. M. Sanders, et al. (1988). "Lymphokine-mediated regulation of the proliferative response of clones of T helper 1 and T helper 2 cells." The Journal of experimental medicine **168**(2): 543-558.

Fernandez-Caldas, E. (2002). "Dust mite allergens: mitigation and control." Current allergy and asthma reports **2**(5): 424-431.

Fernandez, C., M. Martin-Esteban, et al. (1993). "Analysis of cross-reactivity between sunflower pollen and other pollens of the Compositae family." The Journal of allergy and clinical immunology **92**(5): 660-667.

Frank, S. A. (2002). Immunology and evolution of infectious disease. Princeton,, Princeton University Press.

Gajewski, T. F. and F. W. Fitch (1988). "Anti-proliferative effect of IFN-gamma in immune regulation. I. IFN-gamma inhibits the proliferation of Th2 but not Th1 murine helper T lymphocyte clones." Journal of immunology **140**(12): 4245-4252.

Gajhede, M., P. Osmark, et al. (1996). "X-ray and NMR structure of Bet v 1, the origin of birch pollen allergy." Nature structural biology **3**(12): 1040-1045.

Gao, Y. F., Y. Wang de, et al. (2007). "Identification and characterization of a novel allergen from Blomia tropicalis: Blo t 21." The Journal of allergy

and clinical immunology **120**(1): 105-112.

Garman, S. C., B. A. Wurzburg, et al. (2000). "Structure of the Fc fragment of human IgE bound to its high-affinity receptor Fc epsilonRI alpha." Nature **406**(6793): 259-266.

Grzesiek, S., H. Dobeli, et al. (1992). "1H, 13C, and 15N NMR backbone assignments and secondary structure of human interferon-gamma." Biochemistry **31**(35): 8180-8190.

Grzesiek, S., G. W. Vuister, et al. (1993). "A simple and sensitive experiment for measurement of JCC couplings between backbone carbonyl and methyl carbons in isotopically enriched proteins." Journal of biomolecular NMR **3**(4): 487-493.

Hamiaux, C., D. Stanley, et al. (2009). "Crystal structure of Epiphyas postvittana takeout 1 with bound ubiquinone supports a role as ligand carriers for takeout proteins in insects." The Journal of biological chemistry **284**(6): 3496-3503.

Hart, B. J. (1998). "Life cycle and reproduction of house-dust mites: environmental factors influencing mite populations." Allergy **53**(48 Suppl): 13-17.

Hayek, B., L. Vangelista, et al. (1998). "Molecular and immunologic characterization of a highly cross-reactive two EF-hand calcium-binding alder pollen allergen, Aln g 4: structural basis for calcium-modulated IgE recognition." Journal of immunology **161**(12): 7031-7039.

Higgins, D. G. (1994). "CLUSTAL V: multiple alignment of DNA and protein sequences." Methods in molecular biology **25**: 307-318.

Holgate, S. T. (2004). "The epidemic of asthma and allergy." Journal of the Royal Society of Medicine **97**(3): 103-110.

Holm, J., M. Gajhede, et al. (2004). "Allergy vaccine engineering: epitope modulation of recombinant Bet v 1 reduces IgE binding but retains protein folding pattern for induction of protective blocking-antibody responses." Journal of immunology **173**(8): 5258-5267.

Holm, L. and P. Rosenstrom (2010). "Dali server: conservation mapping in 3D." Nucleic acids research **38**(Web Server issue): W545-549.

Holm, L. and C. Sander (1998). "Touring protein fold space with Dali/FSSP." Nucleic acids research **26**(1): 316-319.

Hurtado, I. and M. Parini (1987). "House dust mites in Caracas, Venezuela." Annals of allergy **59**(2): 128-130.

Ichikawa, S., H. Hatanaka, et al. (1998). "Solution structure of Der f 2, the major mite allergen for atopic diseases." The Journal of biological chemistry **273**(1): 356-360.

Johnson, W. C., Jr. (1990). "Protein secondary structure and circular dichroism: a practical guide." Proteins **7**(3): 205-214.

Jutel, M., W. J. Pichler, et al. (1995). "Bee venom immunotherapy results in decrease of IL-4 and IL-5 and increase of IFN-gamma secretion in specific allergen-stimulated T cell cultures." Journal of immunology **154**(8): 4187-4194.

Karamloo, F., P. Schmid-Grendelmeier, et al. (2005). "Prevention of allergy by a recombinant multi-allergen vaccine with reduced IgE binding and preserved T cell epitopes." European journal of immunology **35**(11): 3268-3276.

Karisola, P., J. Mikkola, et al. (2004). "Construction of hevein (Hev b 6.02) with reduced allergenicity for immunotherapy of latex allergy by comutation of six amino acid residues on the conformational IgE epitopes." Journal of immunology **172**(4): 2621-2628.

Kay, A. B. (2008). Allergy and allergic diseases. West Sussex ; Hoboken, NJ, Wiley-Blackwell.

King, T. P., D. Hoffman, et al. (1994). "Allergen nomenclature. WHO/IUIS Allergen Nomenclature Subcommittee." International archives of allergy and immunology **105**(3): 224-233.

Kolodziejczyk, R., G. Bujacz, et al. (2008). "Insect juvenile hormone binding protein shows ancestral fold present in human lipid-binding proteins." Journal of molecular biology **377**(3): 870-881.

Kon, O. M. and N. Barnes (1997). "Immunosuppressive treatment in asthma." British journal of hospital medicine **57**(8): 383-386.

Koradi, R., M. Billeter, et al. (1996). "MOLMOL: a program for display and analysis of macromolecular structures." Journal of molecular graphics **14**(1): 51-55, 29-32.

Kuo, I. C., N. Cheong, et al. (2003). "An extensive study of human IgE cross-reactivity of Blo t 5 and Der p 5." The Journal of allergy and clinical immunology **111**(3): 603-609.

Kussebi, F., F. Karamloo, et al. (2005). "A major allergen gene-fusion protein for potential usage in allergen-specific immunotherapy." The Journal of allergy and clinical immunology **115**(2): 323-329.

Laskowski, R. A., J. A. Rullmannn, et al. (1996). "AQUA and PROCHECK-

NMR: programs for checking the quality of protein structures solved by NMR." Journal of biomolecular NMR **8**(4): 477-486.

Liew, F. Y. and I. B. McInnes (2002). "The role of innate mediators in inflammatory response." Molecular immunology **38**(12-13): 887-890.

McCoy, A. J., R. W. Grosse-Kunstleve, et al. (2007). "Phaser crystallographic software." Journal of applied crystallography **40**(Pt 4): 658-674.

Meno, K., P. B. Thorsted, et al. (2005). "The crystal structure of recombinant proDer p 1, a major house dust mite proteolytic allergen." Journal of immunology **175**(6): 3835-3845.

Midoro-Horiuti, T., V. Mathura, et al. (2003). "Major linear IgE epitopes of mountain cedar pollen allergen Jun a 1 map to the pectate lyase catalytic site." Molecular immunology **40**(8): 555-562.

Mirza, O., A. Henriksen, et al. (2000). "Dominant epitopes and allergic cross-reactivity: complex formation between a Fab fragment of a monoclonal murine IgG antibody and the major allergen from birch pollen Bet v 1." Journal of immunology **165**(1): 331-338.

Montelione, G. T., K. Wuthrich, et al. (1992). "Solution structure of murine epidermal growth factor determined by NMR spectroscopy and refined by energy minimization with restraints." Biochemistry **31**(1): 236-249.

Moverare, R., L. Elfman, et al. (2002). "Development of new IgE specificities to allergenic components in birch pollen extract during specific immunotherapy studied with immunoblotting and Pharmacia CAP System." Allergy **57**(5): 423-430.

Mueller, G. A., D. C. Benjamin, et al. (1998). "Tertiary structure of the major house dust mite allergen Der p 2: sequential and structural homologies." Biochemistry **37**(37): 12707-12714.

Mueller, G. A., L. L. Edwards, et al. (2010). "The structure of the dust mite allergen Der p 7 reveals similarities to innate immune proteins." The Journal of allergy and clinical immunology **125**(4): 909-917 e904.

Mueller, G. A., R. A. Gosavi, et al. (2010). "Der p 5 crystal structure provides insight into the group 5 dust mite allergens." The Journal of biological chemistry **285**(33): 25394-25401.

Mueller, G. A., A. M. Smith, et al. (2001). "Hydrogen exchange nuclear magnetic resonance spectroscopy mapping of antibody epitopes on the house dust mite allergen Der p 2." The Journal of biological chemistry **276**(12): 9359-9365.

Nadler, M. J., S. A. Matthews, et al. (2000). "Signal transduction by the high-

affinity immunoglobulin E receptor Fc epsilon RI: coupling form to function." Advances in immunology **76**: 325-355.

Naik, M. T., C. F. Chang, et al. (2008). "Roles of structure and structural dynamics in the antibody recognition of the allergen proteins: an NMR study on Blomia tropicalis major allergen." Structure **16**(1): 125-136.

Niederberger, V., B. Hayek, et al. (1999). "Calcium-dependent immunoglobulin E recognition of the apo- and calcium-bound form of a cross-reactive two EF-hand timothy grass pollen allergen, Phl p 7." The FASEB journal : official publication of the Federation of American Societies for Experimental Biology **13**(8): 843-856.

Niederberger, V. and R. Valenta (2004). "Recombinant allergens for immunotherapy. Where do we stand?" Current opinion in allergy and clinical immunology **4**(6): 549-554.

Nijhout, H. F. (1994). "Genes on the wing." Science **265**(5168): 44-45.

Norman, P. S., J. L. Ohman, Jr., et al. (1996). "Treatment of cat allergy with T-cell reactive peptides." American journal of respiratory and critical care medicine **154**(6 Pt 1): 1623-1628.

Olsson, S., M. van Hage-Hamsten, et al. (1998). "Contribution of disulphide bonds to antigenicity of Lep d 2, the major allergen of the dust mite Lepidoglyphus destructor." Molecular immunology **35**(16): 1017-1023.

Pearl, F., A. Todd, et al. (2005). "The CATH Domain Structure Database and related resources Gene3D and DHS provide comprehensive domain family information for genome analysis." Nucleic acids research **33**(Database issue): D247-251.

Petersen, T. N., S. Brunak, et al. (2011). "SignalP 4.0: discriminating signal peptides from transmembrane regions." Nature methods **8**(10): 785-786.

Ramachandran, G. N., C. Ramakrishnan, et al. (1963). "Stereochemistry of polypeptide chain configurations." Journal of molecular biology **7**: 95-99.

Robotham, J. M., S. S. Teuber, et al. (2002). "Linear IgE epitope mapping of the English walnut (Juglans regia) major food allergen, Jug r 1." The Journal of allergy and clinical immunology **109**(1): 143-149.

Roos, T. C., S. Geuer, et al. (2004). "Recent advances in treatment strategies for atopic dermatitis." Drugs **64**(23): 2639-2666.

Seiberler, S., O. Scheiner, et al. (1994). "Characterization of a birch pollen allergen, Bet v III, representing a novel class of Ca2+ binding proteins: specific expression in mature pollen and dependence of patients' IgE

binding on protein-bound Ca2+." The EMBO journal **13**(15): 3481-3486.

Shen, H. D., K. Y. Chua, et al. (1993). "Molecular cloning of a house dust mite allergen with common antibody binding specificities with multiple components in mite extracts." Clinical and experimental allergy : journal of the British Society for Allergy and Clinical Immunology **23**(11): 934-940.

Shen, H. D., K. Y. Chua, et al. (1996). "IgE and monoclonal antibody binding by the mite allergen Der p 7." Clinical and experimental allergy : journal of the British Society for Allergy and Clinical Immunology **26**(3): 308-315.

Shen, H. D., K. Y. Chua, et al. (1995). "Characterization of the house dust mite allergen Der p 7 by monoclonal antibodies." Clinical and experimental allergy : journal of the British Society for Allergy and Clinical Immunology **25**(5): 416-422.

Shen, H. D., K. Y. Chua, et al. (1995). "Molecular cloning and immunological characterization of the house dust mite allergen Der f 7." Clinical and experimental allergy : journal of the British Society for Allergy and Clinical Immunology **25**(10): 1000-1006.

Shen, H. D., W. L. Lin, et al. (1997). "Characterization of the allergen Der f 7 from house dust mite extracts by species-specific and crossreactive monoclonal antibodies." Clinical and experimental allergy : journal of the British Society for Allergy and Clinical Immunology **27**(7): 824-832.

Shen, H. D., M. F. Tam, et al. (2011). "Homology modeling and monoclonal antibody binding of the Der f 7 dust mite allergen." Immunology and cell biology **89**(2): 225-230.

Sicherer, S. H. and H. A. Sampson (2000). "Peanut and tree nut allergy." Current opinion in pediatrics **12**(6): 567-573.

Simons, F. E., M. Imada, et al. (1996). "Fel d 1 peptides: effect on skin tests and cytokine synthesis in cat-allergic human subjects." International immunology **8**(12): 1937-1945.

Smith, A. M., D. C. Benjamin, et al. (2001). "The molecular basis of antigenic cross-reactivity between the group 2 mite allergens." The Journal of allergy and clinical immunology **107**(6): 977-984.

Sordet, C., R. Culerrier, et al. (2009). "IgE-binding epitopic peptide mapping on a three-dimensional model built for the 13S globulin allergen of buckwheat (Fagopyrum esculentum)." Peptides **30**(6): 1021-1027.

Spangfort, M. D., O. Mirza, et al. (2003). "Dominating IgE-binding epitope of Bet v 1, the major allergen of birch pollen, characterized by X-ray crystallography and site-directed mutagenesis." Journal of immunology **171**(6): 3084-3090.

Stingl, G. and D. Maurer (1997). "IgE-mediated allergen presentation via Fc epsilon RI on antigen-presenting cells." International archives of allergy and immunology **113**(1-3): 24-29.

Swoboda, I., N. De Weerd, et al. (2002). "Mutants of the major ryegrass pollen allergen, Lol p 5, with reduced IgE-binding capacity: candidates for grass pollen-specific immunotherapy." European journal of immunology **32**(1): 270-280.

Takai, T., S. Ichikawa, et al. (2000). "Effects of proline mutations in the major house dust mite allergen Der f 2 on IgE-binding and histamine-releasing activity." European journal of biochemistry / FEBS **267**(22): 6650-6656.

Thomas, W. R., B. J. Hales, et al. (2005). "Structural biology of allergens." Current allergy and asthma reports **5**(5): 388-393.

Thomas, W. R., W. A. Smith, et al. (2002). "Characterization and immunobiology of house dust mite allergens." International archives of allergy and immunology **129**(1): 1-18.

Trombone, A. P., K. R. Tobias, et al. (2002). "Use of a chimeric ELISA to investigate immunoglobulin E antibody responses to Der p 1 and Der p 2 in mite-allergic patients with asthma, wheezing and/or rhinitis." Clinical and experimental allergy : journal of the British Society for Allergy and Clinical Immunology **32**(9): 1323-1328.

Trompette, A., S. Divanovic, et al. (2009). "Allergenicity resulting from functional mimicry of a Toll-like receptor complex protein." Nature **457**(7229): 585-588.

Turner, H. and J. P. Kinet (1999). "Signalling through the high-affinity IgE receptor Fc epsilonRI." Nature **402**(6760 Suppl): B24-30.

Valenta, R. (2002). "The future of antigen-specific immunotherapy of allergy." Nature reviews. Immunology **2**(6): 446-453.

Valenta, R., B. Hayek, et al. (1998). "Calcium-binding allergens: from plants to man." International archives of allergy and immunology **117**(3): 160-166.

Valenta, R. and D. Kraft (2002). "From allergen structure to new forms of allergen-specific immunotherapy." Current opinion in immunology **14**(6): 718-727.

Valenta, R., K. Niespodziana, et al. (2011). "Recombinant allergens: what does the future hold?" The Journal of allergy and clinical immunology **127**(4): 860-864.

van Neerven, R. J., T. Wikborg, et al. (1999). "Blocking antibodies induced by specific allergy vaccination prevent the activation of CD4+ T cells by inhibiting serum-IgE-facilitated allergen presentation." Journal of immunology **163**(5): 2944-2952.

Van Regenmortel, M. H. (1998). "From absolute to exquisite specificity. Reflections on the fuzzy nature of species, specificity and antigenic sites." Journal of immunological methods **216**(1-2): 37-48.

Visco, V., C. Dolecek, et al. (1996). "Human IgG monoclonal antibodies that modulate the binding of specific IgE to birch pollen Bet v 1." Journal of immunology **157**(2): 956-962.

Vondrasek, J., L. Bendova, et al. (2005). "Unexpectedly strong energy stabilization inside the hydrophobic core of small protein rubredoxin mediated by aromatic residues: correlated ab initio quantum chemical calculations." Journal of the American Chemical Society **127**(8): 2615-2619.

Vrtala, S., C. A. Akdis, et al. (2000). "T cell epitope-containing hypoallergenic recombinant fragments of the major birch pollen allergen, Bet v 1, induce blocking antibodies." Journal of immunology **165**(11): 6653-6659.

Vrtala, S., K. Hirtenlehner, et al. (1999). "Genetic engineering of recombinant hypoallergenic oligomers of the major birch pollen allergen, Bet v 1: candidates for specific immunotherapy." International archives of allergy and immunology **118**(2-4): 218-219.

Wang, H. and E. R. Zuiderweg (1995). "HCCH-TOCSY spectroscopy of 13C-labeled proteins in H2O using heteronuclear cross-polarization and pulsed-field gradients." Journal of biomolecular NMR **5**(2): 207-211.

Weghofer, M., Y. Dall'Antonia, et al. (2008). "Characterization of Der p 21, a new important allergen derived from the gut of house dust mites." Allergy **63**(6): 758-767.

Wills-Karp, M., J. Luyimbazi, et al. (1998). "Interleukin-13: central mediator of allergic asthma." Science **282**(5397): 2258-2261.

Wishart, D. S., B. D. Sykes, et al. (1992). "The chemical shift index: a fast and simple method for the assignment of protein secondary structure through NMR spectroscopy." Biochemistry **31**(6): 1647-1651.

Wopfner, N., O. Dissertori, et al. (2007). "Calcium-binding proteins and their role in allergic diseases." Immunology and allergy clinics of North America **27**(1): 29-44.

Zwart, P. H., P. V. Afonine, et al. (2008). "Automated structure solution with the PHENIX suite." Methods in molecular biology **426**: 419-435.

Appendix I

Recipe for M9 medium

To 773 ml of sterile water, add the following:

200 ml	5X M9
2 ml	1M $MgSO_4$
5 ml	20% Glucose
0.1 ml	1M $CaCl_2$
4 ml	0.25 g/ml NH_4Cl
1 ml	0.1 g/ml Ampicillin

Composition:

1. 5X M9

30 g	Na_2HPO_4
15 g	KH_2PO_4
2.5 g	NaCl

Add water to 1L
(Autoclave)

2. 0.25 g/ml NH4Cl

50 g NH_4Cl, add water to 200 ml
(Autoclave, or filter-sterilize for ^{15}N)

3. 20% Glucose

40 g Glucose, add water to 200 ml
(Autoclave or filter-sterilize for ^{13}C)

4. 1M $MgSO_4$

19.72 g $MgSO_4$, add water to 80 ml
(Autoclave)

5 1M $CaCl_2$

11.76 g $CaCl_2$, add water to 80 ml
(Autoclave)

Appendix II

Buffers for Ni-NTA Affinity Chromatography

• Nickel binding buffer

5 mM	Immidazole
0.5 M	NaCl
20 mM	Tris pH 8.0

• Elution Buffer

0.5 M	Immidazole
0.5 M	NaCl
20 mM	Tris pH 8.0

• Strip Buffer

100 mM	EDTA pH 8.0
0.5 M	NaCl
20 mM	Tris pH 8.0

• Ni-Charge buffer

50 mM $NiSO_4$

Buffers for Glutathione-Sepharose Chromatography

• Phosphate Buffer Saline (PBS)

140 mM	NaCl
2.7 mM	KCl
10 mM	Na_2HPO_4
1.8 mM	KH_2PO_4

• GST Elution Buffer

50 mM	Tris-Cl pH 8.0
10 mM	L-Gluthathione (reduced)

• Column Regeneration Buffer 1

0.1 M	Tris-Cl pH 9.0
0.5 M	NaCl

• Column Regeneration Buffer 2

0.1 M	Sodium acetate pH 4.5
0.5 M	NaCl

Appendix III

Recipe for SDS-PAGE

	15% Separating Gel	4% Stacking Gel
30% Acrylamide/0.8% Bis	3.5 ml	0.4 ml
Resolving Buffer	1.75 ml	-
Stacking Buffer	-	0.75 ml
10% SDS	70 µl	30 µl

Water	1.68 ml	1.8 ml
10% Ammonium	42 µl	30 µl
TEMED	4.2 µl	3 µl

1. Acrylamide solution (30%, 0.8 % Bis)
2. Resolving gel buffer: 1.5 M Tris, pH 8.8

   For 200 ml, 36.3 g of Tris adjust to pH 8.8 with HCl

3. Stacking gel buffer: 0.5 M Tris, pH 6.8

   For 200 ml, 12.1 g Tris, adjust to pH 6.8 with HCl

4. 10% Ammonium persulphate: 1 g Ammonium persulphate in 10 ml water
5. 10X Tank buffer: for 2 liters

   60 g Tris base
   288g Glycine
   200 ml 10% SDS solution
   Add water to 2 liters

6. 2X SDS gel sample buffer: for 50 ml

5 ml	Glycerol
6.25 ml	0.5 M Tris pH 6.8
12.5 ml	10% SDS
2.5 ml	β-mercaptoethanol
0.01 g	Bromophenol blue

   Add water to 50 ml

7. Stain stock: 1% Coomassie Brilliant Blue G (Stir and filter)
8. Destaining solution: for 2 liters

   140 ml Acetic acid
   100 ml Methanol
   Add water to 2 liters